



HAL
open science

Self-management of the umbilical of a ROV for underwater exploration

Christophe Viel

► **To cite this version:**

Christophe Viel. Self-management of the umbilical of a ROV for underwater exploration. 2021.
hal-03286654v1

HAL Id: hal-03286654

<https://hal.science/hal-03286654v1>

Preprint submitted on 15 Jul 2021 (v1), last revised 3 Nov 2021 (v2)

HAL is a multi-disciplinary open access archive for the deposit and dissemination of scientific research documents, whether they are published or not. The documents may come from teaching and research institutions in France or abroad, or from public or private research centers.

L'archive ouverte pluridisciplinaire **HAL**, est destinée au dépôt et à la diffusion de documents scientifiques de niveau recherche, publiés ou non, émanant des établissements d'enseignement et de recherche français ou étrangers, des laboratoires publics ou privés.

Self-management of the umbilical of a ROV for underwater exploration

Journal Title
XX(X):1-37
©The Author(s) 2021
Reprints and permission:
sagepub.co.uk/journalsPermissions.nav
DOI: 10.1177/ToBeAssigned
www.sagepub.com/

SAGE

Christophe Viel¹

Abstract

This article focuses on a passive self-management of the umbilical of a Removed Operated Vehicle (ROV) for underwater exploration. The objective is to give a predictable shape to the umbilical using moving ballast and buoys to stretch the umbilical and so to avoid knots on the cable itself or with environmental obstacles. The ballast and buoys move by themselves to maintain the cable taut without a motorized system. A model of the umbilical is proposed. Case with and without currents are considered. Three configurations of umbilical are proposed, each one to be the most adapted for ROV exploration missions: close-surface, sea exploration, and diving with presence of large obstacles.

Keywords

Underwater robotics, cables management, cables model

1 Introduction

The underwater umbilicals are used to link a submarine Remotely Operated Vehicle (ROV) to a control unit or a Human-Machine interface usually placed on boat. This umbilical, or tether, can have three objectives: first the transmission of data in real time in both directions, *i.e.* real-time video feedback, control orders, instrument measurements... (see [5]), second provide energy for the ROV to supply it completely or to increase its autonomy, third not loose the robot during the exploration [17]. Umbilicals have however many problems like collision with obstacle, umbilical inertia and drag forces impacting the maneuverability of the ROV, knot formation, cable breakage due to its own mass or vehicle mass, etc... . Umbilical is therefore a trade-offs between the umbilical constraint, battery power and real-time feedback in the ROV performance [6].

To solve these constraints, the umbilical have been modeled, equipped and instrumented to provide a feedback on its position and form. Two main categories of methods can be observed in the literature: the detection of the umbilical using vision [15, 14, 16] and/or sensor placed directly on/in the umbilical to obtain a feedback on its shape [10, 7], or a direct modeling of the umbilical using only boat and ROV position [11, 12, 9], sometimes with an a-prior knowledge of underwater current. The main advantage of the first category is the accuracy of the model obtained, often in real time. However, these strategies requires specific umbilical equipment often expensive with a complex installation of the sensors. The second category have the advantage to be implementable for all kind of umbilical, but are often less accurate and can not always provide results in real-time.

Several methods exist to model the cable shape and dynamic, from the simplest geometrical model like catenary curve [19] or the chain of segments with geometrical constraints like in [11]. These methods are perfect to

simulate a large number of segments in real-time and are memory efficient when an accurate physical model is not necessary. When an accurate knowledge of the cable dynamic is required, Lumped-mass-spring method [4, 12, 13] and segmental method [8, 9, 2] are the most used methods. The first method models the umbilical as mass points joined together by massless elastic elements, the second describes the cable as a continuous system and numerically solves resulting partial differential equations.

The umbilical can also be equipped. A TMS (Tether Management System), a system of winches controlled by a human operator and attached to the ROV housing cage [1], can so be used to regulate the amount of tether cable and so keep the umbilical taut. This system is however heavy for the cable when it is operating underwater, and its operation can be a complex task. Some works try to automate or replace it by an other vehicle like a USV [20], secondary ROV or several ROVs [16] or a motorized plug/float assembly [3]. However, all these systems required to be managed automatically by an operator in real time, using the knowledge of several current ROV's parameters like its position.

This paper proposes a passive self-management of the umbilical of a ROV for underwater exploration using moving ballasts and buoys without motorization. Since the shape of the umbilical can be complex to predict when it can move freely, we propose to add ballasts and buoys to introduce tension inside the cable and stretch it, and so make its shape assimilated to straight lines predictable. In this perspective, this paper proposes

- three equipment of the umbilical for three ROV missions : exploration of hull boat and close-surface,

¹CNRS, Lab-STICC, F-29806, Brest, France
Email: firstname.lastname@ensta-bretagne.fr

exploration of sea-ground, and diving exploration with presence of large obstacles.

- to use ballasts and buoys to tend the umbilical and so obtain a model of the umbilical simple to compute,
- the delimitation of areas where the ROV can evolve without risk of knot on the cable itself,
- a passive self-management of the umbilical without motorization nor TMS.

In opposite with [3], the ballast and buoys are not motorized and move by themselves to maintain the cable taut using only weight and Archimedes strength. The umbilical is modeled using geometrical relations and fundamental principle of static for an approach faster and lighter to compute than lumped-mass-spring method or segmental methods studied in [4, 12, 9, 8]. In absence of current, the only required feedback is the ROV position and a limitation of its acceleration in some directions. Case with currents will require knowledge of their strength and orientation to evaluate the shape of the umbilical, but are not required to evaluate areas where absence of knots in the umbilical is guaranteed.

The Section 2 exposes the related work. The problematic and the hypotheses taken in this paper are described in Section 3. The management of the umbilical for surface exploration is presented in Section 4. The management of the umbilical for sea exploration without horizontal currents is exposed in Section 5. The subsections 5.2 and 5.4 described its geometrical and dynamical model. Restricted areas guaranteeing the umbilical is always taut are described in Section 5.4, and the rigidity of the umbilical is studied in Section 5.6. The two-dimensional case with horizontal current is exposed in Section 6, following by the three-dimensional case with horizontal current in Section 7. The last management of the umbilical for diving exploration with presence of large obstacles is described in Section 8. The Section 9 and 11 discuss of the validity of the previous models and hypotheses taken, based on experimentation. Finally, the Section 12 concludes this work.

2 Related work

2.1 Cable modeling

Several methods exist to model the cable shape and dynamic. The simplest model is catenary curve [19], referring to a non-rigid flexible cable whose weight in water is greater than the buoyancy force. Nevertheless, when the cable are very long or heavy, more parameters like bending stiffness must be taken into account. In other methods like [11], neutrally buoyant cables are considering, allowing to ignore gravity and buoyancy strength. The umbilical is represented as a long chain of segments with geometrical constraints between them to take into account rigidity inside the umbilical. When it is not necessarily be physically accurate neither considering dynamic of the cable, these geometrical models allow a fast calculation and are memory efficient.

To obtain a dynamical and physically accurate cable model, two main kind of methods exist [2]: lumped-mass-spring method [4, 12, 13] and segmental method [8, 9]. First method models the umbilical as mass points joined together by massless elastic elements. This approach is very

useful for elastic cables but requires large computational resources. The segmental method describes the cable as a continuous system and numerically solves resulting partial differential equations. These two methods focus on the cable dynamics in simple environments with few forces: gravity, buoyancy, hydrodynamic drag, environment inertial force, axial tension, twisting force and bending force. In [9], a three-dimensional ROV-cable model is presented using Euler-Bernoulli beam theory, modified to allow the compression of the cable. The model is verified experimentally and shows good agreement with the experimental results.

2.2 Cable instrumentation

The umbilical can be equipped and instrumented to provide a feedback on its position and shape. Two main categories exist in the literature: the detection of the umbilical using vision [15, 14, 16], and sensors placed directly on/in the umbilical [10, 7]. These methods allow an accurate model, often in real time, but requires specific umbilical equipment often expensive and complex to install.

In [10], a method named “Smart Tether” gives the shape and the motion of the cable in real time using IMU sensor nodes embedded in the umbilical itself. The main inconvenient of this method, in addition to the difficulty of setting up the sensors and their price, is these nodes induce an irregular shape along the cable, causing problems for winding. In [7], optic fibers are braided within the umbilical and use the interferometry properties to monitor the curve of the whole cable in 3D in real time. Again, this solution has a very high cost again (about 200 000 euros for 50 m length).

For exploring shallow waters, [16] proposes an umbilical composed of mini-ROVs following each other. The shape of cable is controlled by i) the detection of the cable shape using cameras behind the ROV through a color segmentation, see [15, 14], ii) the regulation of the distance between the successive ROVs. Umbilical 3-D shape parameters are estimated in real-time thanks to a curve fitting procedure based on the Gauss-Newton algorithm and then regulated on the cable model based on catenary model or straight line.

Additional components such as TMS, ballasts, buoys or intermediate cables can also be used as dampers to avoid undesired forces on the ROV due to waves/currents or the umbilical weigh. For deep and ultra-deep-water operation for example, [18] proposes alternative configurations for minimizing the tension in the umbilical and reduce the risk of snap, like installing a series of floaters along the umbilical. Three different configurations are numerically investigated and compared. However, the floaters increase the offset of the ROV by making the cable more sensible to currents. The most classic equipment is the TMS, a system of winches attached to the ROV housing cage which regulates the amount of cable [1]. It allows to the robot to move in the working area while keeping the umbilical taut. When the TMS is placed underwater, it acts as a ballast to reduce the ROV offset due to current and wave. However, during ROV operation in deep and ultra-deep waters where total self-weight of the umbilical and ROV is close to the cable limit of the resistance, the elimination of the TMS is a reasonable alternative. TMS can also be set up on the boat to avoid this

problem, but its influence on the cable is much more limited. Finally, TMS is problematic to wind when the umbilical is equipped with buoys or ballasts.

Since the operation of a TMS is a complex task which can be similar to control a secondary ROV, some works try to automate it or replace it by an other vehicle (USV, secondary ROV... see [16, 3, 20]). In [3], a motorized plug/float assembly moves on the umbilical to change the buoyancy of this one, even drop the ROV to become temporary an AUV. A TMS on the boat regulates the cable length. If this system is efficient and allows an important adaptation, it is huge, expensive and can not be adapted for all kind of ROV or exploration. In [20], the system is composed of an USV with an embedded winch, an umbilical and a ROV to offer several ways to manage the cable. The distance between the USV and the ROV is adapted to stretch or loose the umbilical and so avoid collision between the umbilical and underwater obstacle. A method to model its mechanical behavior is proposed, based on a segmental method.

3 Problematic and hypothesis

Let define the referential \mathcal{R} of origin $O = (0, 0)$ corresponding to the coordinate of the boat where the first extremity of the umbilical is attached. $R = (x, y)$ are the coordinates of the ROV, corresponding to the second extremity of umbilical. The vertical axis is oriented to the ground, so for two (y_1, y_2) , $y_1 > y_2$ means y_1 is deeper than y_2 and $y = 0$ corresponds to the sea level.

In absence of tension between its two extremities, a cable takes an irregular shape only limited by its length and its rigidity. In the most shallower dives, a ballast is hung on the umbilical at a defined length to stretch the cable between the boat and the ballast. When the ROV is too close to the ballast, the cable between them floats/falls freely, taking the shape of a bell, subject to entanglement. To pull the cable taut independently of the ROV position, we propose to add an other item on the umbilical.

Since the buoys and ballasts move in opposite direction, alternating the attachment of buoy and ballast on the cable is a good solution to stretch it. However, a ballast/buoy linked to several cables (two parts of the same umbilical in our case) at fixed distances can only taut one of them in most cases, several only in particular configuration. In opposite, a ballast/buoy which can move freely along the cable will always stop its position at the lower/higher point where it stretches the both parts of the cable simultaneously.

This paper proposes several configurations alternating ballasts and buoys, fixed or moving freely along the umbilical to stretch it. Its shape can so be assimilated to configurations of predictable straight lines, where the rigidity of the cable can be modeled by minimal angles between lines. The main advantage of this method is the umbilical is self-managed without motorization and without TMS, using only gravity and Archimedes strength, with a shape predictable at the equilibrium.

Some parameters and particular configurations must however be considered. A ballast heavier than a buoy can makes it dives, and opposite. The action of the ballast on the umbilical becomes equal to a pulley if it is in contact with the sea-ground, same remark with the buoy reaching the surface.

Since a large number of configurations exist (different number of ballasts, buoys, distances fixed between them or sliding, difference of weight...) and most do not guarantee to stretch the umbilical satisfactorily, this paper focus on three chosen configurations with good performances for three different missions: hull boat exploration and close-surface exploration, sea exploration, and diving exploration with presence of large obstacles. These configurations will be exposed in the next sections and are briefly illustrated in Figure 1.

The following assumption are considered in all the study:

A1) The ratio mass/buoyancy of the umbilical is negligible compare to the ballasts' weight and the buoys' buoyancy used in the configuration.

A2) The length of the cable is such that it is reasonable to neglect the length variation of umbilical, considered as constant.

A3) When the umbilical is taut, its geometry can be assimilated to straight lines between defined points, here the ballasts, the buoys, the boat and the ROV. The rigidity of the cable can be modeled by a minimal angle θ_{\min} between them, described in Section 5.6.

A4) Consider the ROV is enough strong and controllable to compensate action of the ballasts and buoys and so (x, y) is perfectly fixed when ROV is not moving.

A5) Let $P = m_m g - F_{cy,m}$ be the strength of the ballast m used in our system, with m_m the mass of the ballast, g is the gravity constant, and $F_{cy,m}$ be the strength of the vertical current apply on the ballast M where $F_{cy,m} < 0$ pushes down to the seafloor and $F_{cy,m} > 0$ pushes up to the surface. One assumes that $P > 0$, *i.e.* the ballast's weight is stronger than the vertical current.

A6) Let $F_{b_i} = (\rho_{water} V_{b_i} - m_{b_i}) g + F_{cy,b_i}$ be the strength of the buoy b_i used in our system, with m_{b_i} the mass of the buoy, V_{b_i} its volume, ρ_{water} the volumetric mass of the water, and F_{cy,b_i} the vertical current applied at the buoy position where $F_{cy,b_i} < 0$ pushes down to the seafloor and $F_{cy,b_i} > 0$ pushes up to the surface. One assumes that $\forall i \in [1 \dots N]$, $F_{b_i} > 0$, *i.e.* the buoy's buoyancy is stronger than its weight and the vertical current strengths.

A7) When a ballast/buoy is considered to move freely on the umbilical, one assumes that there is no friction between the umbilical and the ballast/buoy.

The validity of these hypotheses in practical cases, specifically Assumption A4 and A7, will be discussed in Section 11. Remark if hypothesis A5 or A6 are not respected, the ballast/buoy can not have an action on the umbilical.

4 Umbilical for surface exploration

This section exposes a simple strategy of self-management of the umbilical to explore close to the surface, such as inspection of boat hull, navigation under uniform ice floe,

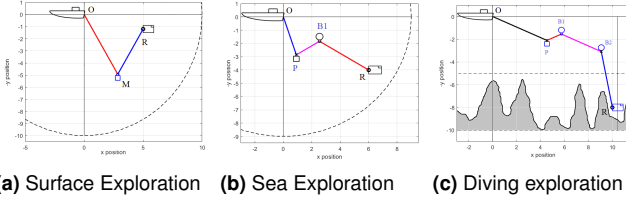


Figure 1. Methods exposed in this works. Square: ballast. Circle: buoy. "x": fixed ballast/buoy. "o": sliding ballast/buoy. Other parameters will be exposed in futur sections.

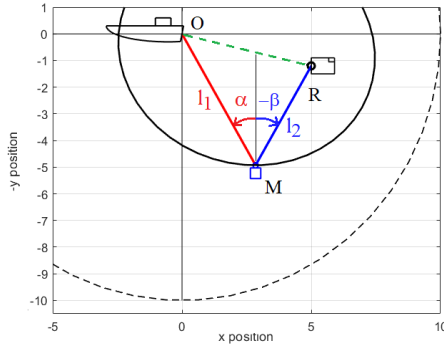


Figure 2. Parameters for Surface Exploration. M : sliding ballast. Black dash line: area where the ROV can move with its umbilical of length L . Black line: ellipse of centers O and R . Green dash line: longest diameter of the ellipse.

etc... . In this configuration, the umbilical remains taut and below the ROV to not disturb it. This configuration is not adapted for seafloor exploration: next sections will proposed strategies for these cases.

Consider in this configuration an umbilical of length L with a sliding ballast M which can move freely between the two extremity of the umbilical, *i.e.* the ROV and the boat, as illustrated in Figure 2. Let α and β be respectively the oriented angle between the sliding ballast and the boat, and between the sliding ballast and the ROV. The parameters are illustrated on the Figure 2. In a configuration where the ballast is not in contact with the sea-ground or an obstacle, the umbilical is taut and the system can be expressed such

$$x = l_1 \sin(\alpha) - l_2 \sin(\beta) \quad (1)$$

$$y = l_1 \cos(\alpha) - l_2 \cos(\beta) \quad (2)$$

with $L = l_1 + l_2$ where $l_1 = ||OM||$ and $l_2 = ||MR||$.

If the environment is free of obstacles, the ROV can move in the area corresponding to the half circle $\mathcal{C}(O, L)$ of radius L and center O , so $x \in [-L, L]$ and $y \in [0, L]$. The ROV must however pass through the position $(0, L)$ to switch from the areas $[-L, 0]$ and $[0, L]$ without creating a knot around the ballast M which would block its displacement.

4.1 Configuration without horizontal current

Consider in a first time there is no horizontal current, vertical current being considered by Assumption A5.

The ballast M is sliding freely on the umbilical of fixed length L , link to the boat and the ROV: due to the umbilical limitation, the ballast can be only inside the ellipse \mathcal{E}_1 of centers O and R and radius $r_1 = \frac{L}{2}$ and

$r_2 = \sqrt{\left(\frac{L}{2}\right)^2 - \frac{x^2 + y^2}{4}}$, and the umbilical is stretched only when the ballast is on the ellipse periphery, as illustrated in Figure 2. Considering Assumption A5 and A7, in absence of horizontal current and since the ballast is sinking, the ballast position is the lowest position and ellipse properties show that

$$\alpha = -\beta \quad (3)$$

Using (3), (1)-(2) becomes

$$x = L \sin(\alpha) \quad (4)$$

$$y = (l_1 - l_2) \cos(\alpha). \quad (5)$$

Since $x \in [-L, L]$ and $y \in [0, L]$, one can deduce from (4)-(5) that

$$\alpha = \text{asin}\left(\frac{x}{L}\right) \quad (6)$$

$$l_1 = \frac{1}{2} \left(L + \frac{y}{\sqrt{1 - \left(\frac{x}{L}\right)^2}} \right) \quad (7)$$

$$l_2 = L - l_1 \quad (8)$$

Proofs of (6)-(8) are provided in Appendix A.1.

Minimum seafloor depth or ROV diving

Let note y_{floor} the minimum depth inside the circle $\mathcal{C}(O, L)$ due to the environment, in most case the seafloor or a rock put on the sea floor. The system (4)-(5) is valid only if the ballast stretches the umbilical, so if the ballast has no contact with the sea-ground or with an obstacle. This condition is always satisfied if $y_{\text{floor}} \geq L$. In other case, since the ballast is always lower than the ROV level, let define the limit depth $y_{\text{lim}}(x)$ for a given position x which guarantee the ballast is always higher than y_{floor} if $y \leq y_{\text{lim}}(x)$.

In absence of current, following steps exposed in Appendix A.2, $y_{\text{lim}}(x)$ can be expressed such

$$y_{\text{lim}}(x) = 2y_{\text{floor}} - L\sqrt{1 - \left(\frac{x}{L}\right)^2}. \quad (9)$$

(9) is illustrated in Figure 3. Remark (9) doesn't take into account the geometries of the ballast which hangs below the umbilical in practice, as illustrated in Figure 3. The limit $y_{\text{lim}}(x)$ must therefore be raised such that

$$y_{\text{lim}}(x) = 2(y_{\text{floor}} - h_M) - L\sqrt{1 - \left(\frac{x}{L}\right)^2} \quad (10)$$

where h_M is the ballast height. Remark also if the position x is unknown, a simple condition to guarantee its hypothesis is to take $y_{\text{lim}} = 2(y_{\text{floor}} - h_M) - L$.

4.2 Configuration with horizontal current

Consider now the presence of horizontal current. Let $F_{cx,m}$ be the strength of the horizontal current applied on the ballast M of mass m on the axis Ox , where $F_{cx,m} > 0$ corresponds to a current in the direction $\vec{O}x$. Consider P the strength of the ballast respecting Assumption A5. Finally, let F_{tp} be the sum of strength P and $F_{cx,m}$ with $\psi_{P,x}$ its orientation such

$$F_{tp} = \sqrt{P^2 + F_{cx,m}^2} \quad (11)$$

$$\psi_{P,x} = \text{atan}\left(\frac{F_{cx,m}}{P}\right). \quad (12)$$

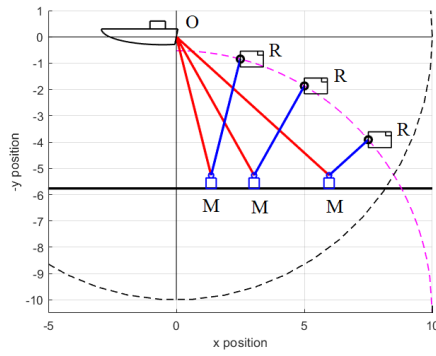


Figure 3. Limit depth y_{lim} which guarantee the ballast is not in contact with the seafloor for Surface Exploration. M : sliding ballast. The dash magenta line: y_{lim} . Large black line: seafloor y_{floor} . Red line: l_1 . Blue line: l_2 .

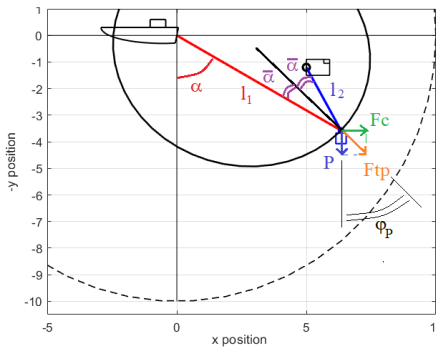


Figure 4. Parameters for Surface Exploration with horizontal current. M : sliding ballast. Black dash line: area where the ROV can move due to the umbilical length. Solid black line: ellipse of centers O and R and radius $\frac{L}{2}$ and $\sqrt{\left(\frac{L}{2}\right)^2 - \frac{x^2+y^2}{4}}$.

Since the ballast M is still sliding on the umbilical, its position is on the ellipse \mathcal{E}_1 defined in Section 4.1 and so F_{tp} creates in the umbilical two angles $\bar{\alpha}$ identical as illustrated in Figure 4 such

$$\bar{\alpha} = \alpha - \psi_{P,x} \quad (13)$$

$$\bar{\alpha} = \psi_{P,x} - \beta \quad (14)$$

leading to

$$\alpha = 2\psi_{P,x} - \beta. \quad (15)$$

Remark (15) is equal to (3) when $F_{cx,m} = 0$. Using (15) and a rotation of the referential \mathcal{R} as described in Appendix A.3, one gets the new expression of the parameters:

$$\alpha = \text{asin} \left(\frac{x \cos(\psi_{P,x}) - y \sin(\psi_{P,x})}{L} \right) + \psi_{P,x} \quad (16)$$

$$l_1 = \frac{1}{2} \left(L + \frac{y \cos(\psi_{P,x}) + x \sin(\psi_{P,x})}{\sqrt{1 - \left(\frac{x \cos(\psi_{P,x}) - y \sin(\psi_{P,x})}{L} \right)^2}} \right) \quad (17)$$

and $l_2 = L - l_1$, $\beta = 2\psi_{P,x} - \alpha$.

A new limit depth y_{lim} noted \bar{y}_{lim} can be defined in this configuration. However, since the current pushes the sliding ballast upward, the new limit depth \bar{y}_{lim} is higher than y_{lim} described for case without current, *i.e.* $\bar{y}_{lim} \leq y_{lim}$.

Since the current can be irregular making the position of M varying between its positions with and without current, it is recommend to use only y_{lim} as limit depth.

The same comment can be made for the 3 dimensions case. The presence of a current $F_{cz,m}$ perpendicular to the plan (O, x, y) pushes the sliding ballast upwards: the limit y_{lim} is so still a sufficient requirement to guarantee the sliding ballast will not touch the seafloor and so the umbilical will stay taut. Note the 3D model is not trivial to solve even for this simple configuration, but this sufficient requirement avoids to solve it. Note also 2D model is applicable for 3D case in absence of horizontal current by choosing the referential such $\vec{O}x$ corresponding to the projection of \vec{OR} on the surface, the ballast M being always inside (O, x, y) at the equilibrium.

5 Umbilical for Sea exploration without horizontal current

This section exposes a simple strategy of self-management of the umbilical to explore the sea and the seafloor. The proposed configuration for this strategy is the following one: a ballast fixed on the umbilical at a constant distance of the boat, and a buoy which can move freely between the ballast and the ROV. The umbilical remains taut as long as the ROV does not enter in a defined forbidden area. In opposite with the strategy proposed in Section 4, the ROV can evolve close to the seafloor in a large area, but its movements are restricted when it is close to the surface. In this section, the problem is studied only for the two dimensional case (2D case) and without horizontal current. The presence of current will be added in Section 6 and three dimensional case (3D case) will be studied in Section 7.

5.1 Introduction of the geometrical model and restricted areas

Consider in this configuration an umbilical of length l divides in two parts: a first part of length l_1 between O and the ballast M fixed on the umbilical, *i.e.* $\|OM\| = l_1$, and a second part of length L where the buoy B can move freely between the ballast and the ROV. Similarly to the problem studied in Section 4, L can be divided in two lengths $l_2 = \|MB\|$ and $l_3 = \|BR\|$ corresponding to the lengths of the left side and right side of the buoy, where $L = l_2 + l_3$. Let γ be the oriented angle between the boat and the ballast M . The oriented angles α and β are respectively the angle between the ballast and the buoy, and between the buoy and the ROV. Parameters are illustrated in Figure 5.

Since the ROV can not go higher than the sea level and to avoid node between l_1 and L , the ROV can move in the area corresponding to the quarter of the circle $\mathcal{C}(O, l)$ of radius $l = l_1 + L$ and center O , so $x \in [0, l]$ and $y \in [0, l]$ (the area $[-x, 0]$ will be discussed later in the section). In a configuration where the umbilical is taut, the system can be expressed such

$$x = l_1 \sin(\gamma) - l_2 \sin(\alpha) + l_3 \sin(\beta) \quad (18)$$

$$y = l_1 \cos(\gamma) - l_2 \cos(\alpha) + l_3 \cos(\beta) \quad (19)$$

$$L = l_2 + l_3. \quad (20)$$

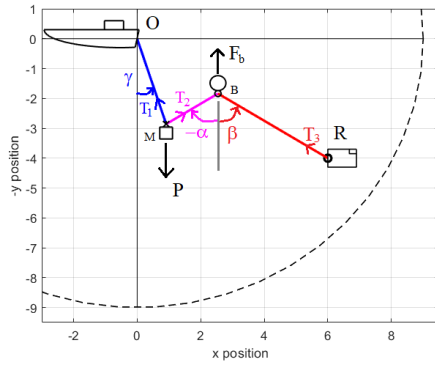


Figure 5. Parameters for Sea Exploration. M is the fixed ballast and B the sliding buoys. In the example here, $P = 3F_b$. The blue, magenta, red lines correspond to l_1, l_2, l_3 . Black dash line: area where the ROV can move with its umbilical length.

where l_1 and L are fixed and known, $L \geq l_2 \geq 0$ and $L \geq l_3 \geq 0$.

Similarly to the problem studied in Section 4, the buoy finds its position on the ellipse \mathcal{E}_2 as long as it does not touch the surface (this condition will be studied below). M and R are the centers of \mathcal{E}_2 , with the two radius $\frac{L}{2}$ and $\sqrt{\left(\frac{L}{2}\right)^2 - \frac{(x-x_M)^2 + (y-y_M)^2}{4}}$ where (x_M, y_M) are the coordinates of the ballast M . In absence of horizontal current, ellipse properties show that

$$\alpha = -\beta. \quad (21)$$

In function of the ROV position, six areas corresponding to specific umbilical configurations can be observed, illustrated in Figure 6:

- Area A: standard behavior of the system. The umbilical is perfectly taut by the action of the ballast and the buoy with $\gamma > 0, l_2 > 0, l_3 > 0$.
- Area B: the buoy is on the surface but the ballast can still taut the cables l_1 and L , with $\gamma \geq 0, l_2 > 0, l_3 > 0$. Note Area B does not exist if $L < l_1$.
- Area C: two cases are possibles
 - if $L \geq l_1$, the buoy is on the surface and ballast can not taut the cable L ,
 - if $L < l_1$, the cable l_1 is not taut because the ROV is too close to the surface for the ballast can stretch l_1 and L (the only solution of the system (18)-(20) is $\gamma < 0$ for $x > 0$, impossible in practice without horizontal current). Moreover, the buoy is in contact with the ROV.

This configuration must be avoid by the ROV.

- Area D1: the umbilical is taut and the buoys is in contact with the ROV, so $l_2 = L$ and $l_3 = 0$.
- Area D2: the umbilical is taut and the buoys is in contact with the ballast M : $l_2 = 0$ and $l_3 = L$.
- Area E: area inaccessible due to the length l .

The system is considered to be inside an area if the ROV coordinate (x, y) is inside this area. The ROV must not enter in the area C because the umbilical cannot be taut inside, making the model (18)-(20) invalid and allowing the appearance of knots. In case where this strategy of self-management of the umbilical is used without need to model

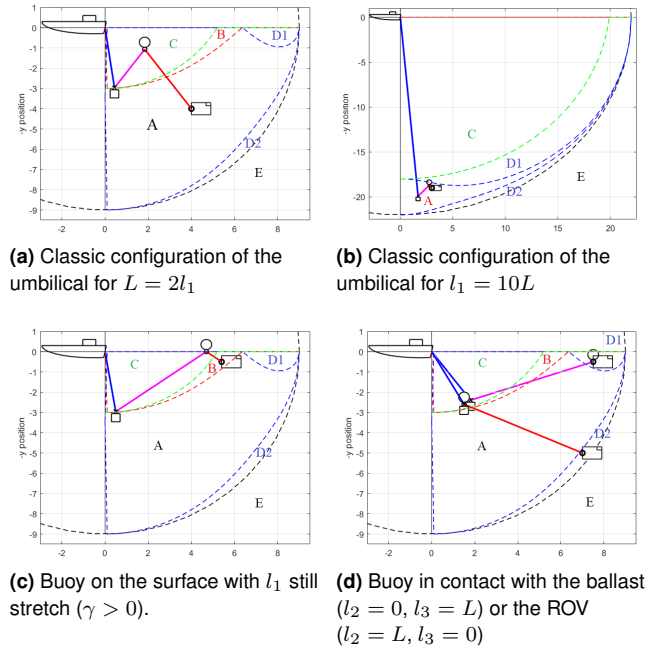


Figure 6. Different areas for Sea Exploration. Green dash line: area C. Red dash line: area B. Blue dash lines : areas D1 and D2. Black dash line: area E. Note the area B does not exist in sub-figure b.

the umbilical in real time, the operator only need to know the areas C and E. All areas are required only to model the umbilical, its shape being different in each area. The shape of the areas depends on different parameters, as it will be shown in Section 5.4.

5.2 Dynamic model

In this section, the ROV is supposed to be inside the area A. Results exposed are not valid in others areas, which will be studied in next sections.

To solve the system (18)-(20), the dynamic of the system is studied at its equilibrium. Let define P and F_b the strength applied on the umbilical by the ballast and the buoy, following assumptions A5 and A6. Moreover, suppose the ballast and the buoy are chosen respecting the following Assumption A8:

Assumption A8) The masses and buoyancy of the ballast and the buoy are chosen such

$$P \geq F_b \max \left(\left[1, \frac{1}{2} \left(\frac{l_1}{L} + 1 \right) \right] \right). \quad (22)$$

This constraint will be shown and used in the appendices, and are only used in this section and Section 6 (case with horizontal current).

In system (18)-(21), the unknown parameters are l_2, l_3, α, β and γ . Since the system (18)-(21) provides 4 equations, a last one must be found. Considering Assumptions A1 to A8, let perform the fundamental principle of static on M and B , as illustrates in Figure 5:

$$\Sigma_M \vec{F} = P\vec{y} + \vec{T}_1 + \vec{T}_2 \quad (23)$$

$$\Sigma_B \vec{F} = -F_b\vec{y} - \vec{T}_3 - \vec{T}_2 \quad (24)$$

where \vec{T}_1 , \vec{T}_2 and \vec{T}_3 are the tension of the umbilical applied on the ballast and the buoy.

Following steps described in Appendix B.2, one can show that

$$\tan(\beta) = \Lambda \tan(\gamma). \quad (25)$$

where $\Lambda = 2\frac{P}{F_b} - 1$ and remark $\Lambda \geq 1$ because $P \geq F_b$.

Adding (25) to (18)-(21), One now has enough equations to solve the system (18)-(20) inside the area A.

5.3 Umbilical model solved in area A

In this section, let's consider the ROV is inside the area A. The Theorem 1 describes the value of parameters γ , α , β , l_2 and l_3 . For this section and the following ones, let not γ_A the evaluation of γ inside the area A, as described in the following theorem.

Theorem 1. Consider the system (18)-(20) with $(x, y) \in [0, l]^2$ and where (x, y) is inside the area A, i.e. $l_2 > 0$, $l_3 > 0$. Considering also the Assumption A8 and the absence of horizontal current, i.e. (25) and (21). The angle γ can be expressed $\gamma = \gamma_A$ such

a) if $x = 0$, the only geometrical solution without current is $\gamma_A = 0$,

b) if $P = F_b$, one has $\Lambda = 1$ and γ_A can be expressed as

$$\sin(\gamma_A) = \frac{x}{l}. \quad (26)$$

c) if $P > F_b$ and $x > 0$, γ_A can be expressed as

$$\sin(\gamma_A) = \min_{i \in [1,2,3,4]} (|X_i|) \quad (27)$$

where

$$\begin{cases} X_1 = \frac{\sqrt{U - \frac{2}{3}A} - \sqrt{\Delta_{Y1}}}{2}, X_2 = \frac{\sqrt{U - \frac{2}{3}A} + \sqrt{\Delta_{Y1}}}{2} & \text{if } \Delta_{Y1} \geq 0, \\ X_1 = \infty, X_2 = \infty & \text{else,} \end{cases} \quad (28)$$

$$\begin{cases} X_3 = \frac{-\sqrt{U - \frac{2}{3}A} - \sqrt{\Delta_{Y2}}}{2}, X_4 = \frac{-\sqrt{U - \frac{2}{3}A} + \sqrt{\Delta_{Y2}}}{2} & \text{if } \Delta_{Y2} \geq 0, \\ X_3 = \infty, X_4 = \infty & \text{else,} \end{cases} \quad (29)$$

$$\text{with } \Delta_{Y1} = - \left(U + \frac{4}{3}A + \frac{2B}{\sqrt{U - \frac{2}{3}A}} \right),$$

$$\Delta_{Y2} = - \left(U + \frac{4}{3}A - \frac{2B}{\sqrt{U - \frac{2}{3}A}} \right) \text{ and}$$

$$A = -\frac{x^2}{2l_1^2} - \frac{(L^2\Lambda^2 - l_1^2)}{l_1^2(\Lambda^2 - 1)} \quad (30)$$

$$B = -\frac{l_1^2 + L^2\Lambda^2}{l_1^3(\Lambda^2 - 1)}x \quad (31)$$

$$C = \frac{x^4}{16l_1^4} + \frac{x^2(l_1^2 - L^2\Lambda^2)}{4l_1^4(\Lambda^2 - 1)} \quad (32)$$

$U =$

$$\begin{cases} \left(-\frac{q}{2} + \sqrt{\frac{q^2}{4} + \frac{p^3}{27}} \right)^{1/3} + \left(-\frac{q}{2} - \sqrt{\frac{q^2}{4} + \frac{p^3}{27}} \right)^{1/3} & \text{if } \Delta_U > 0, \\ 2 \cos \left(\frac{1}{3} \arccos \left(-\frac{q}{2\sqrt{-\frac{p^3}{27}}} \right) \right) \sqrt{-\frac{p}{3}} & \text{if } \Delta_U < 0, \\ -\sqrt{-\frac{p}{3}} & \text{if } \Delta_U = 0 \end{cases} \quad (33)$$

and $\Delta_U = \frac{q^2}{4} + \frac{p^3}{27}$, $p = -4C - \frac{A^2}{3}$ and $q = \frac{2A^3}{27} + (4AC - B^2) + \frac{-4CA}{3}$. Moreover, other parameters can be expressed such

$$\beta = \text{atan}(\Lambda \tan(\gamma_A)) \quad (34)$$

$$l_2 = \frac{L}{2} - \frac{y - l_1 \cos(\gamma_A)}{2 \cos(\beta)}, \quad (35)$$

and $l_3 = L - l_2$, $\alpha = -\beta$.

The proofs of Theorem 1 are described in Appendix B.3 and B.4. If several configurations must be considered to evaluate γ in Theorem 1, a solution always exists and the solution is analytic, so can be evaluated quickly.

The Theorem 1 is evaluated for $x \geq 0$. Since the system (18)-(20) is symmetric for $[0, x]$ and $[-x, 0]$ in absence of horizontal current, the following corollary can be made.

Corollary 1. In absence of horizontal current, the system (18)-(20) is symmetric for $[0, x]$ and $[-x, 0]$, and the Theorem 1 can be extended to the case $x < 0$ by taking $|x|$ instead of x inside the Theorem 1 and take the solution $\sin(\gamma_A) = \min_{i \in [1,2,3,4]} (|X_i|) \text{sgn}(x)$.

If Corollary gives a solution for areas $(x, y) \in [0, l] \times [0, l]$ and $(x, y) \in [-l, 0] \times [0, l]$, the ROV must however pass through the position $(0, L)$ to switch from the two areas to not create a knot around the buoy B, which would block its displacement.

5.4 Evaluation of the areas

To solve completely the geometrical model (18)-(20), the different areas must be considered because they represent particular geometrical configurations. This section present the boundaries of areas B, C, D1, D2 and E, area A corresponding to the default configuration. The calculation of these boundaries is described in Appendix B.6.

The boundary $y_{\text{area B}}(x)$ between the areas A and B correspond to the depth where the buoy is in contact with the surface $y = l_3 \cos(\beta)$, with $l_3 \geq 0$. The area B does not exist if $L < l_1$ because the buoy can not reach the surface without let the cable l_1 becomes loose (area C) or come in contact with the ROV (area D1). Following step from Appendix B.6.1, $y_{\text{area B}}(x)$ can be expressed as

$$y_{\text{area B}}(x) = \begin{cases} \max \left(\frac{L - l_1 \sqrt{1 + (\Lambda^2 - 1) \sin(\gamma_A(x))^2}}{\sqrt{1 + \Lambda^2 \tan(\gamma_A(x))^2}}, 0 \right) & \text{if } L \geq l_1, \\ 0 & \text{else.} \end{cases} \quad (36)$$

The area C is in contact with 1) the areas B if $L \geq l_1$, when the buoy is on the surface but ballast can not taut the cable L, 2) the areas A or D1 if $L < l_1$, when the cable l_1 is not taut because the ROV is too close to the surface. Following step from Appendix B.6.2, $y_{\text{area C}}(x)$ can be expressed as

$$y_{\text{area C}}(x) = \begin{cases} \sqrt{l_1^2 - x^2} - L & \text{if } \left(|x| < \sqrt{l_1^2 - L^2} \right) \& (l_1 > L), \\ \sqrt{L^2 - x^2} - l_1 & \text{if } \left(|x| < \sqrt{L^2 - l_1^2} \right) \& (L > l_1), \\ 0 & \text{else.} \end{cases} \quad (37)$$

In area D1, the buoy is in contact with the ROV, so $l_3 = 0$ and $l_2 = L$. Following step from Appendix B.6.3, $y_{area D1}(x)$ can be expressed as

$$y_{area D1}(x) = \max\left(\frac{l_1\sqrt{1 + (\Lambda^2 - 1)\sin(\gamma_A(x))^2} - L}{\sqrt{1 + \Lambda^2 \tan(\gamma_A(x))^2}}, 0\right). \quad (38)$$

In area D2, the buoy is in contact with the ballast, so $l_3 = L$ and $l_2 = 0$. Following step from Appendix F.4.3, $y_{area D2}(x)$ can be expressed as

$$y_{area D2}(x) = \max\left(\frac{l_1\sqrt{1 + (\Lambda^2 - 1)\sin(\gamma_A(x))^2} + L}{\sqrt{1 + \Lambda^2 \tan(\gamma_A(x))^2}}, 0\right). \quad (39)$$

Finally, since the area E corresponds to the limit of the umbilical length, $y_{area E}(x)$ can be expressed as described in Appendix B.6.5 such

$$y_{area E}(x) = \sqrt{l^2 - x^2}. \quad (40)$$

Note limits $y_{area B}(x)$ and $y_{area C}(x)$ between areas B and C described above don't take into account the geometries of the buoy which, in practice, hang above the umbilical as illustrated in Figure (3). For a given x , the area B and C must so be lowered such

$$y_{area B}(x) = \bar{y}_{area B}(x) + h_B \quad (41)$$

$$y_{area C}(x) = \bar{y}_{area C}(x) + h_B, \quad (42)$$

where h_B is the height of the submerged part of the buoy when the buoy floats freely on the surface without constraints, $\bar{y}_{area B}$ and $\bar{y}_{area C}$ are evaluated using (36) and (37).

As shown in (36)-(40) and illustrated on Figure 23 in the Appendix, areas C and E depend of l_1 , L and x , and areas B, D1 and D2 depend of l_1 , L , x , γ_A , P and F_b . The area B converges to area C when the ration $\frac{P}{F_b}$ increases, and area C increases with the discrepancy between l_1 and L , and do not exist if $l_1 = L$. Note areas C and E depend only of l_1 , L and x , so can be modelled easily. Since the umbilical is stretched when, the ROV stays outside the area C, area C is a sufficient information for an operator to avoid knot.

Minimum seafloor depth

The previous areas show the minimum depth where the ROV must dive to guarantee the umbilical stay taut due to the presence of the buoy, but assumes that the depth is sufficient in all cases. In practice, conditions on the minimum deep y_{floor} must also be respected.

Let note y_{floor} the minimum depth inside the circle $\mathcal{C}(O, l)$, in most cases the seafloor or a rock put on the sea floor. The system (18)-(19) is valid only if the two following conditions are respected

1. The ballast has no contact with the sea-ground or with an obstacle during its displacement, so y_{floor} must be lower than the circle of center O and radius l_1 ,
2. The ROV does not go inside the area C defined previously, so $y_{floor}(x) \geq y_{area C}(x)$.

Thus, for a given position x , the minimum seafloor depth $y_{floor}(x)$ can be expressed as

$$y_{floor}(x) \geq \max([y_{area C}(x), y_{ballast}(x)]) \quad (43)$$

where

$$y_{ballast}(x) = h_M + \sqrt{l_1^2 - x^2} \quad (44)$$

with h_M is the ballast height. Note (43) is always satisfied if the seafloor respects the following condition

$$y_{floor} \geq h_M + \max([l_1, L - l_1]). \quad (45)$$

5.5 Umbilical model solved for all areas

As exposed in Section 5.4, the different areas must be considered because they represent particular geometrical configurations. In areas D1 or D2 for example, angle β or α does not exist because the distances l_2 or l_3 are equal to zero. Let first define γ_D the value of γ outside the area A:

1) If $y \neq 0$, γ_D can be expressed as

$$\sin(\gamma_D) = \frac{a_D b_D - \sqrt{a_D^2 b_D^2 - (1 + b_D^2)(a_D^2 - 1)}}{(1 + b_D^2)} \quad (46)$$

with $a_D = \frac{x^2 + y^2 + l_1^2 - L^2}{2yl_1}$ and $b_D = \frac{x}{y}$.

2) else, $y = 0$, γ_D can be expressed as

$$\sin(\gamma_D) = \frac{x^2 + l_1^2 - L^2}{-2l_1 x}. \quad (47)$$

Note one has $x \neq 0$ because the ROV can only be inside the area A or C if $x = 0$, so γ_D does not exist if $x = 0$.

The following Theorem 2 exposes the evaluation of the parameters γ , α , β , l_2 and l_3 in function of the area where the ROV is located.

Theorem 2. Consider the system (18)-(20) for $(x, y) \in [0, l]^2$ and $y < y_{area E}(x)$. Considering the assumption A8 and the absence of current, i.e. (25) and (21), one gets

(1) if $y < y_{area C}(x)$, the model is not valid and the system (18)-(20) cannot be solved.

(2) else if $y_{area B}(x) \neq 0$ and $y_{area C}(x) \leq y \leq y_{area B}(x)$, then (x, y) is in the area B and one has $\gamma = \gamma_D(x)$, $l_2 = L - l_3$ and

$$\cos(\beta) = \frac{y + l_1 \cos(\gamma_D)}{L} \quad (48)$$

$$l_3 = \frac{Ly}{l_1 \cos(\gamma_D) + y}. \quad (49)$$

(3) else if $y_{area D1}(x) \neq 0$ and $y_{area C}(x) \leq y \leq y_{area D1}(x)$, then (x, y) is in the area D1 and one has $l_2 = L$, $l_3 = 0$, $\beta = 0$, $\gamma = \gamma_D(x)$ and

$$\alpha = -\text{acos}\left(\frac{-y + l_1 \cos(\gamma_D)}{L}\right). \quad (50)$$

(4) else if $y_{area D2}(x) \leq y$, then (x, y) is in the area D2 and one has $l_2 = 0$, $l_3 = L$, $\alpha = 0$, $\gamma = \gamma_D(x)$ and

$$\cos(\beta) = \frac{y - l_1 \cos(\gamma_D)}{L}. \quad (51)$$

(5) else, then (x, y) is in the area A and one has the parameters defined in Theorem 1 such $\gamma = \gamma_A(x)$, $\alpha = -\beta$, $l_3 = L - l_2$ with $\tan(\beta) = \Lambda \tan(\gamma_A)$ and $l_2 = \frac{l}{2} - \frac{y - l_1 \cos(\gamma_A)}{2 \cos(\beta)}$.

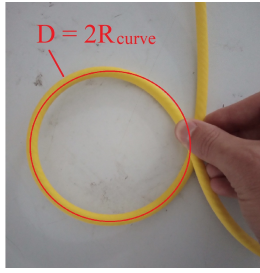


Figure 7. Characterization of umbilical rigidity

The proofs of previous results are described in Appendix B.7. Note if Theorem 2 (1) is true, the ROV must dive to $y = y_{area C}(x)$ to make the system valid. Remark also case $y > y_{area E}(x)$ is not physically possible due to the umbilical length.

The Theorem 2 is evaluated for $x \geq 0$. Again, since the system (18)-(20) is symmetric for $[0, x]$ and $[-x, 0]$ in absence of horizontal current, the following corollary can be made.

Corollary 2. *In absence of horizontal current, the system (18)-(20) is symmetric for $[0, x]$ and $[-x, 0]$, and the Theorem 2 can be extended to the case $x < 0$ by doing the following changes :*

- 1) take $|x|$ instead of x in Theorem 1 and (46) for the evaluation of γ_A and γ_D ,
- 2) take the solution $\sin(\gamma_A) = \min_{i \in \{1,2,3,4\}} (|X_i|) \operatorname{sgn}(x)$ in Theorem 1 and $\sin(\gamma_D) = \frac{a_D b_D - \sqrt{a_D^2 b_D^2 - (1+b_D^2)(a_D^2-1)}}{(1+b_D^2)} \operatorname{sgn}(x)$ in (46),
- 3) take the value $\beta = \beta \operatorname{sgn}(x)$ for cases (2)-(4) in Theorem 2.

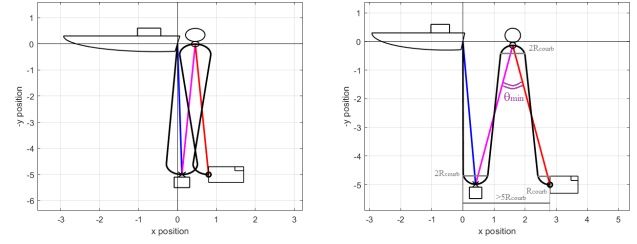
5.6 Model of umbilical rigidity and security angle

In practice, the umbilical has a rigidity which does not allow angles $|\alpha| + |\gamma|$ and $|\alpha| + |\beta|$ to become smaller than a minimum value. This rigidity can lead to collisions between the different part of the umbilical, as illustrated in Figure 8. To guarantee the absence of collision with the cable itself, this rigidity can be taken into consideration by introducing conditions $|\alpha| + |\beta| \geq \theta_{\min}$ and $|\alpha| + |\gamma| \geq \theta_{\min}$, or a minimum distance x_{\min} to respect such $x > x_{\min}$.

Let define R_{curve} the cable rigidity, such $D = 2\pi R_{curve}$ is the perimeter of the smallest circle which can be performed with the umbilical, see Figure 7. To guarantee the absence of collision in the umbilical, the distance x must allow the cable to perform two half circles around the ballast and the buoy, and a quarter of circle at the connection between the ROV and the umbilical, as illustrated in Figure 8. It is considered the umbilical drops straight without problem of rigidity problem at the boat level. Thus, the distance x must be larger than

$$x_{\min} = 5R_{curve}. \quad (52)$$

From (25) and Theorem 2, one has $|\gamma| \leq |\beta|$ in all cases. The minimum angle $\theta_{\min} = |\alpha| + |\beta| = 2|\beta|$ guaranteeing



(a) Collision due to umbilical rigidity **(b)** Absence of collision

Figure 8. Umbilical shape considering its rigidity. Black line: shape of the umbilical due to cable rigidity. Blue: l_1 . Magenta: l_2 . Red: l_3 . In the example here, $R_{curve} = 0.4\text{m}$ and $l = 15\text{m}$.

the absence of collision can so be defined such that

$$\theta_{\min} = 2\operatorname{asin}\left(\frac{4R_{curve}}{L}\right). \quad (53)$$

(53) is shown in Appendix B.1 and θ_{\min} is respected if $x \geq x_{\min}$. Note the value of θ_{\min} can be oversized for safety or for taking into account some other constraint, for example the presence of an optical fiber inside the umbilical requiring a larger curve to not break.

The parameter θ_{\min} will be more used in future sections with presence of horizontal currents.

5.7 3-Dimensionnal case in absence of horizontal current

In absence of horizontal current, the three dimensions case can be simply solved using the two dimensions case. Let define the 3D referential $\mathcal{R}_{3D} = (x, y, z)$ of origin $O = (0, 0, 0)$, where y is the vertical axis oriented to the ground. $(x, 0, z)$ is the horizontal plan at the sea level. $(x, y, 0)$ is the vertical plan such $\vec{OR} \cdot \vec{z} = 0$, where \vec{OR} is the vector between the boat and the ROV. One observes the umbilical is always at the equilibrium inside $(x, y, 0)$, so the solution of the 3D case without current is the solution of the 2D-case performed inside $(x, y, 0)$.

5.8 Practical case: Forces applied on the ROV

This section exposes the strengths applied by the umbilical on the ROV, to choose the ballast and the buoy in the capabilities of the ROV. Let $\vec{F}_{cable \rightarrow ROV}$ be the strength applied by the umbilical on the ROV and $\vec{T}_3 = -\vec{F}_{cable \rightarrow ROV}$ where \vec{T}_3 is exposed in Section 5.2. Then, one has from (24)

$$\sum_B \vec{F} \cdot \vec{x} = 0 \quad (54)$$

$$-T_2 \cos(\alpha) + T_3 \cos(\beta) = 0 \quad (55)$$

$$T_3 \cos(\beta) = T_2 \cos(\alpha). \quad (56)$$

Since $\alpha = -\beta$, one has $T_3 = T_2$. Moreover, since $F_{cable \rightarrow ROV} = T_3$ and $T_2 = F_b \frac{\sin(\beta)}{\sin(2\beta)} = \frac{F_b}{2} \tan(\beta)$ from (179) in Appendix B.2, one gets

$$F_{cable \rightarrow ROV} = \frac{F_b}{2} \tan(\beta). \quad (57)$$

Deduce from (57) and Theorem 2 that $F_{cable \rightarrow ROV}$ increases with the distance $d = \sqrt{x^2 + y^2}$. Since β is

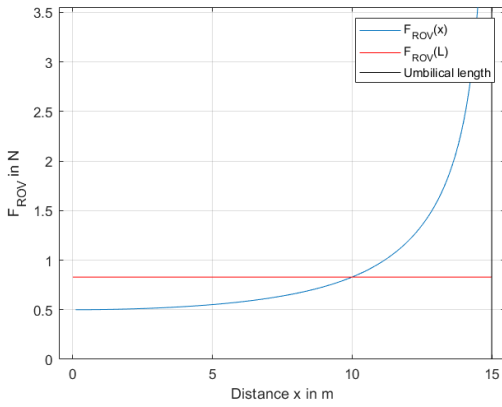


Figure 9. $F_{cable \rightarrow ROV}$ in function of the distance x , inside the area A. $P = 2F_b$, $F_b = 1N$, $L = 10m$ and $l_1 = 5m$.

independent of y in area A (see Theorem 2), one deduces that $F_{cable \rightarrow ROV}$ increases only with x in area A. Figure 9 shows the evolution of $F_{cable \rightarrow ROV}$ in function of x . An observation made for different values of P and F_b is that $F_{cable \rightarrow ROV}$ stays relatively low for $x \leq L$, because the boat carries most of the ballast's weight when the length L is fold.

5.9 Practical case: choice of umbilical length

Previous sections describe the umbilical shape and areas in function of predefined parameters like the umbilical length l . In practice, an operator searches the best umbilical length to explore an area approximately known. This section proposes a simple method to choose the parameters l , L and l_1 in function of several environmental constraints. More elaborate algorithms are proposed in Appendix H, and others choices can be made.

Remind y_{floor} is the dept of the seafloor. Let's define $[y_{\text{min}}, y_{\text{max}}]$ the desired minimum depth and maximum depths for the ROV exploration, where $y_{\text{max}} \leq y_{\text{floor}} - h_M$. Let's also define $[x_{\text{min}}, x_{\text{max}}]$ the desired minimum and maximum horizontal distances for the ROV exploration, where x_{min} has been defined in Section 5.6. Compromises must be made because not all the parameters x_{max} , y_{min} , y_{max} will be respected simultaneously. In this perspective, since the boat can move on the surface, the respect of parameters $[y_{\text{min}}, y_{\text{max}}]$ is favored over $[x_{\text{min}}, x_{\text{max}}]$.

To go the deepest possible without the ballast touching the seafloor, take $l_1 = y_{\text{floor}} - h_B$. Then,

- if y_{min} is favored over y_{max} , take $L = l_1 + y_{\text{min}}$, and $l = L + l_1$. To respect y_{min} for all $x \leq x_{\text{max}}$, one takes $x_{\text{max}} = \sqrt{l^2 - y_{\text{min}}^2}$ and has $y_{\text{max}}(x) = \sqrt{l^2 - x^2}$.
- if y_{max} is favored over y_{min} and respected for all $x \leq x_{\text{max}}$, takes $L \in \left[\sqrt{y_{\text{max}}^2 + x_{\text{max}}^2} - l_1, 2l_1 \right]$ with $x_{\text{max}} = \sqrt{9l_1^2 - y_{\text{max}}^2}$. One has $y_{\text{min}}(x) = y_{\text{area C}}(x)$.

The umbilical respected simultaneously y_{min} and y_{max} for $x \in [x_{\text{min}}, x_{\text{max}}]$ if there exist L such

$$\sqrt{y_{\text{max}}^2 + x_{\text{max}}^2} - l_1 \leq L \leq l_1 + y_{\text{min}}, \quad (58)$$

which is possible iff

$$x_{\text{max}} \leq \sqrt{(2l_1 + y_{\text{min}})^2 - y_{\text{max}}^2} \quad (59)$$

where $x_{\text{max}} \geq 0$ because here $l_1 = y_{\text{floor}} - h_B \geq y_{\text{max}}$.

6 Umbilical for Sea exploration with horizontal current

This section extends results of the configuration studied in Section (5) by adding presence of horizontal current. The presence of currents makes the system asymmetric and changes the position of the ballast and buoy, as well as the shape of areas exposed in the previous section.

6.1 Influence of current on the geometrical model and restricted areas

Consider the same configuration exposed in Section 5 with the geometrical model (18)-(20) and constraint on P and F_b . The presence of a vertical current is considering inside P and F_b , see Assumption A5 and A6.

Let $F_{cx,m}$ and $F_{cx,b}$ be the strengths of the current horizontal applied on the ballast M and buoy B on the axis \vec{Ox} such $F_{cx,m} > 0$ corresponds to a current in the direction \vec{Ox} , same for $F_{cx,b}$, as illustrated on Figure 10. Let also define the sums of strengths $F_{tm,x}$ and $F_{tb,x}$ such

$$F_{tm,x} = \sqrt{P^2 + F_{cx,m}^2} \quad (60)$$

$$F_{tb,x} = \sqrt{F_b^2 + F_{cx,b}^2} \quad (61)$$

with their incidence angles

$$\tan(\psi_{P,x}) = \frac{F_{cx,m}}{P} \quad (62)$$

$$\tan(\psi_{B,x}) = -\frac{F_{cx,b}}{F_b}. \quad (63)$$

Since the buoy is still moving freely on the umbilical and does not touch the surface (not inside areas B and C), its position is still on the ellipse \mathcal{E}_2 described in Section 5. In presence of horizontal current, ellipse properties shows that two angles $\bar{\alpha}$ identical are created by the strength $F_{tb,x}$ such $\bar{\alpha} = \alpha - \psi_{B,x}$ and $\bar{\alpha} = \psi_{B,x} - \beta$, illustrated on Figure 10. This property leads to

$$\alpha = 2\psi_{B,x} - \beta. \quad (64)$$

Remark (64) becomes equal to (3) when $F_{cx,b} = 0$.

As illustrated in Figure 11, the six areas defined in previous Section 5 still exist. However, since the ballast and the buoy are pushed in the same direction than the current, the areas are not symmetric, and area C does not exist theoretically when $L > l_1$ because the umbilical can always be taut by the current. The disappearance of area C must however be carefully considered in practice if the current is weak: it can be recommend to use the area C without horizontal current described in Section 5.

An additional area F can be defined in presence of horizontal current, corresponding to the area where cables l_2 and l_3 or l_1 and l_3 are crossed, *i.e.* lines associated to $\alpha = \beta$ and $\alpha = \gamma$. The crossing of cables can lead to a

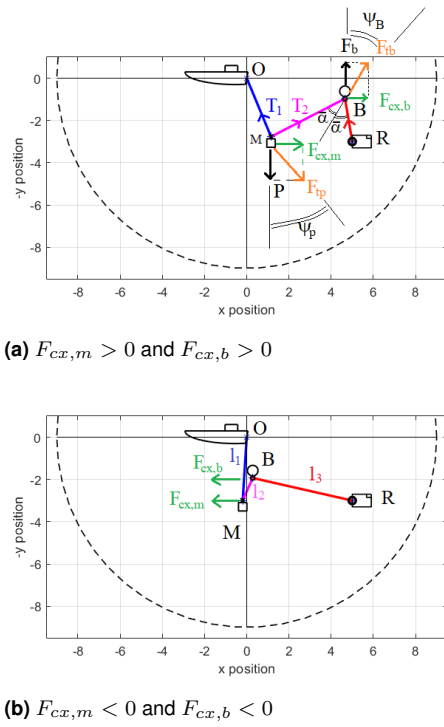


Figure 10. Parameters for Sea Exploration with current. M is the fixed ballast, B is the sliding buoys, such $P = 3.4F_b$ and $F_{cx,m} = F_{cx,b} = 0.5F_b$. The blue, magenta, red lines correspond to l_1, l_2, l_3 . Black dash line: area where the ROV can move due to the umbilical length.

knot in the umbilical, or simply obstruct the displacement of the buoy on the umbilical, making the umbilical self-management strategy invalid. Area F must therefore be avoid by the ROV like area C. As illustrated in Figure 11, area F is superposed with the other areas A, B, C, and D2: the area F has priority over the other areas to avoid cables crossing, except the area D2 where $l_2 = 0$ and so no knot can happen.

Figure 24 in Appendix illustrates the evolution of the areas with the current strength.

6.2 Dynamic model with horizontal current

In this section, the ROV is supposed to be inside the area A. Results exposed here are not valid in others areas, which will be studied in next sections.

Let add the presence of horizontal current $F_{cx,m}$ and $F_{cx,b}$ to the strengths studying in Section 5.2. The unknown parameters are still l_2, l_3, α, β and γ , with 4 equations provided by (18)-(21), one equation missing to solve the system. Let perform the fundamental principle of static on M and B illustrated in Figure 10 (a):

$$\Sigma_M \vec{F} = P\vec{y} + \vec{T}_1 + \vec{T}_2 + \vec{F}_{cx,m} \quad (65)$$

$$\Sigma_B \vec{F} = -F_b\vec{y} - \vec{T}_3 - \vec{T}_2 + \vec{F}_{cx,b} \quad (66)$$

which can be rewritten such as

$$\Sigma_M \vec{F} = \vec{F}_{tm,x} + \vec{T}_1 + \vec{T}_2 \quad (67)$$

$$\Sigma_B \vec{F} = \vec{F}_{tb,x} - \vec{T}_3 - \vec{T}_2 \quad (68)$$

Following Appendix C.1, one gets

$$F_{tm,x} \frac{\sin(\Gamma)}{\sin(\Gamma + B + \Delta\psi_x)} = F_{tb,x} \frac{\sin(B)}{\sin(2B)}. \quad (69)$$

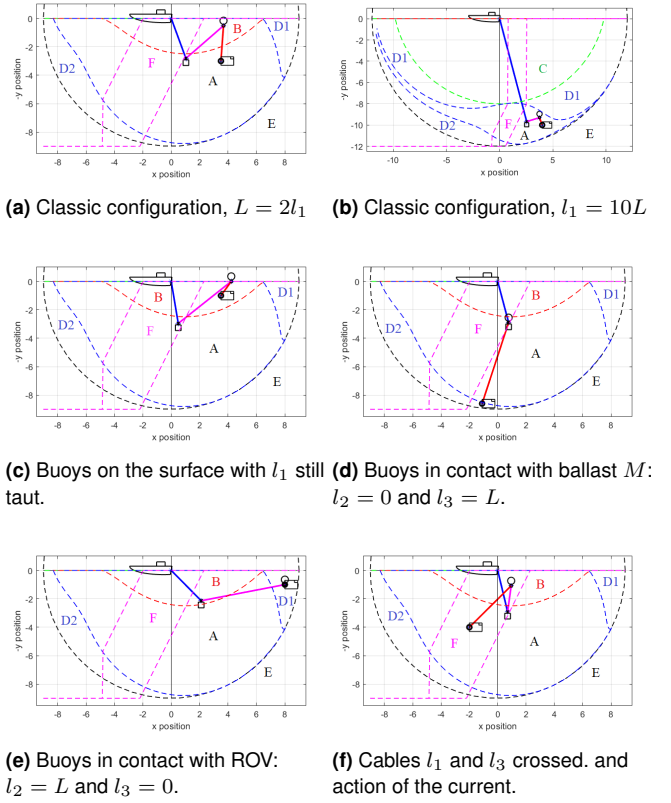


Figure 11. The different areas for Sea Exploration with current. M : fixed ballast, B : sliding buoys. $P = 3F_b$, and $F_{cx,m} = F_{cx,b} = 0.5F_b$. Black dash line: area where the ROV can move due to the umbilical length. Note the area B does not exist in sub-figure b where $L < l_1$ and area C does not exist in sub-figure where $L > l_1$.

and

$$\tan(B) = \frac{\left(2 \frac{F_{tm,x}}{F_{tb,x}} - \cos(\Delta\psi_x)\right) \tan(\Gamma) - \sin(\Delta\psi_x)}{\cos(\Delta\psi_x) - \tan(\Gamma) \sin(\Delta\psi_x)}. \quad (70)$$

with $\Gamma = \gamma - \psi_{P,x}$, $B = \beta - \psi_{B,x}$ and $\Delta\psi_x = \psi_{P,x} - \psi_{B,x}$. Note if $F_{cx,m} = 0$ and $F_{cx,b} = 0$, one has $\psi_{P,x} = 0$ and $\psi_{B,x} = 0$, so (70) is equal to (25).

6.3 Evaluation of the areas in presence of current

The presence of currents changes the shape of areas exposed in previous Section 5.4. This section presents the new boundaries of areas B, C, D1, D2 and E, solved analytically when it is possible, numerically else. Let note $\alpha_A, \beta_A, \gamma_A, l_{2A}, l_{3A}$ the value of $\alpha, \beta, \gamma, l_2, l_3$ inside the area A, which will be evaluated in Section 6.4.

6.3.1 Boundaries of areas B, D1 and D2: numerical approach

Due to the strong non-linearity of the relation (70), only a numerical approach has been found to find a boundary of areas B, D1 and D2. However, since these areas are not required for the ROV control but only for the umbilical model, the numerical approach is less constraining than for the areas C and F.

The proposed method is similar for the three areas. Several values of γ are chosen to scan the entire interval $I_\gamma = \left[-\frac{\pi}{2} + \psi_{P,x}, \frac{\pi}{2} - \psi_{P,x}\right]$. Since areas B, D1 and D2 are at the boundary of area A, the value of β and α are evaluated using (64) and (70) for each value of γ chosen inside I_γ . Using the obtained values of α , β and γ , one deduces the value of l_2 and l_3 such

- **Area B:** the buoy is in contact with the surface, so $y = l_3 \cos(\beta)$,
 $l_2 = \min\left(L, \max\left(l_1 \frac{\cos(\gamma)}{\cos(\alpha)}, 0\right)\right)$ and $l_3 = L - l_2$.
- **Area D1:** the buoy is in contact with the ROV, so $l_2 = L$ and $l_3 = 0$.
- **Area D2:** the buoy is in contact with the ballast, so $l_2 = 0$ and $l_3 = L$.

Using the parameters $\alpha, \beta, \gamma, l_2$ and l_3 , one gets the boundary $y_{area B}$, $y_{area D1}$ and $y_{area D2}$ using (19), associated to a value of x evaluated using (18). By storing the couple (x, y) in a tabular, the boundaries can be found and drawn as illustrated in Figures 11 and 12.

Note the evaluation of boundaries of area B, D1 and D2 are not necessary to consider their influence in the model (18)-(20). Indeed, using α_A, β_A and l_{3A} which will be evaluated with Theorem 3 in Section 6.4, one can deduce

- if $y \geq l_{3A} \cos(\beta_A)$, the ROV is inside the area B,
- if $y \leq l_1 \cos(\gamma_A) - L \cos(\alpha_A)$, The ROV is inside the area D1 Then, the current value of α and γ can be evaluated using Theorem 2 (3),
- if $y \geq l_1 \cos(\gamma_A) - L \cos(\beta_A)$, the ROV is inside the area D2. Then, the current value of β and γ can be evaluated using Theorem 2 (4).

6.3.2 Boundary of area C

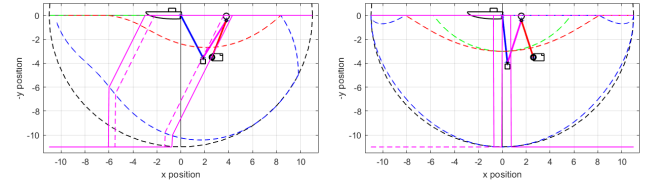
Since the ballast and the buoy are pushed in the same direction than the current, the area C does not exist theoretically when $L > l_1$ because the umbilical can always be stretched by the current. In opposite, the case $L < l_1$ stay unchanged because the buoy cannot reach the surface while stretch the both part of the umbilical. Following step from Appendix C.2.1 and in presence of horizontal current, $y_{area C}(x)$ can be expressed as

$$y_{area C}(x) = \begin{cases} \sqrt{l_1^2 - x^2} - L & \text{if } (|x| < \sqrt{l_1^2 - L^2}) \& (l_1 > L), \\ 0 & \text{else} \end{cases} \quad (71)$$

It is however recommended to use the area C described in Section 5 for the case without horizontal current in practice.

6.3.3 Boundary of area F

The area F can be defined in presence of horizontal current, corresponding to area where cables l_1 and l_3 are crossed. There are two boundaries between the areas A-F, the first corresponding to $|\alpha - \beta| = 0$, the second $|\alpha - \gamma| = 0$. To take into account the rigidity of the umbilical and consider a safety margin, the area F is evaluated for $|\alpha - \beta| = \theta_{\min}$ and $|\alpha - \gamma| = \theta_{\min}$, where $\theta_{\min} \geq 0$ is the value defined in (53) in Section 5.6. Figure 12 illustrates the area F for $\theta_{\min} = 10^\circ$.



(a) $F_{cx,m} = F_{cx,b} = 0.5F_b$ (b) $F_{cx,m} = F_{cx,b} = 0$

Figure 12. Area F with $\theta_{\min} = 10^\circ$. The plain magenta line corresponds to the area F with $\theta_{\min} = 10^\circ$ and the dash magenta line to the area F with $\theta_{\min} = 0$.

Following step from Appendix C.2.2, the ROV is inside the area F if $y_{area F1} \leq y \leq y_{area F2}$ where $y_{area F1}$ and $y_{area F2}$ can be expressed such

$$y_{area F1}(x) = \begin{cases} l_1 \cos(\gamma_F) - (L - l_{33}) \cos(\psi_{B,x} + \frac{\theta_{\min}}{2}s) \\ + l_{33} \cos(\psi_{B,x} - \frac{\theta_{\min}}{2}s) & \text{if } 0 \leq l_{33} \leq L \\ l & \text{if } l_{33} > L \\ 0 & \text{else,} \end{cases} \quad (72)$$

$$y_{area F2}(x) = \begin{cases} l_1 \cos(\psi_{P,x} + \frac{\theta_{\min}}{2}s) - l_{22} \cos(\psi_{P,x} + \frac{\theta_{\min}}{2}s) \\ + (L - l_{22}) \cos(2\psi_{B,x} - \psi_{P,x} - \frac{\theta_{\min}}{2}s) & \text{if } 0 \leq l_{22} \leq L \\ l & \text{if } (l_{22} < 0) \& (l_{33} \geq L) \\ 0 & \text{else} \end{cases} \quad (73)$$

where γ_F can be evaluated with (70) using $\beta = \psi_{B,x} - \frac{\theta_{\min}}{2}s$, and

$$l_{22} = \frac{l_1 \sin(\psi_{P,x} + \frac{\theta_{\min}}{2}s) + L \sin(2\psi_{B,x} - \psi_{P,x} + \frac{\theta_{\min}}{2}s) - x}{\sin(2\psi_{B,x} - \psi_{P,x} + \frac{\theta_{\min}}{2}s) + \sin(\psi_{P,x} - \frac{\theta_{\min}}{2}s)} \quad (74)$$

$$l_{33} = \frac{x - l_1 \sin(\gamma_{F1}) + L \sin(\psi_{B,x} + \frac{\theta_{\min}}{2}s)}{\sin(\psi_{B,x} + \frac{\theta_{\min}}{2}s) + \sin(\psi_{B,x} - \frac{\theta_{\min}}{2}s)} \quad (75)$$

with $s = \text{sign}(\psi_{B,x})$ if $\psi_{B,x} \neq 0$, $s = -\text{sign}(x)$ else.

Remark if there is no current, i.e. $F_{cx,m} = F_{cx,b} = 0$, and $\theta_{\min} > 0$, the area F corresponds to $[-x_{\min}, x_{\min}]$, where x_{\min} is evaluated using (52) exposed in Section 5.6 to guarantee the absence of collision in the umbilical due to the rigidity of the cable. Finally, remark the area F stops always when it reaches the area D2. Indeed, no knot can be made between l_2 and l_3 or between l_2 and l_1 when $l_2 = 0$.

6.4 Numerical solution of umbilical model

In opposite with the case without current studied in Section 5.3, the strong non-linearity of the relation (70) makes the system (18)-(20) too complex to be solved analytically.

Theorem 3 proposes a numerical solution of system (18)-(20) and values of parameters $\gamma, \alpha, \beta, l_2$ and l_3 inside the

area A. Let note $\alpha_A, \beta_A, \gamma_A, l_{2A}, l_{3A}$ the evaluations of $\alpha, \beta, \gamma, l_2, l_3$ inside the area A described in the following theorem.

Theorem 3. Consider the system (18)-(20) with (x, y) such $|x| \leq l$ and $0 \leq y \leq l$ and suppose (x, y) are inside the area A. Considering also the assumption A8 and presence of horizontal current, i.e. (70) and (64). The parameters $\gamma = \gamma_A$ and $l_3 = l_{3A}$ where $\gamma_A \in [-\frac{\pi}{2}, \frac{\pi}{2}]$ and $l_{3A} \in [0, L]$ are the solutions of the system

$$\begin{cases} x = l_1 \sin(\gamma_A) - l_2 \sin(\alpha_A) + l_{3A} \sin(\beta_A) \\ y = l_1 \cos(\gamma_A) - l_2 \cos(\alpha_A) + l_{3A} \cos(\beta_A) \end{cases} \quad (76)$$

with

$$\beta_A = \psi_{B,x} + \operatorname{atan} \left(\frac{\left(2 \frac{F_{tm,x}}{F_{tb,x}} - \cos(\Delta\psi_x) \right) \tan(\gamma_A - \psi_{P,x}) - \sin(\Delta\psi_x)}{\cos(\Delta\psi_x) - \tan(\gamma_A - \psi_{P,x}) \sin(\Delta\psi_x)} \right) \quad (77)$$

$$\text{and } l_2 = L - l_{3A}, \alpha_A = 2\psi_{B,x} - \beta_A.$$

Consider now the system inside the area B. Since the buoy reaches the surface, one has $y = l_3 \cos(\beta)$. Due to the current, the umbilical can always be taut, but the relation (64) does not hold because the buoy is not on the ellipse \mathcal{E}_2 in this configuration. Theorem 4 proposes a numerical solution of system (18)-(20) and values of parameters $\gamma, \alpha, \beta, l_2$ and l_3 in all areas.

Theorem 4. Consider the system (18)-(20) with (x, y) and such $y_{area E}(x) > y$, i.e. the configuration is possible. Considering also the assumption A8 and presence of horizontal current. Let β_A, γ_A and l_{3A} be the value of β, γ and l_3 estimated using Theorem 3 for the couple (x, y) . Consider the following cases:

(1) if $y < y_{area C}(x)$, the ROV is inside the area C, so the model (18)-(20) is not valid.

(2) if $y < l_{3A} \cos(\beta_A)$, the ROV is inside the area B and $\alpha = \alpha_B, \beta = \beta_B, \gamma = \gamma_B$ where

$$\alpha_B \in \left[-\frac{\pi}{2}, \frac{\pi}{2} \right] \quad (79)$$

$$\beta_B \in \begin{cases} [-\pi, 0] & \text{if } F_{cx} < 0 \\ [0, \pi] & \text{else.} \end{cases} \quad (80)$$

$$\gamma_B \in \begin{cases} [\psi_{P,x}, \frac{\pi}{2}] & \text{if } (F_{cx} > 0) \& (x > 0) \\ [-\frac{\pi}{2}, \psi_{P,x}] & \text{if } (F_{cx} < 0) \& (x < 0) \\ [-\frac{\pi}{2}, \frac{\pi}{2}] & \text{else.} \end{cases} \quad (81)$$

are the solutions of the system

$$\begin{cases} x = l_1 \sin(\gamma_B) - l_2 \sin(\alpha_B) + l_3 \sin(\beta_B) \\ y = l_3 \cos(\beta_B) \\ 0 = \frac{F_{tb,x}}{F_{tm,x}} \sin(\beta_B - \psi_{B,x}) \sin(\gamma_B - \alpha_B) \\ - \sin(\gamma_B - \psi_{P,x}) \sin(\beta_B - \alpha_B) \end{cases} \quad (82)$$

with $l_2 = l_1 \frac{\cos(\gamma_B)}{\cos(\alpha_B)}, l_3 = L - l_2$.

(3) if $y > l_{3A} \cos(\beta_A)$ and $y \leq l_1 \cos(\gamma_A) - L \cos(\alpha_A)$, the ROV is inside the area D1 with $l_2 = L, l_3 = 0, \beta = 0$ and values of α, γ can be evaluated using Theorem 2 (3).

(4) if $y > l_{3A} \cos(\beta_A)$ and $y \geq l_1 \cos(\gamma_A) - L \cos(\beta_A)$, the ROV is inside the area D2 with $l_2 = 0, l_3 = L, \alpha = 0$ and values of β, γ can be evaluated using Theorem 2 (4).

(5) else, the ROV is inside the area A with $\beta = \beta_A, \gamma = \gamma_A$ and $l_3 = l_{3A}$, and other parameters can be evaluated using Theorem 3.

Again, if Theorem 4(1) is true, ROV must dive to $y = y_{area C}(x)$ to make the system valid. In addition, if the ROV is inside the area F and not inside the area D2 simultaneously, it is strongly recommended to leave it by the same side the ROV is entered to avoid the creation of a knot. Remark Theorem 4 is valid in area F, this area pointing only if the umbilical makes knot or not.

6.5 Forces applied on the ROV with presence of current

This section extends results of Section 5.8 by considering the presence of currents. Remind $\vec{F}_{cable \rightarrow ROV}$ is the strength applied by the umbilical on the ROV. Excluding the ROV propulsion, the sum $F_{ROV,x}$ and $F_{ROV,y}$ of the external strengths applied on the ROV on axis Ox and Oy can be expressed as

$$\vec{F}_{ROV,x} = (-T_3 \sin(\beta) + F_{cx,ROV}) \vec{x} \quad (83)$$

$$\vec{F}_{ROV,y} = (T_3 \cos(\beta) + F_{cy,ROV}) \vec{y} \quad (84)$$

where $F_{cx,ROV}$ and $F_{cy,ROV}$ are the strengths of the horizontal and vertical currents applied on the ROV and T_3 has been introduced in Section 6.2.

Following step of Appendix D, the strengths $F_{ROV,x}$ and $F_{ROV,y}$ can be expressed as

$$\vec{F}_{ROV,x} \cdot \vec{x} = - \left(F_{tb,x} \frac{\cos(2\psi_{B,x} - \beta)}{2 \cos(\beta - \psi_{B,x})} - F_{cx,b} \right) \tan(\beta) + F_{cx,ROV} \quad (85)$$

$$\vec{F}_{ROV,y} \cdot \vec{y} = F_{tb,x} \frac{\cos(2\psi_{B,x} - \beta)}{2 \cos(\beta - \psi_{B,x})} - F_{cx,b} + F_{cy,ROV}. \quad (86)$$

7 Umbilical for Sea exploration: 3D case with currents

In this section, the 3-Dimensionnal case with presence of horizontal current is studied, 3D case without current already exposed in Section 5.7. This case is more complex and can be solved only using numerical method.

7.1 Geometrical model

The 3D case introduces new degrees of freedom, described by parameters defined in the plans $P_{oxy} = (O, x, y)$ and $P_{ozy} = (O, z, y)$. Let γ and ϕ be respectively the angles between the boat and the ballast M in P_{oxy} and P_{ozy} , α and μ be the angles between the ballast and the buoy in P_{oxy} and P_{ozy} , and β and η be the angles between the buoy and the ROV in P_{oxy} and P_{ozy} . The length l_{1x} and l_{1z} are the projections of l_1 on P_{oxy} and P_{ozy} , same for l_{2x}, l_{2z}, l_{3x} and l_{3z} . All these parameters are illustrated in the Figure 13.

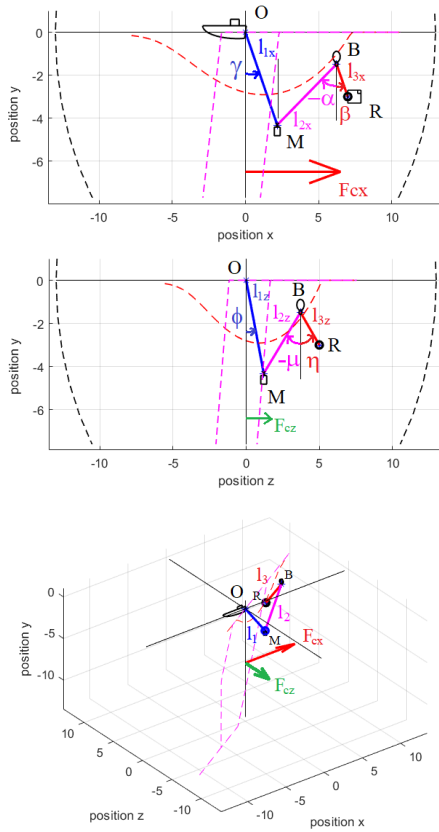


Figure 13. Parameters for Sea Exploration with current in 3D case, for $(x, y, z) = (5, 2.5, 3)$. M : fixed ballast. B : sliding buoys. The blue, magenta, red lines correspond to l_1, l_2, l_3 . Black dash line: area where the ROV can move due to the umbilical length. Red and green arrows: horizontal currents F_{cx} and F_{cz} in direction \vec{Ox} and \vec{Oz} with $F_{cx} = 3F_{cz}$.

In a configuration where the umbilical is taut, and using the coordinates of the ROV, the system can be expressed such

$$x = l_{1x} \sin(\gamma) - l_{2x} \sin(\alpha) + l_{3x} \sin(\beta) \quad (87)$$

$$y = l_{1x} \cos(\gamma) - l_{2x} \cos(\alpha) + l_{3x} \cos(\beta) \quad (88)$$

$$z = l_{1z} \sin(\phi) - l_{2z} \sin(\mu) + l_{3z} \sin(\eta) \quad (89)$$

with

$$l_1^2 = l_{1x}^2 + \sin(\phi)^2 l_{1z}^2 \quad (90)$$

$$l_2^2 = l_{2x}^2 + \sin(\mu)^2 l_{2z}^2 \quad (91)$$

$$l_3^2 = l_{3x}^2 + \sin(\eta)^2 l_{3z}^2 \quad (92)$$

$$L = l_2 + l_3 \quad (93)$$

Let expressed (x_M, y_M, z_M) the coordinate of the ballast M , $L_x = l_{1x} + l_{2x}$ and $L_z = l_{1z} + l_{2z}$. Since the buoy is still moving freely on the umbilical, its position is on

- the ellipse \mathcal{E}_2 of centers M and R with the two radius $\frac{L_x}{2}$ and $\sqrt{\left(\frac{L_x}{2}\right)^2 - \frac{(x-x_M)^2 + (y-y_M)^2}{4}}$ in P_{oxy} ,
- the ellipse \mathcal{E}_3 of centers M and R with the two radius $\frac{L_z}{2}$ and $\sqrt{\left(\frac{L_z}{2}\right)^2 - \frac{(z-z_M)^2 + (y-y_M)^2}{4}}$ in P_{ozy} .

Thus, since the buoy does not touch the surface (not inside area B and C), these properties lead to

$$\alpha = 2\psi_{B,x} - \beta \quad (94)$$

$$\mu = 2\psi_{B,z} - \eta \quad (95)$$

where $\psi_{B,x}$ has been defined in Section 6.1 in P_{oxy} and $\psi_{B,z}$ is the orientation of the strength $F_{tb,z}$, similarly to $\psi_{B,x}$ but inside P_{ozy} , which will be described in Section 7.2.

7.2 Study of the dynamic model

Let $F_{cx,m}$ and $F_{cx,b}$ be the strengths of the horizontal current applied on the ballast M and buoy B on the axis \vec{Ox} , as exposed in Section 6.1. Since they exist only in P_{oxy} , the strengths applied on the system in P_{oxy} are similar to the 2D case studied in Section 6.1 and 6.2.

Let $F_{cz,m}$ and $F_{cz,b}$ be the strengths of the horizontal current applied on the ballast M and buoy B on the axis \vec{Oz} such $F_{cz,m} > 0$ corresponds to a current in the direction \vec{Oz} , same for $F_{cz,b}$, as illustrated on Figure 13. These ones exist only in P_{ozy} . Let also define the sums of strengths $F_{tm,z}$ and $F_{tb,z}$ such

$$F_{tm,z} = \sqrt{P^2 + F_{cz,m}^2} \quad (96)$$

$$F_{tb,z} = \sqrt{F_b^2 + F_{cz,b}^2} \quad (97)$$

with their incidence angles

$$\tan(\psi_{P,z}) = \frac{F_{cz,m}}{P} \quad (98)$$

$$\tan(\psi_{B,z}) = -\frac{F_{cz,b}}{F_b}. \quad (99)$$

When the buoy does not touch the surface, the relations (70) linking $F_{tm,x}$, $F_{tb,x}$, γ and β are still valid in the plan P_{oxy} . Following the same steps than in Section 6.1, 6.2 and Appendix C.1, one may write

$$F_{tm,z} \frac{\sin(\Phi)}{\sin(\Phi + H + \Delta\psi_z)} = F_{tb,z} \frac{\sin(H)}{\sin(2H)} \quad (100)$$

and

$$\tan(H) = \frac{\left(2 \frac{F_{tm,z}}{F_{tb,z}} - \cos(\Delta\psi_z)\right) \tan(\Phi) - \sin(\Delta\psi_z)}{\cos(\Delta\psi_z) - \tan(\Phi) \sin(\Delta\psi_z)} \quad (101)$$

with $\Phi = \phi - \psi_{P,z}$, $H = \eta - \psi_{B,z}$ and $\Delta\psi_z = \psi_{P,z} - \psi_{B,z}$. Note if $F_{cz,m} = F_{cz,b} = 0$, one has $\psi_{P,z} = \psi_{B,z} = 0$, and so (95) is equal to $\mu = -\eta$ and (101) is equal to $\tan(\eta) = \left(2 \frac{F_{tm,z}}{F_{tb,z}} - 1\right) \tan(\phi)$.

7.3 Numerical solution of umbilical model

The system (87)-(89) have 14 unknown parameters: $l_{1x}, l_{1z}, l_{2x}, l_{2z}, l_{3x}, l_{3z}, l_2, l_3, \alpha, \beta, \gamma, \phi, \mu, \eta$. Enough equations must be found to solve the system, and a small number of variables must be selected to obtain a numerical resolution with a reduced computing time. Using relations found in previous sections and other presented in this section, the Theorem 5 proposes a numerical resolution of system (87)-(89) using only variables γ, ϕ, l_3 .

Following steps described in Appendix E.1, one can obtain

$$l_{1x}^2 = \frac{l_1^2}{\left(1 + \tan(\phi)^2 \cos(\gamma)^2\right)} \quad (102)$$

$$l_{1z}^2 = \frac{l_1^2}{\left(\sin(\phi)^2 + \left(\frac{\cos(\phi)}{\cos(\gamma)}\right)^2\right)} \quad (103)$$

and the same for l_{2x}, l_{2z} and l_{3x}, l_{3z} replacing l_1, γ, ϕ by l_2, α, μ and l_3, β, η .

Using (102)-(103) and their equivalent for $l_{2x}, l_{2z}, l_{3x}, l_{3z}$, the system (87)-(89) has now only 8 unknown parameters: $l_2, l_3, \alpha, \beta, \gamma, \phi, \mu, \eta$. (93) solves $l_2 = L - l_3$ and (94)-(95) express β, η with α, μ , leaving 5 unknown parameters. (70) and (101) provide two other relations to express β, η with γ, ϕ . The system (87)-(89) provide the last three equations, to solve for the variables γ, ϕ, l_3 .

Theorem 5. Consider the system (87)-(89) with (x, y, z) such $|x| \leq l, |z| \leq l$ and $0 \leq y \leq l$ not inside the areas B and C. Considering also the assumption A8 and presence of horizontal current. The parameters γ, ϕ, l_3 such

$$\gamma \in \begin{cases} [\psi_{P,x}, \frac{\pi}{2}] & \text{if } (F_{cx} > 0) \& (x > 0) \\ [-\frac{\pi}{2}, \psi_{P,x}] & \text{if } (F_{cx} < 0) \& (x < 0) \\ [-\frac{\pi}{2}, \frac{\pi}{2}] & \text{else.} \end{cases} \quad (104)$$

$$\phi \in \begin{cases} [\psi_{P,z}, \frac{\pi}{2}] & \text{if } (F_{cz} > 0) \& (z > 0) \\ [-\frac{\pi}{2}, \psi_{P,z}] & \text{if } (F_{cz} < 0) \& (z < 0) \\ [-\frac{\pi}{2}, \frac{\pi}{2}] & \text{else.} \end{cases} \quad (105)$$

$$l_3 \in [0, L] \quad (106)$$

are the solutions of the system

$$\begin{cases} x = l_{1x} \sin(\gamma) - l_{2x} \sin(\alpha) + l_{3x} \sin(\beta) \\ y = l_{1x} \cos(\gamma) - l_{2x} \cos(\alpha) + l_{3x} \cos(\beta) \\ z = l_{1z} \sin(\phi) - l_{2z} \sin(\mu) + l_{3z} \sin(\eta) \end{cases} \quad (107)$$

with

$$\beta = \psi_{B,x} + \operatorname{atan} \left(\frac{\left(2 \frac{F_{tm,x}}{F_{tb,x}} - \cos(\Delta\psi_x) \right) \tan(\gamma - \psi_{P,x}) - \sin(\Delta\psi_x)}{\cos(\Delta\psi_x) - \tan(\gamma - \psi_{P,x}) \sin(\Delta\psi_x)} \right) \quad (108)$$

$$\eta = \psi_{B,z} + \operatorname{atan} \left(\frac{\left(2 \frac{F_{tm,z}}{F_{tb,z}} - \cos(\Delta\psi_z) \right) \tan(\phi - \psi_{P,z}) - \sin(\Delta\psi_z)}{\cos(\Delta\psi_z) - \tan(\phi - \psi_{P,z}) \sin(\Delta\psi_z)} \right) \quad (109)$$

where (α, μ) are evaluated using (94)-(95), $l_2 = L - l_3$, (l_{1x}, l_{1z}) evaluated using (102)-(103), and (l_{2x}, l_{2z}) and (l_{3x}, l_{3z}) evaluated similarly to (l_{1x}^2, l_{1z}^2) using l_2, α, μ and l_3, β, η .

The Theorem 5 does not consider specific cases for the areas D1 and D2 because these configurations can be solved by taking $l_3 = 0$ or $l_3 = L$ if required. Since the Theorem 5 provides a solution only outside the areas B and C, the following Theorem 6 describes the solution of the system in all cases. Let define l_{3xA} and β_A the evaluation of l_{3x} and β by Theorem 5.

Theorem 6. Consider the system (87)-(89) with (x, y, z) such $|x| \leq l, |z| \leq l$ and $0 \leq y \leq l$ inside the area B. Considering also the assumption A8 and presence of horizontal current. If $y < l_{3xA} \cos(\beta_A)$, the ROV is inside

the area B and $\alpha_B, \beta_B, \gamma_B, \phi_B, \mu_B$ and η_B where

$$\alpha_B \in \left[-\frac{\pi}{2}, \frac{\pi}{2}\right], \quad \mu_B \in \left[-\frac{\pi}{2}, \frac{\pi}{2}\right] \quad (110)$$

$$\beta_B \in \begin{cases} [-\pi, 0] & \text{if } F_{cx} < 0 \\ [0, \pi] & \text{else.} \end{cases}, \quad \eta \in \begin{cases} [-\pi, 0] & \text{if } F_{cz} < 0 \\ [0, \pi] & \text{else.} \end{cases} \quad (111)$$

$$\gamma_B \in \begin{cases} [\psi_{P,x}, \frac{\pi}{2}] & \text{if } (F_{cx} > 0) \& (x > 0) \\ [-\frac{\pi}{2}, \psi_{P,x}] & \text{if } (F_{cx} < 0) \& (x < 0) \\ [-\frac{\pi}{2}, \frac{\pi}{2}] & \text{else.} \end{cases} \quad (112)$$

$$\phi_B \in \begin{cases} [\psi_{P,z}, \frac{\pi}{2}] & \text{if } (F_{cz} > 0) \& (z > 0) \\ [-\frac{\pi}{2}, \psi_{P,z}] & \text{if } (F_{cz} < 0) \& (z < 0) \\ [-\frac{\pi}{2}, \frac{\pi}{2}] & \text{else.} \end{cases} \quad (113)$$

are the solutions of the system

$$\begin{cases} x = l_{1x} \sin(\gamma_B) - l_{2x} \sin(\alpha_B) + l_{3x} \sin(\beta_B) \\ z = l_{1z} \sin(\phi_B) - l_{2z} \sin(\mu_B) + l_{3z} \sin(\eta_B) \\ 0 = l_{2x} \cos(\alpha_B) - l_{1x} \cos(\gamma_B) \\ 0 = l_{2z} \cos(\mu_B) - l_{1z} \cos(\phi_B) \\ 0 = \frac{F_{tb,x}}{F_{tm,x}} \sin(\beta_B - \psi_{B,x}) \sin(\gamma_B - \alpha_B) \\ - \sin(\gamma_B - \psi_{P,x}) \sin(\beta_B - \alpha_B) \\ 0 = \frac{F_{tb,z}}{F_{tm,z}} \sin(\eta_B - \psi_{B,z}) \sin(\phi_B - \mu_B) \\ - \sin(\phi_B - \psi_{P,z}) \sin(\eta_B - \mu_B) \end{cases} \quad (114)$$

where $l_{3x} = \frac{y}{\cos(\beta_B)}$, $l_{3z} = \frac{y}{\cos(\eta_B)}$, $l_3 = \sqrt{l_{3x}^2 + l_{3z}^2}$, $l_2 = L - l_3$, (l_{1x}, l_{1z}) evaluated using (102)-(103), and (l_{2x}, l_{2z}) evaluated similarly to (l_{1x}^2, l_{1z}^2) using l_2, α, μ .

7.4 Evaluation of the areas in 3D

To evaluate the areas in 3D case with presence of horizontal current, numerical approaches similar to those from Section 6.3 can be used. However, in order to obtain a fast computation, approximations of the areas B, C, F are proposed here. These approximate areas are sufficient requirements to guarantee the umbilical is taut and absence of knot. Areas D1 and D2 are not studied because useless for Theorems 5 and 6 and the control of the ROV. Area E is of course unchanged.

Let $F_{c,m} = \sqrt{F_{cx,m}^2 + F_{cz,m}^2}$ and $F_{c,b} = \sqrt{F_{cx,b}^2 + F_{cz,b}^2}$ be the sum of the horizontal currents applied on the ballast and the buoy, associated to orientations $\zeta_m = \operatorname{atan}\left(\frac{F_{cz,m}}{F_{cx,m}}\right)$ and $\zeta_b = \operatorname{atan}\left(\frac{F_{cz,b}}{F_{cx,b}}\right)$. Let define also $\varepsilon = \operatorname{atan}\left(\frac{z}{x}\right)$ the orientation of the ROV projected on the plan (O, x, z) .

The lengths $\mathcal{L}_{xz} = \{l_{1x}, l_{1z}, l_{2x}, l_{2z}, l_{3x}, l_{3z}\}$ are respectively smallest or equal to l_1, l_2 and l_3 . When $\varepsilon = \zeta_m = \zeta_b$, the 3D case can be assimilated to a 2D case in the plan (O, \vec{OR}, \vec{Oy}) with $F_{c,m}$ and $F_{c,b}$ as horizontal currents. In the same way, when $\cos(\varepsilon - \zeta_m) = \cos(\varepsilon - \zeta_b) = 0$, the horizontal currents push the ballast upward and the sliding buoy downward perpendicularly to the plan, reducing values of \mathcal{L}_{xy} without influencing their position in the direction \vec{OR} : the 3D case can so be assimilated to a 2D case in the plan (O, \vec{OR}, \vec{Oy}) without horizontal current and with shorter lengths l_1, l_2 and l_3 .

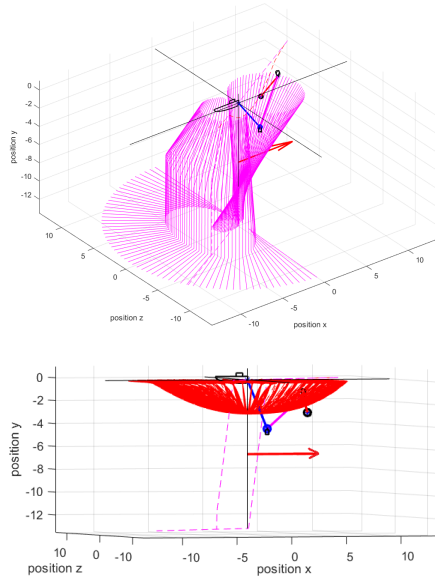


Figure 14. Approximate areas F (magenta) and B (red) in the 3D case.. The red arrow: horizontal current $F_{c,m} = F_{c,b}$

Considering previous points, 3D areas B, C and F can so be upper-bounded such

$$y_{area B} \leq \bar{y}_{area B} \quad (115)$$

$$y_{area C} \leq \bar{y}_{area C} \quad (116)$$

$$y_{area F1} \leq \bar{y}_{area F1} \quad (117)$$

$$y_{area F2} \leq \bar{y}_{area F2} \quad (118)$$

where $\bar{y}_{area B}$, $\bar{y}_{area C}$, $\bar{y}_{area F1}$ and $\bar{y}_{area F2}$ are evaluated using the expression of $y_{area B}$, $y_{area F1}$ and $y_{area F2}$ exposed in Section 6.3 by replacing x by $d = \sqrt{x^2 + y^2}$, and replacing $F_{cx,m}$ and $F_{cx,b}$ by $\bar{F}_{cx,m}$ and $\bar{F}_{cx,b}$ such

$$\bar{F}_{cx,m} = F_{c,m} \cos(\varepsilon - \zeta_m) \quad (119)$$

$$\bar{F}_{cx,b} = F_{c,b} \cos(\varepsilon - \zeta_b). \quad (120)$$

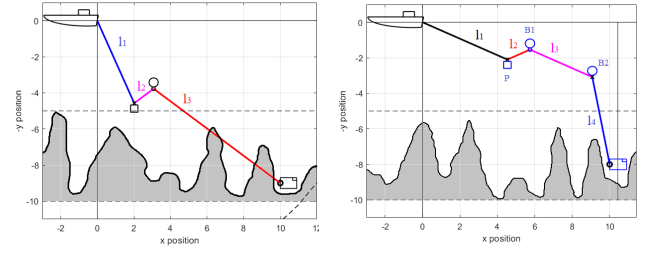
The boundaries $\bar{y}_{area B}$, $\bar{y}_{area F1}$ and $\bar{y}_{area F2}$ provide sufficient requirements for the umbilical to stay taut outside this area B and F without creating knots.

One can observe the area F should theoretically exist only in the plane \mathcal{F} where $\varepsilon = \zeta_m = \zeta_b$, else the projections of cables l_1 , l_2 and l_3 are crossed on (O, \vec{OR}, \vec{Oy}) but not the true cables in the three dimensional space. However, the ROV must bypass the area F to not make a knot when it wants to cross the plane \mathcal{F} (ex: if \mathcal{F} is the plan (O, x, y) , there is a risk of knot if the ROV takes the shortest pass from coordinate $z = 1$ to $z = -1$). The area created by the boundaries $\bar{y}_{area F1}$ and $\bar{y}_{area F2}$ allows to bypass the area F softly without risk of creating a knot, as illustrated in Figure 14.

8 Umbilical for diving exploration with presence of large obstacles

8.1 The main idea

In the strategy exposed in previous sections, the presence of obstacles higher than the minimum seafloor level is



(a) Sea exploration strategy

(b) Diving exploration strategy

Figure 15. Comparison between methods exposed in Section 5 and 8. For the same exploration area $[0, 10] \times [5, 10]$, the diving exploration strategy allows to keep the cable l_4 close to the vertical and so avoid contact with obstacle.

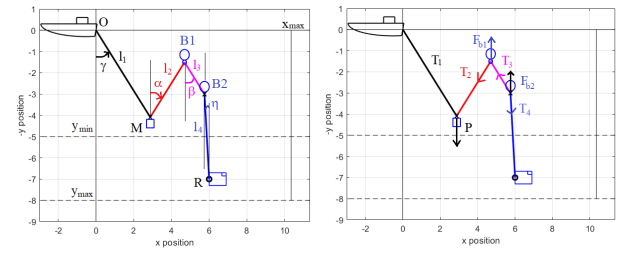


Figure 16. Parameters of diving exploration strategy. M : fixed ballast. $B1$: sliding buoys. $B2$: fixed buoy. $P = F_{b1}$ and $F_{b2} = 63P$. Black dash lines: exploration area where the ROV can move due to the constraint taken for umbilical shape.

not considered. The operator must watch the model of the umbilical and its knowledge of the environment to check if the position of the umbilical does not coincide with the presence of an obstacle. In presence of large/high obstacles on the seafloor, the angles performed by the umbilical can be very restrictive for the navigation and lead to a contact between the umbilical and an obstacle, specifically when the ROV is far from the boat, see Figure 15.

In this section, a third strategy is proposed where the umbilical stays close to the vertical behind the ROV in all situations since it is inside a defined area, allowing to dive vertically without risk of collision between the umbilical and a possible obstacle.

Consider in this configuration an umbilical of length l divided in three parts of fixed lengths: a first part length l_1 between the boat O and a ballast M fixed on the umbilical, *i.e.* $\|OM\| = l_1$, a second part of length L where a first buoy $B1$ can move freely between the ballast and a second fixed buoy $B2$, and finally a third part l_4 between the fixed buoy $B2$ and the ROV, *i.e.* $\|B2R\| = l_4$. Similarly to case studied in Section 4 and 5, the second part of umbilical L can be divided in two lengths $l_2 = \|MB1\|$ and $l_3 = \|B1R\|$ corresponding to the lengths of the right side and left side of the buoy $B1$, such $L = l_2 + l_3$. Let γ be the oriented angle between the boat and the ballast M . α and β are respectively the oriented angles between the ballast and the sliding buoy, and between the sliding buoy and the second buoy. η is the oriented angle between the second buoy and the ROV. Parameters are illustrated in Figure 16.

8.2 Umbilical model solved

In a configuration where the umbilical is taut, the system can be expressed such

$$x = l_1 \sin(\gamma) - l_2 \sin(\alpha) + l_3 \sin(\beta) + l_4 \sin(\eta) \quad (121)$$

$$y = l_1 \cos(\gamma) - l_2 \cos(\alpha) + l_3 \cos(\beta) + l_4 \cos(\eta) \quad (122)$$

$$L = l_2 + l_3. \quad (123)$$

with L , l_1 and l_4 fixed.

The objective is to define a configuration where the ROV can explore an area $[x_{\min}, x_{\max}] \times [y_{\min}, y_{\max}]$ where $\eta \leq \eta_{\max}$ with $\eta_{\max} \geq 0$ is taken small to avoid collision with obstacles.

To respect these objectives, some conditions are taken:

- The minimum depth $y_{\min} > 0$ is chosen such there is no obstacle in the area $[x_{\min}, x_{\max}] \times [0, y_{\min}]$,
- The ballast M and buoys must stay inside $[0, y_{\min}] \times [x_{\min}, x_{\max}]$ to avoid collision with an obstacle, and buoys must not touch the surface. Thus, one takes $L = l_1$, and y_{\min} can be expressed such

$$y_{\min} = \max(l_1 + h_M, l_4) \quad (124)$$

where h_M is the ballast height,

- Since the buoy B_2 must stay inside $[x_{\min}, x_{\max}] \times [0, y_{\min}]$, the maximal depth y_{\max} can be expressed

$$y_{\max} = y_{\min} + l_4, \quad (125)$$

- x_{\min} is evaluated using (52) defined in Section 5.6.
- The ballast M and the buoy B_1 are chosen such $P = F_{b1}$ where P and F_{b1} are defined following Assumptions A4 and A5. The Assumption A8 is respected because $L = l_1$.

Some observations can be made:

- l_1 and l_4 are chosen to satisfy (124) and (125): y_{\min} is favor to avoid collision between ballast/buoys and obstacles, which limits the value of y_{\max} due to (125),
- The system (121)-(123) is designed such the ROV evolves only inside the working area $[x_{\min}, x_{\max}] \times [y_{\min}, y_{\max}]$. Due to the chosen parameters, the areas A, B, C and D1 like in Section 5 is excluded inside the working area, but area D2 exists, as shown in Appendix F.4.
- The horizontal currents are considered absent for this configuration, or small enough to be ignore compare to the ballast and buoys.

The position of the buoy B_2 can be assimilated to the ROV position of the Section 5. In absence of horizontal currents, (21) and (25) are still valid such $\alpha = -\beta$ and $\tan(\beta) = \Lambda_1 \tan(\gamma)$ with $\Lambda_1 = 2 \frac{P}{F_{b1}} - 1 = 1$, so

$$\beta = \gamma. \quad (126)$$

Following steps described in Appendix F.1, it can be shown that

$$\tan(\beta) = \Lambda_2 \tan(\eta) \quad (127)$$

with $\Lambda_2 = 2 \frac{F_{b2}}{F_{b1}} + 1$.

The boundary $y_{area D2}$ can be expressed as

$$y_{area D2}(x) = \max \left(\left[\frac{2L}{\sqrt{1 + \Lambda_2^2 \tan(\eta_A(x))^2}} + l_4 \cos(\eta_A(x)), 0 \right] \right) \quad (128)$$

where $\eta_A(x)$ is evaluated in Theorem 8.

For these conditions, the Theorems 7 and 8 describe the value of parameters γ , α , β , l_2 and l_3 .

Theorem 7. Consider the system (121)-(123) for $x \in [x_{\min}, x_{\max}]$ and $y \in [y_{\min}, y_{\max}]$, where y_{\min} , y_{\max} and x_{\min} are defined following (124)-(125) and (52). Consider also $P = F_{b1}$ and the absence of horizontal current, i.e. (25), (126) and (21), (127). For a chosen $\eta_{\max} \geq 0$, the condition

$$0 \leq \eta \leq \eta_{\max} \quad (129)$$

is satisfied if

$$F_{b2} \geq \frac{F_{b1}}{2} \left(\frac{|x_{\max} - l_4 \sin(\eta_{\max})|}{\tan(\eta_{\max}) \sqrt{4l_1^2 - (x_{\max} - l_4 \sin(\eta_{\max}))^2}} - 1 \right) \quad (130)$$

and

$$x_{\max} \leq (l_1 + L) + l_4 \sin(\eta_{\max}). \quad (131)$$

In these conditions,

1) If $y < y_{area D2}(x)$, one has $\eta = \eta_A$ where η_A can be evaluated following Theorem 8, and

$$\beta = \text{atan}(\Lambda_2 \tan(\eta_A)) \quad (132)$$

$$l_2 = \frac{L + l_1}{2} - \frac{y - l_4 \cos(\eta_A)}{2 \cos(\gamma)} \quad (133)$$

and $l_3 = L - l_2$, $\alpha = -\beta$, $\gamma = \beta$.

2) Else, the ROV is inside the area D2 and one has $\alpha = 0$, $\beta = \gamma$, $l_2 = 0$, $l_3 = L$ and

$$\sin(\gamma) = \frac{a_D b_D + \sqrt{a_D^2 b_D^2 - 4(1 + b_D^2)(a_D^2 - 1)}}{(a_D^2 - 1)} \quad (134)$$

$$\cos(\eta) = \frac{y - 2L \cos(\gamma)}{l_4} \quad (135)$$

where $a_D = \frac{x^2 + y^2 + 4L^2 - l_4^2}{4yL}$ and $b_D = \frac{x}{y}$.

Theorem 8. Consider the conditions exposed in Theorem 7 are respected. Thus, η can be expressed such as

$$\sin(\eta) = \min_{i \in [1,2,3,4]} (|W_i|) \quad (136)$$

where

$$\begin{cases} W_1 = \frac{\sqrt{U_\eta - \frac{2}{3}A_\eta - \sqrt{\Delta_{W1}}}}{2}, & \text{if } \Delta_{W1} \geq 0 \\ W_1 = \infty & \text{else,} \end{cases} \quad (137)$$

$$\begin{cases} W_2 = \frac{\sqrt{U_\eta - \frac{2}{3}A_\eta + \sqrt{\Delta_{W1}}}}{2}, & \text{if } \Delta_{W1} \geq 0 \\ W_2 = \infty & \text{else,} \end{cases} \quad (138)$$

$$\begin{cases} W_3 = \frac{-\sqrt{U_\eta - \frac{2}{3}A_\eta} - \sqrt{\Delta_{W2}}}{2} & \text{if } \Delta_{W2} \geq 0 \\ W_3 = \infty & \text{else,} \end{cases} \quad (139)$$

$$\begin{cases} W_4 = \frac{-\sqrt{U_\eta - \frac{2}{3}A_\eta} + \sqrt{\Delta_{W2}}}{2} & \text{if } \Delta_{W2} \geq 0 \\ W_4 = \infty & \text{else,} \end{cases} \quad (140)$$

$$\text{with } \Delta_{W1} = -\left(U_\eta + \frac{4}{3}A_\eta + \frac{2B_\eta}{\sqrt{U_\eta - \frac{2}{3}A_\eta}}\right), \quad \Delta_{W2} = -\left(U_\eta + \frac{4}{3}A_\eta - \frac{2B_\eta}{\sqrt{U_\eta - \frac{2}{3}A_\eta}}\right), \text{ and}$$

$$A_\eta = -\frac{x^2}{2l_4^2} - \frac{(4l_1^2\Lambda_2^2 - l_4^2)}{l_4^2(\Lambda_2^2 - 1)} \quad (141)$$

$$B_\eta = -\frac{l_4^2 + 4l_1^2\Lambda_2^2}{l_4^3(\Lambda_2^2 - 1)}x \quad (142)$$

$$C_\eta = \frac{x^4}{16l_4^4} + \frac{x^2(l_4^2 - 4l_1^2\Lambda_2^2)}{4l_4^4(\Lambda_2^2 - 1)} \quad (143)$$

$$U_\eta = \begin{cases} \begin{cases} \left(-\frac{q}{2} + \sqrt{\frac{q^2}{4} + \frac{p^3}{27}}\right)^{1/3} \\ + \left(-\frac{q}{2} - \sqrt{\frac{q^2}{4} + \frac{p^3}{27}}\right)^{1/3} \end{cases} & \text{if } \Delta_{U_\eta} > 0, \\ 2 \cos\left(\frac{1}{3}\arccos\left(-\frac{q}{2\sqrt{-\frac{p^3}{27}}}\right)\right)\sqrt{-\frac{p}{3}} & \text{if } \Delta_{U_\eta} < 0, \\ = -\sqrt{-\frac{p}{3}} & \text{if } \Delta_{U_\eta} = 0 \end{cases} \quad (144)$$

$$\text{with } \Delta_{U_\eta} = \frac{q^2}{4} + \frac{p^3}{27}, \quad p = -4C_\eta - \frac{A_\eta^2}{3} \text{ and } q = \frac{2A_\eta^3}{27} + (4A_\eta C_\eta - B_\eta^2) + \frac{-4C_\eta A_\eta}{3}.$$

Proofs of Theorems 7 and 8 are provided in Appendix F.2, F.3 and F.4.4.

8.3 Practical case: Forces applied on the ROV

This section exposes the strengths applied by the umbilical on the ROV, to help to choose the ballast and the buoys within the capabilities of the ROV.

Let $\vec{F}_{cable \rightarrow ROV}$ be the strength apply by the umbilical on the ROV, and $\vec{T}_4 = -\vec{F}_{cable \rightarrow ROV}$ is the tension of the cable l_4 between the buoy $B2$ and the ROV. Let perform the principle of the fundamental principle of static on $B1$ and $B2$:

$$\Sigma_{B1} \vec{F} = -F_{b1}\vec{y} - \vec{T}_3 + \vec{T}_2 \quad (145)$$

$$\Sigma_{B2} \vec{F} = -F_{b2}\vec{y} + \vec{T}_3 + \vec{T}_4 \quad (146)$$

where \vec{T}_2, \vec{T}_3 are the tension on the cable on $B1$ as defined in Section 5.2 and illustrated in Figure 16.

Following Appendix F.5 and since we desire $\eta \leq \eta_{\max}$, the strength applied on the ROV can be bounded such

$$F_{cable \rightarrow ROV} \leq \frac{F_{b2} + \frac{1}{2}F_{b1}}{\cos(\eta_{\max})}. \quad (147)$$

Using (130) and (147) in Theorem 7, the choice of ballast and buoys strengths P , F_{b1} and F_{b2} can be made in function of the maximum strength of the ROV and desired η_{\max} .

8.4 Practical case: choice of umbilical length

To satisfied all constraints exposed in previous sections, the choice of parameters l_1 , L and l_4 is simple:

$$l_1 = y_{\min} - h_M \quad (148)$$

$$l_4 = y_{\max} - y_{\min} \quad (149)$$

$$y_{\min} \leq y_{\max} \leq 2y_{\min}. \quad (150)$$

and $L = l_1 \cdot x_{\max}$ chosen with Theorem 7. Since the choice of y_{\min} restricts all other parameters, y_{\min} must be taken the largest possible.

9 ROV control

The systems exposed in previous sections are studied at the equilibrium. However, each time the ROV dives, rises or backs off, a part of the umbilical becomes temporary loosen. Since a loosen cable can lead to a knot, and the loosen model can be complex and/or heavy to compute, an alternative approach is proposed here by controlling the ROV to make the transitory phases short and the discrepancy between the models studied and the reality small. Thus, the ROV is controlled to move slower than the fall of the ballast and/or the rise of the buoy. As long as their behavior are faster than ROV's velocity, the umbilical stays globally taut.

9.1 Main idea and hypotheses

For this work, the ROV never makes a complete turn on itself and goes backwards to come closer to the position $x = 0$: this assumption reduces the stress inside the umbilical and avoid the formation of knot by twisting. In 2D case, it means the ROV is always oriented in the direction $\vec{O}x$. In 3D case, its mean its yaw orientation ω_{ROV} respected always the following condition

$$\omega_{ROV}\vec{y} \in \left(\omega_{OR} + \left[-\frac{\pi}{2}, \frac{\pi}{2}\right]\right)\vec{y}, \quad (151)$$

where ω_{OR} is the angle between the ROV position and the origin O in the plan (O, x, z) .

The reasoning developed below is performed for the sea exploration strategy developed in Section 5, 6 and 7, but it is also valid for the diving exploration strategy developed in Section 8, and can be easily adapted for surface exploration in Section 4 by replacing the sliding buoy by the sliding ballast.

The three behaviors illustrated in Figure 17 can be observed. When the ROV moves forward, the umbilical is always taut because 1) its displacement is in opposition with the torque created by the ballast, 2) the ellipse created by the system ballast/buoy/ROV becomes flatter, so the strength of the buoy is also opposed to the cable displacement. During the ascent of the ROV or while it is moving backward, the umbilical is temporary loosen between the buoy and the ROV because the movement gives slack to the buoy. Finally, during the ROV dive, the umbilical is temporary loosen between the weight and the buoy because the ballast and the ROV share the same direction while the buoy pushes in the opposite direction, keeping umbilical stretched between them.

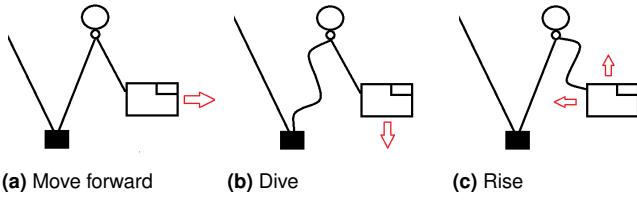


Figure 17. Umbilical is temporary loosen when the ROV dives, rises to surface or backs off. The umbilical is always taut when the ROV moves straight ahead.

When the displacement of the ROV slackens the umbilical, the fall of the ballast and the rise of the buoy try to retighten it. However, the fall of the ballast is constrained by the cable l_1 , making its displacement similar to a pendulum link to the boat. On its side, the buoy is as if released freely in the water when the umbilical is not taut, only submitted by its weight and Archimedes strength. Since the displacement of the ballast is limited when it is close to the vertical position, and so its influence to retighten the umbilical, the control of the ROV will be performed as if the buoy is the only strength which can stretch the umbilical during the transition period. Even if this hypothesis is false in practical case, it gives a sufficient condition to restrict ROV behavior. This hypothesis can be only taken when the ROV is not inside the area B or C, *i.e.* when the buoy does not touch the surface.

When the buoy touches the surface, the umbilical can be stretched only by the ballast and the horizontal current applied on the buoy. Note the ballast's weight is stronger or equal than the buoy's buoyancy, which can compensate the pendulum effect in this configuration. However, the ballast can stretch the umbilical only if $\gamma \neq \psi_{P,x}$ ($\psi_{P,x} = 0$ when there is no current). Else, only the horizontal current applied on the buoy (so the surface current) can taut the umbilical. Since a buoy on the surface can be subject to other strengths like wind or wave, it is best to avoid working inside the area B in practice. Remind umbilical cannot be stretched inside the area C.

Thus, when the ROV rises, dives or goes back, its velocity and acceleration must be bounded by buoy's velocity and acceleration since this one does not touch the surface, as defined in the following Section 9.2.

9.2 Maximum velocity

When the umbilical is not taut between the ROV and the buoy, the buoy is like dropped freely in the water with only its weight and Archimedes strength. Consider the fluid friction $\vec{F}_{fb} = -K_b \vec{v}_b$, where \vec{v}_b is the buoy velocity such $\vec{v}_b = v_{b,x} \vec{x} + v_{b,y} \vec{y}$ and $v_b = \sqrt{v_{b,x}^2 + v_{b,y}^2}$, and K_b is the fluid friction coefficient associated to the buoy. For a spherical buoy of radius R_b , one has $K_b = 6\pi R_b \rho_{water}$ with ρ_{water} is the water mass density. Let m_b , ρ_b and a_b be the mass, the mass density and the vertical acceleration of the buoy. Remind $F_b = (\rho_{water} V_b - m_b)g + F_{cy,b}$ with V_b the volume of the buoy.

By performing the fundamental principle of dynamic on the axis x and y as exposed in Appendix G, one gets

$$v_b(t) = \left(1 - \exp\left(-\frac{K_b}{m_b}t\right)\right) \times \sqrt{\left(\frac{F_{cx,b}}{K_b}\right)^2 + \left(\frac{m_b}{K_b} \left(\left(\frac{\rho_{water} V_b}{m_b} - 1\right)g + \frac{F_{cy,b}}{m_b}\right)\right)^2} \quad (152)$$

$$a_b(t) = \exp\left(-\frac{K_b}{m_b}t\right) \times \sqrt{\left(\frac{F_{cx,b}}{m_b}\right)^2 + \left(\left(\frac{\rho_{water} V_b}{m_b} - 1\right)g + \frac{F_{cy,b}}{m_b}\right)^2} \quad (153)$$

The maximal velocity and acceleration can be expressed as

$$v_{b,max} = \sqrt{\left(\frac{F_{cx,b}}{K_b}\right)^2 + \left(\frac{m_b}{K_b} \left(\left(\frac{\rho_{water} V_b}{m_b} - 1\right)g + \frac{F_{cy,b}}{m_b}\right)\right)^2} \quad (154)$$

$$a_{b,max} = \sqrt{\left(\frac{F_{cx,b}}{m_b}\right)^2 + \left(\left(\frac{\rho_{water} V_b}{m_b} - 1\right)g + \frac{F_{cy,b}}{m_b}\right)^2} \quad (155)$$

Thus, when the ROV rises, dives or goes back from a starting instant $t = 0$ and is not inside the area B and C, its velocity and acceleration must be bounded by $v_b(t)$ and $a_b(t)$ for $t \geq 0$. Note if the value of $F_{cx,b}$ is unknown, (152)-(155) can be lower bound by taking $F_{cx,b} = 0$ or a known lower bound of $F_{cx,b}$, and so will be the velocity and acceleration of the ROV. Same method can be used if $F_{cy,b}$ is unknown and $F_{cy,b} > 0$. If $F_{cy,b} < 0$, an upper bound of $|F_{cy,b}|$ must be known and guarantee that $(\rho_{water} V_{buoy,i} - m_{buoy,i})g + F_{cy,b} > 0$ (Assumption A6): its upper bound can be used inside (152)-(155). It is recommended to take F_b such that $(\rho_{water} V_{buoy,i} - m_{buoy,i})g > \frac{-F_{cy,b}}{2}$ in practice.

10 Reversed and transferred models

In previous section, a model to explore hull boat, seafloor or hilly seafloor have been proposed. However, there exist some configuration where it is the surface which is hilly, under the ice or in underground caves for example. There exist also configuration where the seafloor is very deep, and so the length l_1 is too long to be approximated by a straight line. To solve these problems and explore new environment, the previous models can be "reversed" or "transferred".

In reversed model, an anchor is used instead of the boat as origin, and ballast are reversed by buoys and opposite, as illustrated in Figure 18 (a) and (c). The same resolutions of the models can be used, changing the buoyancy of the buoy by ballast weight and opposite in the equation. The axis y is also reversed such $\vec{O}y$ point to the surface, $y = 0$ corresponds to the depth of the anchor y_{anchor} , and $y_1 < y_2$, y_1 is deeper than y_2 .

In transferred models, the origin O is translated deeper using an anchor at the end of a cable l_0 , not in contact with the seafloor, as illustrated in Figure 18 (b). The anchor becomes the new origin like the boat before. The main advantage of this technique is the cable l_0 linking the anchor to the boat takes all the cable deformation due to its length, while cables l_1 , l_2 and l_3 can still respect the Assumptions A1-A7. Surface exploration and diving exploration strategies

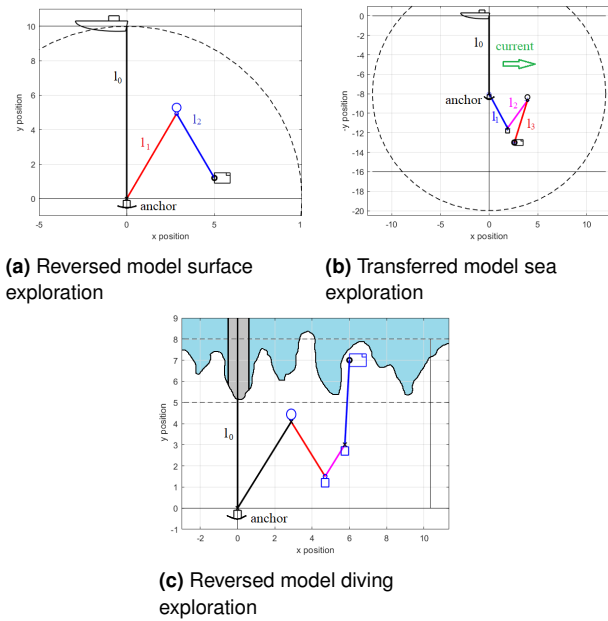


Figure 18. Example of reversed model and transferred model. An anchor is used instead of the boat as origin, and ballast and buoys are reversed in the reversed models.

can easily be transferred by evaluating the system for $y - l_0$ and adding the distance l_0 at the result. In case of the Sea Exploration configuration, the areas are impacted and must be redefined. The areas D1, D2, E and F must be lower than the value of l_0 , *i.e.* for $U \in \{D1, D2, E, F\}$ $y_{areaU} = y_{areaU} + l_0$. Cases of areas B and C are more complex. If $L < l_1$, the area C is also lower of the value of l_0 (and area B still does not exist). If $L > l_1$ and $L - l_1 > l_0$ the area B and C must be elevated of l_0 , *i.e.* $y_{areaU} = y_{areaU} - l_0$ for $U \in \{B, C\}$, because there is more space before the buoy reaches the surface. Else if $l_0 \geq L - l_1$, the buoy can not reach the surface without loose cable l_0 or l_1 , so the area B does not exist and the area C can be assimilate to a roof at level $y_{areaC} = l_0 + l_1 - L$.

In all situations, the anchor must be chosen enough heavy to make strength of ballasts, buoy, ROV and current negligible compared to it.

11 Practical case and experimental tests

This section discusses the validity of the assumptions made in the paper, exposes some problems in practical case and provides some experimental results to illustrate the validity of the study.

11.1 Validity of assumptions taken and choice of ballast and buoy

Consider first the assumptions made in this study. The Assumptions A1, A4, A5, A6 and A8 can easily be respected by the choice of the ballast mass and buoy volume. However, the Assumptions A2 and A3 can be satisfied only when the umbilical is relatively short (50m or less between the points). In case of deep dive where cable l_1 is too long to respect these assumptions, the problem can be solved using the transferred model exposed in Section 10: the additional cable

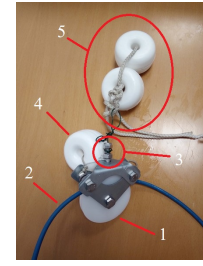


Figure 19. Pulley to obtain a sliding buoy. 1: pulley. 2: umbilical. 3: ball joint to reduce twist effort between the buoy and the pulley. 4: additional buoy and ballast to give a neutral buoyancy to the pulley assembly (without considering the buoys in 5). 5: buoys F_b for the self-management strategy.

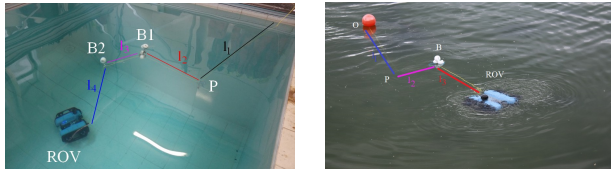
l_0 takes all the cable deformation due to its length, while cables l_1 , l_2 and l_3 can respect A2 and A3.

Assumption A7 considers the friction between the umbilical and the sliding ballast/buoy is quite negligible to allow the ballast/buoy to reach its theoretical equilibrium position. A pulley has been used in practice to let the buoy slide with few friction, as illustrated in Figure 19. Others tests have been performed using karabiner or ring, but the performances obtained are insufficient to correspond to the theory, the fault of a too strong friction making the equilibrium position strongly dependent of the starting position. Tests show Assumption A7 can be respected mostly, but cannot be taken lightly, see next section. Note the radius of the pulley R_p must be taken larger than the radius made by cable rigidity, involving to take $R_{curve} = R_p$ and so the value of angle θ_{min} and x_{min} exposed in Section 5.6. The pulley shown in Figure 19 has been produced to respect perfectly the diameter of our umbilical, but first tests performed using commercial pulleys provided very good results: the method can so be easily adapted for all kind of umbilical. The buoy is linked to the pulley by a mechanical ball joint to avoid twist strength on the umbilical by the buoy.

The choice of the ballast and buoy can be more complex. First, a ratio $\frac{P}{F_b}$ must be chosen such 1) Assumption A8 is respected, 2) P and F_b are taken such the umbilical weight/buoyancy is negligible compare to it, and can be deformed by them. Theoretically, any ballast and buoy respecting ratio $\frac{P}{F_b}$ works, however the biggest P and F_b are, the fastest the dynamic of the system is but the strongest the strength applied on the ROV by the umbilical is too: choice of the ballast and buoy is a trade-off between perturbation on the ROV, its maximum velocity and cable parameters.

11.2 Materials and experimentation

As illustrated in Figure 20 for the sea exploration and diving exploration, the three configurations have been tested in pool and in sea, in absence of current yet. To make measurements, the results exposed in this section have been performed in a pool of size $3m \times 4m$ with a depth of $3m$ for the sea exploration strategy, but similar conclusion can be taken for the two others strategies. To obtain a configuration immobile during the measurement, the ROV has been replaced by an anchor immersed at a controlled distance and depth from the origin (0, 0). Let however call it “ROV” in the text below. The measurement have been made with a measuring tape.



(a) BlueROV during test in pool. Umbilical for diving exploration with presence of large obstacles. $P = 80\text{g}$, $F_{b1} = 80\text{g}$, $F_{b2} = 280\text{g}$, $l_1 = l_4 = L = 1.5\text{m}$, so $\eta_{\max} = 10^\circ$.

(b) BlueROV during test in sea. Umbilical for sea exploration, the boat is replaced here by the orange buoy. $P = 255\text{g}$, $F_b = 135\text{g}$, $l_1 = 2.5\text{m}$ and $L = 3.5\text{m}$.

Figure 20. Materials for experimental tests in pool and sea.

The strength of a buoy is evaluated in gram, corresponding to the maximum mass it can lift. One takes $P = 255\text{g}$ and $F_b = 135\text{g}$. The umbilical is floating with the following parameters: diameter 4mm, $R_{\text{curve}} = 18\text{mm}$. One takes the lengths $l_1 = 2.5\text{m}$ and $L = 3.5\text{m}$. The mass for 6m of umbilical is 85g. The pulley has an internal radius of $R_p = 20\text{mm}$.

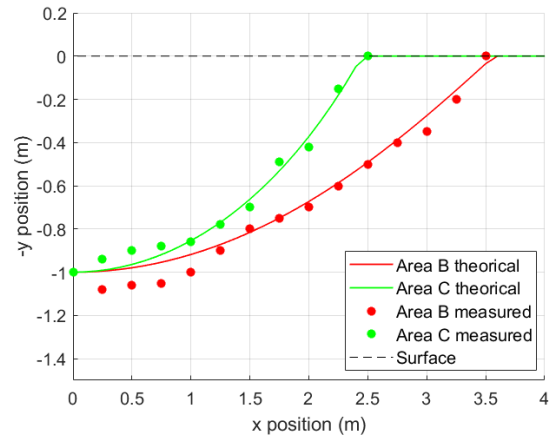
Let defined E_B the discrepancy between the measured position $(x_{B,m}, y_{B,m})$ and its theoretical position $(x_{B,th}, y_{B,th})$ of the buoy B for a ROV position (x_{ROV}, y_{ROV}) such as

$$E_B(x_{ROV}, y_{ROV}) = \sqrt{(x_{B,th} - x_{B,m})^2 + (y_{B,th} - y_{B,m})^2}. \quad (156)$$

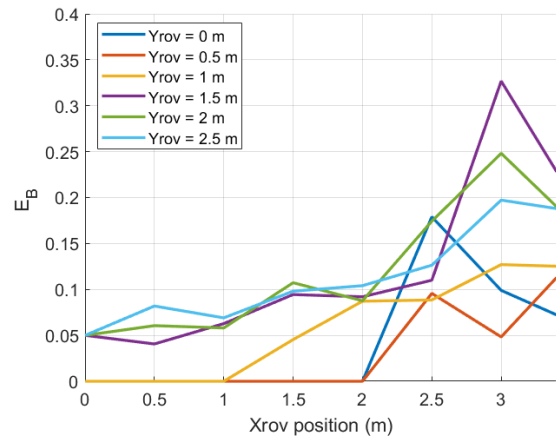
Since the movement of the buoy are larger than that of the ballast, the accuracy of the method is studied using E_B .

The Figure 21 (a) shows the difference between the areas B and C measured and theoretical. One can observe the both results are closed, the most discrepancies between the measured and theoretical areas are mostly due to the measurement error. Indeed, the boundary between the areas B and C, *i.e.* the beginning of the umbilical release, is not always simple to observe in practice. During our experimentation, the boundary has been measured when ballast reaches its resting position $(0, l_1)$ or when the umbilical starts to twist due to the lack of tension between the ballast and the buoy. Remind the height of the buoy (element 5 in Figure 19) must be taking into account in the evaluation of the areas B and C.

The Figure 22 illustrates two examples of the difference between theory and practice, and Figure 21 (b) shows the discrepancy E_B for several position (x_{ROV}, y_{ROV}) . These figures show the discrepancy between the theoretical model and the experimental results is small when the ROV is close to the origin and becomes larger when it moves always. The first reason of this discrepancy is the difference between the angles α, β, γ of the model and the curves performed by the umbilical in practice. Moreover, tests show the frictions cannot be totally neglect, and so the immobilization of the buoy's position is not always identical in function of the buoy's starting point and the movement performed by the ROV. Results exposed in the Figure 21 (b) are so the mean of three measurements. The maximum error measured before averaging was 0.38m for $(x_{ROV}, y_{ROV}) =$



(a) Areas B and C. Plain lines: theoretical areas. Dots: experimental measurement.



(b) Error E_B

Figure 21. Experimental measurement of discrepancy E_B and areas B and C. Each point is the mean of three measurements for the same position (x_{ROV}, y_{ROV}) .

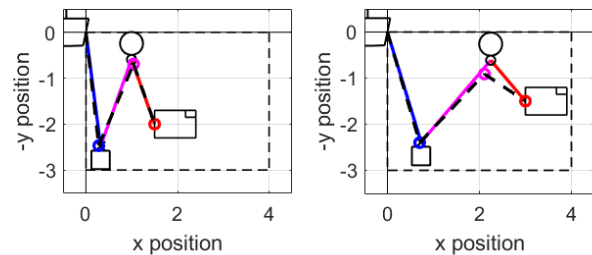


Figure 22. Comparison between theoretical umbilical (colored plain lines) and measured umbilical (large dash black lines). Small black dash lines: poolside. Left: $E_B = 0.107\text{m}$. Right: $E_b = 0.327\text{m}$, largest discrepancy of the experimentation.

$(3.5\text{m}, 2\text{m})$. Note this problem of friction is proportional with the horizontability of the cable, and so is negligible when the ROV is close to the origin and increase with the distance, like the discrepancy.

Despite the gap between theory and practice, the umbilical remained perfectly taut during all tests since the ROV is outside the area C, even during the transition phases, and its shape is predictable with a margin error. Note also the ballast and buoy used are small, inducing a small constraints on the cable.

11.3 Other practical problems

To perform the model of the umbilical in real time, this work supposes the position of the ROV is known. To obtain this position, the simple method is to use an Ultra Short Baseline (USBL). In absence of USBL, the vertical position y of the ROV can be found using a barometer, and the distance d between the ROV and the boat can be found using a sonar or by vision for example.

An other practical problem is the knowledge of the horizontal current F_{cx} , required for the model or the areas' evaluation. Since F_{cx} is in the most case unknown, the areas can be defined for two cases: absence of current, *i.e.* $F_{cx} = 0$, and the maximum current $F_{cx,max}$ against which the ROV will not be able to go upstream, and so the navigation of the ROV is impossible in these conditions. The area B must be evaluated considering $F_{cx} = 0$, and area F must be evaluated considering $F_{cx,max}$. Since it can be very restrictive for area F, an upper-bound on an a priori knowledge of the current F_{cx} can also be taken instead of $F_{cx,max}$. Note the buoy and/or ballast can be instrumented to know their position and so simplified model evaluation. Angles between the boat and the umbilical and/or the ROV and the umbilical can also be measured using a camera for example.

Finally, a last practical problem is the raising of the cable and ROV after a deep sea mission. The cable l_1 (or l_0) coiling and the ROV raising must be synchronized to avoid a knot formation inside the area C.

12 Conclusion

This work proposes three passive self-management strategies of the umbilical for a ROV, without motorized system on the umbilical. Using moving ballast and buoys to tend the umbilical, two dimensional and three dimensional models of the umbilical shape have been provided, considering absence or presence of currents. Cables are assimilated to straight lines with minimum angle between them to consider umbilical rigidity. Several areas have been defined where the umbilical behavior are different. These areas and a limitation of the ROV's velocity and acceleration define a safe exploration area without risk of knot on the umbilical itself. To implement these methods, the only required feedback is the ROV position. The strengths applied on the umbilical and the ROV have been studied. Finally, reversed and transferred models allow a large adaptation of the three basic configurations to extend them to other environments while respecting hypotheses taken.

Future works will study other umbilical configurations, *e.g.* for large area to explore with shallow water depth. A general model to create easily new configurations could also be proposed. Variations of current, presence of waves and uncertainty on parameters will be considered. Finally, measurements in sea during a true mission will be performed.

References

- [1] BA Abel. Underwater vehicle tether management systems. In *Proceedings of OCEANS'94*, volume 2, pages II-495, 1994.
- [2] O. Blintsov. Development of the mathematical modeling method for dynamics of the flexible tether as an element of the underwater complex. *Eastern-European Journal of Enterprise Technologies*, 1 (7):4-14, 2017.
- [3] L. Brignone, E. Raugel, J. Opderbecke, V. Rigaud, R. Piasco, and S. Ragot. First sea trials of hrov the new hybrid vehicle developed by ifremer. In *Oceans 2015-genova*, pages 1-7, 2015.
- [4] B. Buckham and M. Nahon. Dynamics simulation of low tension tethers. In *IEEE Conference Proceedings Oceans*, volume 2, pages 757-766, 1999.
- [5] R. D. Christ and R. L. Wernli Sr. *The ROV manual: a user guide for observation class remotely operated vehicles*. Elsevier, 2011.
- [6] T. Crandle, G. Cook, and E. Celkis. Tradeoffs between umbilical and battery power in rovs performance. In *IEEE OCEANS 2017-Anchorage*, pages 1-6, 2017.
- [7] R. G. Duncan, Mark E. Froggatt, S. T Kreger, R. J. Seeley, D. K. Gifford, A. K. Sang, and M. S. Wolfe. High-accuracy fiber-optic shape sensing. In *Sensor Systems and Networks*, volume 6530, page 65301S, 2007.
- [8] O. A. Eidsvik and I. Schjølberg. Time domain modeling of rovs umbilical using beam equations. *IFAC*, 49(23):452-457, 2016.
- [9] O. A. N. Eidsvik and I. Schjølberg. Finite element cable-model for remotely operated vehicles (rovs) by application of beam theory. *Ocean Engineering*, 163:322-336, 2018.
- [10] J. E. Frank, R. Geiger, D. R. Kraige, and A. Murali. Smart tether system for underwater navigation and cable shape measurement, 2013. US Patent 8,437,979, URL <https://patents.google.com/patent/US8437979B2/en>.
- [11] O. Ganoni, R. Mukundan, and R. Green. Visually realistic graphical simulation of underwater cable. 2018.
- [12] F. González, A. de la Prada, A. Luaces, and M. González. Real-time simulation of cable pay-out and reel-in with towed fishing gears. *Ocean Engineering*, 131:295-307, 2017.
- [13] Sung Min Hong, Kyoung Nam Ha, and Joon-Young Kim. Dynamics modeling and motion simulation of usv/uuv with linked underwater cable. *Journal of Marine Science and Engineering*, 8(5):318, 2020.
- [14] M. Laranjeira, C. Dune, and V. Hugel. Catenary-based visual servoing for tethered robots. In *IEEE International Conference on Robotics and Automation*, pages 732-738, 2017.
- [15] M. Laranjeira, C. Dune, and V. Hugel. Embedded visual detection and shape identification of underwater umbilical for vehicle positioning. In *OCEANS 2019-Marseille*, pages 1-9, 2019.

- [16] M. Laranjeira, C. Dune, and V. Hugel. Catenary-based visual servoing for tether shape control between underwater vehicles. *Ocean Engineering*, 200:107018, 2020.
- [17] A. Lasbouygues, S. Louis, B. Ropars, L. Rossi, H. Jourde, H. Délas, P. Balordi, R. Bouchard, M. Dighouth, M. Dugrenot, et al. Robotic mapping of a karst aquifer. In *IFAC: International Federation of Automatic Control*, 2017.
- [18] M. B. Lubis, M. Kimiaei, and M. Efthymiou. Alternative configurations to optimize tension in the umbilical of a work class rov performing ultra-deep-water operation. *Ocean Engineering*, 225:108786, 2021.
- [19] M. Such, J. R. Jimenez-Octavio, A. Carnicero, and O. Lopez-Garcia. An approach based on the catenary equation to deal with static analysis of three dimensional cable structures. *Engineering structures*, 31(9):2162–2170, 2009.
- [20] O. Tortorici, C. Anthierens, V. Hugel, and H. Barthelemy. Towards active self-management of umbilical linking rov and usv for safer submarine missions. *IFAC-PapersOnLine*, 52(21):265–270, 2019.

A Proof of umbilical model for surface exploration

A.1 Proof of (6)-(8)

Since $x \leq L$, (6) is obvious from (4). The relation $L = l_1 + l_2$ shows (8). Consider now (5):

$$\begin{aligned} y &= (l_1 - l_2) \cos(\alpha) \\ y &= (-L + 2l_1) \cos(\alpha) \\ l_1 &= \frac{1}{2} \left(L + \frac{y}{\cos(\alpha)} \right). \end{aligned} \quad (157)$$

From (4), one can write

$$\begin{aligned} \cos(\alpha) &= \cos\left(\arcsin\left(\frac{x}{L}\right)\right) \\ &= \sqrt{1 - \left(\frac{x}{L}\right)^2} \end{aligned} \quad (158)$$

so

$$l_1 = \frac{1}{2} \left(L + \frac{y}{\sqrt{1 - \left(\frac{x}{L}\right)^2}} \right). \quad (159)$$

A.2 Proofs of (9) and (10)

Let define the mass depth y_M . Using (6)-(8), one gets

$$\begin{aligned} y_M &= l_1 \cos(\alpha) \\ &= l_1 \sqrt{1 - \left(\frac{x}{L}\right)^2} \\ &= \frac{1}{2} \left(L + \frac{y}{\sqrt{1 - \left(\frac{x}{L}\right)^2}} \right) \sqrt{1 - \left(\frac{x}{L}\right)^2} \\ &= \frac{1}{2} \left(L \sqrt{1 - \left(\frac{x}{L}\right)^2} + y \right). \end{aligned} \quad (160)$$

To guarantee $y_{\text{floor}} \geq y_M$, one must have

$$\begin{aligned} y_{\text{floor}} &\geq y_M \\ y_{\text{floor}} &\geq \frac{1}{2} \left(L \sqrt{1 - \left(\frac{x}{L}\right)^2} + y \right) \\ 2y_{\text{floor}} - L \sqrt{1 - \left(\frac{x}{L}\right)^2} &\geq y, \end{aligned} \quad (161)$$

and to take into account the mass height h_M , one gets

$$\begin{aligned} y_{\text{floor}} &\geq y_M(x) + h_M \\ y_{\text{floor}} - h_M &\geq \frac{1}{2} \left(L \sqrt{1 - \left(\frac{x}{L}\right)^2} + y \right) \\ 2(y_{\text{floor}} - h_M) - L \sqrt{1 - \left(\frac{x}{L}\right)^2} &\geq y. \end{aligned} \quad (162)$$

A.3 Proofs of umbilical model for surface exploration with current

By making a rotation of the referential \mathcal{R} by an angle of $\frac{\pi}{2} - \psi_{P,x}$, this problem can be assimilate to the case without current studied in Section 4.1. Let define \mathcal{R}^* the

new referential obtained with the parameters α^* , β^* where $\alpha^* = \bar{\alpha}$ and $\beta^* = -\bar{\alpha}$. Then

$$\alpha = \alpha^* + \psi_{P,x} \quad (163)$$

$$\beta = 2\psi_{P,x} - \alpha. \quad (164)$$

Let define x^*, y^* the coordinate in referential \mathcal{R}^* such

$$x^* = x \cos(\psi_{P,x}) - y \sin(\psi_{P,x}) \quad (165)$$

$$y^* = y \cos(\psi_{P,x}) + x \sin(\psi_{P,x}). \quad (166)$$

Note l_1 and l_2 stay unchanged. Using result described in Appendix A.1, one gets

$$\alpha^* = \text{asin}\left(\frac{x^*}{L}\right) \quad (167)$$

$$l_1 = \frac{1}{2} \left(L + \frac{y^*}{\sqrt{1 - \left(\frac{x^*}{L}\right)^2}} \right) \quad (168)$$

$$l_2 = L - l_1 \quad (169)$$

Using (163) and (165)-(166) to go back to the referential \mathcal{R} , one obtains

$$\alpha = \text{asin}\left(\frac{x \cos(\psi_{P,x}) - y \sin(\psi_{P,x})}{L}\right) + \psi_{P,x} \quad (170)$$

$$\beta = 2\psi_{P,x} - \alpha \quad (171)$$

$$l_1 = \frac{1}{2} \left(L + \frac{y \cos(\psi_{P,x}) + x \sin(\psi_{P,x})}{\sqrt{1 - \left(\frac{x \cos(\psi_{P,x}) - y \sin(\psi_{P,x})}{L}\right)^2}} \right) \quad (172)$$

$$l_2 = L - l_1. \quad (173)$$

All the parameters have been defined.

B Proof for umbilical for sea exploration

B.1 Proof of θ_{\min} in (53)

To perform two half circles of radius R_{curve} around the ballast and the buoy, one must have

$$4R_{curve} = l_2 \sin(-\alpha) + l_3 \sin(\beta). \quad (174)$$

Since $\alpha = -\beta$ and $L = l_2 + l_3$, one gets

$$\begin{aligned} 4R_{curve} &= L \sin(\beta) \\ \sin(\beta) &= \frac{4R_{curve}}{L} \\ \theta_{\min} &= 2\text{asin}\left(\frac{4R_{curve}}{L}\right). \end{aligned} \quad (175)$$

B.2 Proof of (25) in area A

Since \vec{T}_1 , \vec{T}_2 and \vec{T}_3 are unknown, (23) and (24) are projected on the axis perpendiculars to \vec{T}_1 and \vec{T}_3 , noted respectively $\vec{v}_{\perp T1}$ and $\vec{v}_{\perp T3}$:

$$\Sigma_M \vec{F} \cdot \vec{v}_{\perp T1} = P \sin(\gamma) - T_2 \sin(\gamma - \alpha) \quad (176)$$

$$\Sigma_B \vec{F} \cdot \vec{v}_{\perp T3} = -F_b \sin(\beta) - T_2 \sin(\beta - \alpha). \quad (177)$$

Remind $\beta = -\alpha$. Since $\Sigma_M \vec{F} \cdot \vec{v}_{\perp T1} = 0$ and $\Sigma_B \vec{F} \cdot \vec{v}_{\perp T3} = 0$, one gets

$$T_2 = P \frac{\sin(\gamma)}{\sin(\gamma + \beta)} \quad (178)$$

$$T_2 = F_b \frac{\sin(\beta)}{\sin(2\beta)} \quad (179)$$

so

$$P \frac{\sin(\gamma)}{\sin(\gamma + \beta)} = F_b \frac{\sin(\beta)}{\sin(2\beta)}. \quad (180)$$

From (180), one may write

$$\begin{aligned} \frac{P}{F_b} \sin(\gamma) \sin(2\beta) &= \sin(\beta) \sin(\gamma + \beta) \\ \frac{P}{F_b} \sin(\gamma) [2 \sin(\beta) \cos(\beta)] &= \sin(\beta) [\sin(\beta) \cos(\gamma) \\ &\quad + \sin(\gamma) \cos(\beta)] \end{aligned} \quad (181)$$

If $\gamma = 0$, one has $\beta = 0$ and so $\alpha = 0$. The case $\gamma = \frac{\pi}{2}$ is possible only if $\beta = \frac{\pi}{2}$ and $\alpha = -\frac{\pi}{2}$ because the buoy can not go higher than the sea level. Consider now the case $\gamma \neq 0$ and $\gamma \neq \frac{\pi}{2}$. (181) becomes

$$\begin{aligned} 2 \frac{P}{F_b} \tan(\gamma) &= \tan(\beta) + \tan(\gamma) \\ \left(2 \frac{P}{F_b} - 1\right) \tan(\gamma) &= \tan(\beta). \end{aligned} \quad (182)$$

(182) provides a relation between γ and β in the area A.

B.3 Calculation of γ in area A

Let first remind $\Lambda \tan(\gamma) = \tan(\beta)$. For a given θ , one has $\sin(\text{atan}(\theta)) = \frac{\theta}{\sqrt{1+\theta^2}}$, so

$$\begin{aligned} \sin(\beta) &= \sin(\text{atan}(\Lambda \tan(\gamma))) \\ &= \frac{\Lambda \tan(\gamma)}{\sqrt{1 + (\Lambda \tan(\gamma))^2}}. \end{aligned} \quad (183)$$

Put $X = \sin(\gamma)$. Thus, one has

$$\tan(\gamma) = \frac{X}{\sqrt{1-X^2}} \quad (184)$$

and so (183) becomes

$$\begin{aligned} \sin(\beta) &= \frac{\frac{\Lambda X}{\sqrt{1-X^2}}}{\sqrt{1 + \left(\frac{\Lambda X}{\sqrt{1-X^2}}\right)^2}} \\ &= \frac{\Lambda X}{\sqrt{1 + (\Lambda^2 - 1) X^2}}. \end{aligned} \quad (185)$$

By introducing (21) and (20) inside (18), one gets

$$x = l_1 \sin(\gamma) + L \sin(\beta). \quad (186)$$

Let's introduce X and (185) inside (186):

$$x = l_1 X + \frac{L \Lambda X}{\sqrt{1 + (\Lambda^2 - 1) X^2}}$$

$$\begin{aligned}(x - l_1 X) \sqrt{1 + (\Lambda^2 - 1) X^2} &= L \Lambda X \\ (x - l_1 X)^2 (1 + (\Lambda^2 - 1) X^2) &= (L \Lambda X)^2 \\ (x^2 - 2x l_1 X + l_1^2 X^2) (1 + (\Lambda^2 - 1) X^2) &= L^2 \Lambda^2 X^2\end{aligned}$$

$$\begin{aligned}x^2 + x^2 (\Lambda^2 - 1) X^2 - 2x l_1 X - 2x l_1 (\Lambda^2 - 1) X^3 \\ + l_1^2 X^2 + l_1^2 (\Lambda^2 - 1) X^4 - L^2 \Lambda^2 X^2 = 0\end{aligned}\quad (187)$$

which can be reorganised such

$$aX^4 + bX^3 + cX^2 + dX + E = 0 \quad (188)$$

with

$$a = l_1^2 (\Lambda^2 - 1) \quad (189)$$

$$b = -2x l_1 (\Lambda^2 - 1) \quad (190)$$

$$c = x^2 (\Lambda^2 - 1) - L^2 \Lambda^2 + l_1^2 \quad (191)$$

$$d = -2x l_1 \quad (192)$$

$$e = x^2. \quad (193)$$

(188) is a quartic function which can be solved using Ludovico Ferrari, described for our parameters in Section B.5.

Remark if $P = F_b$, on gets $\Lambda^2 = 1$ so $a = 0$ and $b = 0$. (188) becomes a second order polynomial whom the solution which interest us is

$$\sin(\gamma) = \frac{-d - \sqrt{d^2 - 4ce}}{2c} \quad (194)$$

which is equal to

$$\begin{aligned}\sin(\gamma) &= \frac{x(l_1 - L)}{l_1^2 - L^2} \\ &= \frac{x(l_1 - L)}{(l_1 - L)(l_1 + L)} \\ &= \frac{x}{l}\end{aligned}\quad (195)$$

since $l = l_1 + L$. Moreover, if $x = 0$, the only geometrical solution without current is $\sin(\gamma) = 0$.

B.4 Calculation of l_2 and l_3 in area A

Suppose β and γ have been previously evaluated using (25) and results of Appendix B.3. Then (19) can be rewritten such

$$\begin{aligned}y &= l_1 \cos(\gamma) - l_2 \cos(\beta) + (L - l_2) \cos(\beta) \\ y &= l_1 \cos(\gamma) + (L - 2l_2) \cos(\beta) \\ -2l_2 &= -L + \frac{y - l_1 \cos(\gamma)}{\cos(\beta)} \\ l_2 &= \frac{L}{2} - \frac{y - l_1 \cos(\gamma)}{2 \cos(\beta)}\end{aligned}\quad (196)$$

and so $l_3 = L - l_2$.

B.5 Solve quartic function

Considering our application, only one solution of the quartic function corresponds to our configuration. This section summarized the Ludovico Ferrari's method to solve quartic

function and add the knowledge of ours parameters to exclude some cases and pick the appropriate solution.

Let solve the quartic function

$$aX^4 + bX^3 + cX^2 + dX + e = 0. \quad (197)$$

Suppose $P > F_b$, so $a \neq 0$ and $b \neq 0$, else the solution of (188) is described in (194). Suppose also $x > 0$, else the only geometric solution is $X = 0$.

Theorem 9. Consider $x > 0$ and $P > F_b$. The solution of (197) considering the relation between the parameters l_1, L, x, P and F_b is

$$X = \min_{i \in \{1, 2, 3, 4\}} (|X_i|) \quad (198)$$

where

$$\begin{cases} X_1 = \frac{\sqrt{U - \frac{2}{3}A} - \sqrt{\Delta_{Y1}}}{2}, X_2 = \frac{\sqrt{U - \frac{2}{3}A} + \sqrt{\Delta_{Y1}}}{2}, & \text{if } \Delta_{Y1} \geq 0 \\ X_1 = \infty, X_2 = \infty & \text{else,} \end{cases}\quad (199)$$

$$\begin{cases} X_3 = \frac{-\sqrt{U - \frac{2}{3}A} - \sqrt{\Delta_{Y2}}}{2}, X_4 = \frac{-\sqrt{U - \frac{2}{3}A} + \sqrt{\Delta_{Y2}}}{2}, & \text{if } \Delta_{Y2} \geq 0 \\ X_3 = \infty, X_4 = \infty & \text{else,} \end{cases}\quad (200)$$

$$\begin{aligned}\text{for } \Delta_{Y1} &= -\left(U + \frac{4}{3}A + \frac{2B}{\sqrt{U - \frac{2}{3}A}}\right) \text{ and } \Delta_{Y2} = \\ &= -\left(U + \frac{4}{3}A - \frac{2B}{\sqrt{U - \frac{2}{3}A}}\right) \text{ with}\end{aligned}$$

$$A = -\frac{x^2}{2l_1^2} - \frac{(L^2 \Lambda^2 - l_1^2)}{l_1^2 (\Lambda^2 - 1)} \quad (201)$$

$$B = -\frac{l_1^2 + L^2 \Lambda^2}{l_1^3 (\Lambda^2 - 1)} x \quad (202)$$

$$C = \frac{x^4}{16l_1^4} + \frac{x^2 (l_1^2 - L^2 \Lambda^2)}{4l_1^4 (\Lambda^2 - 1)} \quad (203)$$

$U =$

$$\begin{cases} \left(-\frac{q}{2} + \sqrt{\frac{q^2}{4} + \frac{p^3}{27}}\right)^{\frac{1}{3}} + \left(-\frac{q}{2} - \sqrt{\frac{q^2}{4} + \frac{p^3}{27}}\right)^{\frac{1}{3}} & \text{if } \Delta_U > 0, \\ 2 \cos\left(\frac{1}{3} \arccos\left(-\frac{q}{2\sqrt{-\frac{p^3}{27}}}\right)\right) \sqrt{-\frac{p}{3}} & \text{if } \Delta_U < 0, \\ -\sqrt{-\frac{p}{3}} & \text{if } \Delta_U = 0 \end{cases}\quad (204)$$

$$\text{with } \Delta_U = \frac{q^2}{4} + \frac{p^3}{27}, \quad p = -4C - \frac{A^2}{3} \text{ and } q = \frac{2A^3}{27} + (4AC - B^2) + \frac{-4CA}{3}.$$

B.5.1 Proof of Theorem 9

Suppose here $x > 0$ and $P > F_b$, so $\Lambda^2 > 1$ and $a \neq 0$ and $b \neq 0$. By putting $X = Y - \frac{b}{4a}$, (197) becomes

$$Y^4 + AY^2 + BY + C = 0 \quad (205)$$

with

$$A = \frac{-3b^2}{8a^2} + \frac{c}{a} \quad (206)$$

$$B = \frac{\left(\frac{b}{2}\right)^3}{a^3} - \frac{1}{2} \frac{bc}{a^2} + \frac{d}{a} \quad (207)$$

$$C = -3 \left(\frac{b}{4a}\right)^4 + c \left(\frac{b}{4a}\right)^2 - \frac{1}{4} \frac{bd}{a^2} + \frac{e}{a}. \quad (208)$$

Let show that in our case, $B \neq 0$. We introduce the value of (189)-(193) inside B :

$$\begin{aligned} B &= \frac{\left(\frac{b}{2}\right)^3}{a^3} - \frac{1}{2} \frac{bc}{a^2} + \frac{d}{a} \\ &= \frac{(-xl_1(\Lambda^2 - 1))^3}{(l_1^2(\Lambda^2 - 1))^3} + \frac{-2xl_1}{l_1^2(\Lambda^2 - 1)} \\ &\quad - \frac{1}{2} \frac{(-2xl_1(\Lambda^2 - 1))(x^2(\Lambda^2 - 1) - L^2\Lambda^2 + l_1^2)}{(l_1^2(\Lambda^2 - 1))^2} \\ &= -\left(\frac{x}{l_1}\right)^3 - \frac{2x}{l_1(\Lambda^2 - 1)} + \frac{x(x^2(\Lambda^2 - 1) - L^2\Lambda^2 + l_1^2)}{l_1^3(\Lambda^2 - 1)} \\ &= \frac{-x^2(\Lambda^2 - 1) - 2l_1^2 + (x^2(\Lambda^2 - 1) - L^2\Lambda^2 + l_1^2)}{l_1^3(\Lambda^2 - 1)}x \\ &= \frac{-l_1^2 - L^2\Lambda^2}{l_1^3(\Lambda^2 - 1)}x \end{aligned} \quad (209)$$

and since $x > 0$, $L > 0$, $l_1 > 0$ and $\Lambda > 0$, one has $B < 0$.

Since $B \neq 0$, (205) can be rewritten

$$\left(Y^2 + \frac{u}{2}\right)^2 = (u - A)(Y - Z)^2 \quad (210)$$

where $Z = \frac{B}{2(u-A)}$ and u is the solution of

$$\begin{aligned} u^3 - Au^2 - 4Cu + (4AC - B^2) &= 0 \\ \bar{a}u^3 + \bar{b}u^2 + \bar{c}u + \bar{d} &= 0 \end{aligned} \quad (211)$$

with

$$\bar{a} = 1 \quad (212)$$

$$\bar{b} = -A \quad (213)$$

$$\bar{c} = -4C \quad (214)$$

$$\bar{d} = 4AC - B^2. \quad (215)$$

and where (211) can be evaluated using **Cardan formula**.

Evaluation of u

Using Cardan approach, (211) can be rewritten such that

$$U^3 + pU + q = 0 \quad (216)$$

where

$$u = \left(U - \frac{\bar{b}}{3\bar{a}}\right) = U + \frac{A}{3} \quad (217)$$

$$p = \left(\frac{\bar{c}}{\bar{a}} - \frac{\bar{b}^2}{3\bar{a}^2}\right) = -4C - \frac{A^2}{3} \quad (218)$$

$$q = \left(\frac{2\bar{b}^3}{27\bar{a}^3} + \frac{\bar{d}}{\bar{a}} - \frac{\bar{b}\bar{c}}{3\bar{a}^2}\right) = \frac{2A^3}{27} + (4AC - B^2) + \frac{-4CA}{3} \quad (219)$$

Still following the Cardan approach, let define the determinant $\Delta_U = \frac{q^2}{4} + \frac{p^3}{27}$ and consider cases $\Delta_U > 0$, $\Delta_U < 0$ and $\Delta_U = 0$:

- If $\Delta_U > 0$, p and q are necessarily negative (property of Cardan formula) and the solution of (216) is

$$U = \left(-\frac{q}{2} + \sqrt{\frac{q^2}{4} + \frac{p^3}{27}}\right)^{\frac{1}{3}} + \left(-\frac{q}{2} - \sqrt{\frac{q^2}{4} + \frac{p^3}{27}}\right)^{\frac{1}{3}} \quad (220)$$

and so $U > 0$.

- If $\Delta_U < 0$, one has necessarily $p < 0$ (property of Cardan formula) and the solution of (216) is

$$U = 2 \cos\left(\frac{t}{3}\right) \sqrt{-\frac{p}{3}} \quad (221)$$

with

$$t = \arccos\left(-\frac{q}{2r}\right) \quad (222)$$

$$r = \sqrt{-\frac{p^3}{27}} \quad (223)$$

and so $U > 0$.

- If $\Delta_U = 0$, one has necessarily $p < 0$ (property of Cardan formula) and the solution of (216) is

$$U = -\sqrt{-\frac{p}{3}}, \quad (224)$$

so $U \geq 0$.

Evaluation of Y

Let's go back to (210):

$$\left(Y^2 + \frac{u}{2}\right)^2 = (u - A)(Y - Z)^2 \quad (225)$$

with

$$\begin{aligned} Z &= \frac{B}{2(u - A)} \\ &= \frac{B}{2\left(U - \frac{2A}{3}\right)} \end{aligned} \quad (226)$$

Let's show first $u - A \geq 0$. Since $u = U + \frac{A}{3}$, one has $u - A = U - \frac{2A}{3}$ where $U \geq 0$. Let's show $A < 0$:

$$\begin{aligned} A &= \frac{-3b^2}{8a^2} + \frac{c}{a} \\ &= \frac{-3(2xl_1(\Lambda^2 - 1))^2}{8l_1^4(\Lambda^2 - 1)^2} + \frac{x^2(\Lambda^2 - 1) - L^2\Lambda^2 + l_1^2}{l_1^2(\Lambda^2 - 1)} \\ &= \frac{-12x^2l_1^2(\Lambda^2 - 1)^2}{8l_1^4(\Lambda^2 - 1)^2} + \frac{x^2(\Lambda^2 - 1) - L^2\Lambda^2 + l_1^2}{l_1^2(\Lambda^2 - 1)} \\ &= \frac{-12x^2l_1^2(\Lambda^2 - 1)^2}{8l_1^4(\Lambda^2 - 1)^2} \\ &\quad + \frac{8x^2l_1^2(\Lambda^2 - 1)^2 - 8l_1^2L^2\Lambda^2(\Lambda^2 - 1) + 8l_1^4(\Lambda^2 - 1)}{8l_1^4(\Lambda^2 - 1)^2} \\ &= \frac{-4x^2l_1^2(\Lambda^2 - 1)^2 - 8l_1^2(L^2\Lambda^2 - l_1^2)(\Lambda^2 - 1)}{8l_1^4(\Lambda^2 - 1)^2} \\ &= -\frac{x^2}{2l_1^2} - \frac{(L^2\Lambda^2 - l_1^2)}{l_1^2(\Lambda^2 - 1)} \end{aligned} \quad (227)$$

so $A < 0$ if $L^2\Lambda^2 - l_1^2 \geq 0$, so if $LA \geq l_1$. Due to the Assumption A8, one has

$$P \geq \frac{F_b}{2} \left(\frac{l_1}{L} + 1\right)$$

$$L \left(2\frac{P}{F_b} - 1\right) \geq l_1$$

$$LA \geq l_1 \quad (228)$$

so the condition is true and $A < 0$, so $u - A > 0$.

Since it has been proven that $(u - A) > 0$, Y of (225) is the solution of one of the two equations

$$\begin{cases} Y^2 + \frac{u}{2} = T(Y - Z) \\ Y^2 + \frac{u}{2} = -T(Y - Z) \end{cases} \quad (229)$$

with $T = \sqrt{u - A}$ and $Z = \frac{B}{2(u - A)}$

$$\begin{cases} Y^2 - YT + (ZT + \frac{u}{2}) = 0 \\ Y^2 + YT + (-ZT + \frac{u}{2}) = 0. \end{cases} \quad (230)$$

For (230), we can define two discriminates Δ_{Y1} and Δ_{Y2} . Consider first Δ_{Y1}

$$\begin{aligned} \Delta_{Y1} &= T^2 - 4 \left(ZT + \frac{u}{2} \right) \\ &= (u - A) - 4 \left(\frac{B\sqrt{u - A}}{2(U - \frac{2A}{3})} + \frac{u}{2} \right). \end{aligned} \quad (231)$$

Since $u = U + \frac{A}{3}$, one gets

$$\begin{aligned} \Delta_{Y1} &= \left(U - \frac{2}{3}A \right) - 4 \left(\frac{B\sqrt{U - \frac{2}{3}A}}{2(U - \frac{2A}{3})} + \frac{U}{2} + \frac{1}{6}A \right) \\ &= \left(U - \frac{2}{3}A \right) - \left(\frac{2B}{\sqrt{U - \frac{2}{3}A}} + 2U + \frac{2}{3}A \right) \\ &= - \left(U + \frac{4}{3}A + \frac{2B}{\sqrt{U - \frac{2}{3}A}} \right). \end{aligned} \quad (232)$$

In the same way, one can get

$$\Delta_{Y2} = - \left(U + \frac{4}{3}A - \frac{2B}{\sqrt{U - \frac{2}{3}A}} \right). \quad (233)$$

and obtain the four solution of (230):

$$Y_1 = \frac{\sqrt{U - \frac{2}{3}A} - \sqrt{\Delta_{Y1}}}{2} \quad (234)$$

$$Y_2 = \frac{\sqrt{U - \frac{2}{3}A} + \sqrt{\Delta_{Y1}}}{2} \quad (235)$$

$$Y_3 = \frac{-\sqrt{U - \frac{2}{3}A} - \sqrt{\Delta_{Y2}}}{2} \quad (236)$$

$$Y_4 = \frac{-\sqrt{U - \frac{2}{3}A} + \sqrt{\Delta_{Y2}}}{2}. \quad (237)$$

Remind $X = Y - \frac{b}{4a}$, so $X = Y + \frac{x}{2l_1}$. Then from (234)-(237), one gets the four solution X_k for $k \in [1, \dots, 4]$:

$$X_1 = \frac{\sqrt{U - \frac{2}{3}A} - \sqrt{\Delta_{Y1}}}{2} \quad (238)$$

$$X_2 = \frac{\sqrt{U - \frac{2}{3}A} + \sqrt{\Delta_{Y1}}}{2} \quad (239)$$

$$X_3 = \frac{-\sqrt{U - \frac{2}{3}A} - \sqrt{\Delta_{Y2}}}{2} \quad (240)$$

$$X_4 = \frac{-\sqrt{U - \frac{2}{3}A} + \sqrt{\Delta_{Y2}}}{2}. \quad (241)$$

For our case, the solution is the smallest real absolute value of the X_k solution, so

$$X = \min_{i \in [1, 2, 3, 4]} (|X_i|). \quad (242)$$

Simplification of C

$$\begin{aligned} C &= -3 \left(\frac{b}{4a} \right)^4 + c \frac{\left(\frac{b}{4} \right)^2}{a^3} - \frac{1}{4} \frac{bd}{a^2} + \frac{e}{a} \\ &= -3 \left(\frac{-2xl_1(\Lambda^2 - 1)}{4l_1^2(\Lambda^2 - 1)} \right)^4 \\ &\quad + \frac{(x^2(\Lambda^2 - 1) - L^2\Lambda^2 + l_1^2)}{(l_1^2(\Lambda^2 - 1))^3} \left(\frac{-2xl_1(\Lambda^2 - 1)}{4} \right)^2 \\ &\quad - \frac{1}{4} \frac{(-2xl_1(\Lambda^2 - 1))(-2xl_1)}{(l_1^2(\Lambda^2 - 1))^2} + \frac{x^2}{l_1^2(\Lambda^2 - 1)} \\ &= -3 \frac{x^4}{16l_1^4} + \frac{(x^2(\Lambda^2 - 1) - L^2\Lambda^2 + l_1^2)}{l_1^6(\Lambda^2 - 1)^3} \\ &\quad \times \left(\frac{x^2l_1^2(\Lambda^2 - 1)^2}{4} \right) - \frac{(xl_1)^2(\Lambda^2 - 1)}{l_1^4(\Lambda^2 - 1)^2} + \frac{x^2}{l_1^2(\Lambda^2 - 1)} \\ &= -\frac{3}{16} \frac{x^4}{l_1^4} + \frac{(x^2(\Lambda^2 - 1) - L^2\Lambda^2 + l_1^2)}{l_1^4(\Lambda^2 - 1)} \left(\frac{x^2}{4} \right) \\ &\quad - \frac{x^2}{l_1^2(\Lambda^2 - 1)} + \frac{x^2}{l_1^2(\Lambda^2 - 1)} \\ &= -\frac{3}{16} \frac{x^4}{l_1^4} + \frac{x^4(\Lambda^2 - 1) - x^2L^2\Lambda^2 + x^2l_1^2}{4l_1^4(\Lambda^2 - 1)} \\ &= -\frac{3x^4(\Lambda^2 - 1)}{16l_1^4} + \frac{4x^4(\Lambda^2 - 1) - 4x^2L^2\Lambda^2 + 4x^2l_1^2}{16l_1^4(\Lambda^2 - 1)} \\ &= \frac{x^4(\Lambda^2 - 1) - 4x^2L^2\Lambda^2 + 4x^2l_1^2}{16l_1^4(\Lambda^2 - 1)} \\ &= \frac{x^4}{16l_1^4} + \frac{x^2(l_1^2 - L^2\Lambda^2)}{4l_1^4(\Lambda^2 - 1)} \end{aligned} \quad (243)$$

B.6 Calculation of the boundary between areas

B.6.1 Boundary areas A-B: $y = l_3 \cos(\beta)$

The boundary between the areas A and B corresponds to the depth $y = l_3 \cos(\beta)$ with $l_3 \geq 0$ because the buoy must stay on the surface. So (19) becomes

$$\begin{aligned} l_3 \cos(\beta) &= l_1 \cos(\gamma) - l_2 \cos(\alpha) + l_3 \cos(\beta) \\ 0 &= l_1 \cos(\gamma) - l_2 \cos(\beta) \\ l_2 &= l_1 \frac{\cos(\gamma)}{\cos(\beta)} \end{aligned} \quad (244)$$

and since $L = l_2 + l_3$, one gets

$$l_3 = L - l_1 \frac{\cos(\gamma)}{\cos(\beta)}. \quad (245)$$

At the boundary of areas A and B, β can still be evaluated using (25) and γ_A can be evaluated using Theorem 1. Let $\gamma_A(x)$ be the value of γ inside the area A for a position

$x > 0$. Thus, one has

$$\begin{aligned} \cos(\beta) &= \cos(\operatorname{atan}(\Lambda \tan(\gamma_A(x)))) \\ &= \frac{1}{\sqrt{1 + \Lambda^2 \tan^2(\gamma_A(x))}}. \end{aligned} \quad (246)$$

Using (245) and (246), for a given x , the associate depth $y_{area B}$ can be expressed as

$$\begin{aligned} y_{area B}(x) &= \max([l_3 \cos(\beta), 0]) \\ &= \max([L \cos(\beta) - l_1 \cos(\gamma_A(x)), 0]) \\ &= \max\left(\left[\frac{L}{\sqrt{1 + \Lambda^2 \tan^2(\gamma_A(x))}} - l_1 \cos(\gamma_A(x)), 0\right]\right) \end{aligned} \quad (247)$$

and the ROV is inside the area B if $y < y_{area B}(x)$. Remark $y_{area B}$ can be rewritten

$$y_{area B}(x) = \max\left(\left[\frac{L - l_1 \sqrt{1 + (\Lambda^2 - 1) \sin^2(\gamma_A(x))}}{\sqrt{1 + \Lambda^2 \tan^2(\gamma_A(x))}}, 0\right]\right). \quad (248)$$

B.6.2 Boundary areas B-C, A-C or D1-C

The area C can correspond to two cases : 1) if $L \geq l_1$, the buoy is on the surface but ballast can not taut the cable L , 2) if $L < l_1$, the cable l_1 is not taut because the ROV is too close to the surface. In the first case, the boundary is between the area B and the area C. In the second, the boundary is between the area A or D1 and area C.

Case 1: $L \geq l_1$

In this configuration, area B exist and we search the boundary between the areas B and C. At the boundary of the two areas, the buoy is on the surface and ballast can still taut the cable L . In absence of current, the ballast can apply a tension simultaneously on the cable l_1 and L only for angles γ such $\gamma \in [0, \frac{\pi}{2}]$. Else, the part L of the umbilical will not be taut. Since (21) is still valid at the boundary between areas B and C, one can deduce from (18) and that

$$x = l_1 \sin(\gamma) + L \sin(\beta) \quad (249)$$

For its limit angle $\gamma = 0$, one gets

$$\sin(\beta) = \frac{x}{L}, \quad (250)$$

which is possible only if $x \leq L$.

Put the condition $x \leq L$. Since the buoy is on the surface, one has $y = l_3 \cos(\beta)$. From (19) and since (21), one gets

$$\begin{aligned} y &= l_1 \cos(\gamma) - l_2 \cos(\beta) + l_3 \cos(\beta) \\ 0 &= l_1 - l_2 \cos\left(\operatorname{asin}\left(\frac{x}{L}\right)\right) \\ l_2 &= \frac{l_1}{\sqrt{1 - \frac{x^2}{L^2}}}. \end{aligned} \quad (251)$$

and $l_3 = L - l_2$.

Introducing (251) into $y = l_3 \cos(\beta)$, one gets if $x \leq L$

$$\begin{aligned} y_{area C,1}(x) &= \max\left(\left[\left(L - \frac{l_1}{\sqrt{1 - \frac{x^2}{L^2}}}\right) \sqrt{1 - \frac{x^2}{L^2}}, 0\right]\right) \\ &= \max\left(\left[\sqrt{L^2 - x^2} - l_1, 0\right]\right). \end{aligned} \quad (252)$$

and

$$y_{area C,1}(x) = 0 \quad \text{if } x > L. \quad (253)$$

Remark (252) converges to zero when x converges to $\sqrt{L^2 - l_1^2}$, so $y_{area C,1}(x)$ is continuous and one gets

$$y_{area C,1}(x) = \begin{cases} \sqrt{L^2 - x^2} - l_1 & \text{if } x < \sqrt{L^2 - l_1^2} \\ 0 & \text{else.} \end{cases} \quad (254)$$

where $L > l_1$.

Case 2: $L < l_1$

In this configuration, area B does not exist and the buoy is in contact with the ROV, so we search the boundary of areas A or D1 and C. At the boundary and in absence of current, the buoy is in contact with the ROV, so $\beta = 0$, $l_2 = L$ and $l_3 = 0$, and the ballast can apply a tension simultaneously on the cable l_1 and L only if $\alpha \in [0, \pi]$. For its limit angle $\alpha = 0$, one can deduce from (18) that

$$\sin(\gamma) = \frac{x}{l_1} \quad (255)$$

which is possible only if $x \leq l_1$.

Since the buoy is in contact with the ROV, one has $l_2 = L$ and $l_3 = 0$. Introducing these results in (19) and for $\alpha = 0$, one gets

$$\begin{aligned} y &= l_1 \cos(\gamma) - L \\ &= l_1 \cos\left(\operatorname{asin}\left(\frac{x}{l_1}\right)\right) - L \\ &= l_1 \sqrt{1 - \frac{x^2}{l_1^2}} - L \\ &= \sqrt{l_1^2 - x^2} - L. \end{aligned} \quad (256)$$

Thus, in similar way than for the case 1, one may write

$$y_{area C,2}(x) = \begin{cases} \sqrt{l_1^2 - x^2} - L & \text{if } x < \sqrt{l_1^2 - L^2} \\ 0 & \text{else.} \end{cases} \quad (257)$$

where $l_1 > L$.

Conclusion

The result of the two previous cases can be summarized by

$$y_{area C}(x) = \begin{cases} \sqrt{l_1^2 - x^2} - L, & \text{if } (x < \sqrt{l_1^2 - L^2}) \& (l_1 > L), \\ \sqrt{L^2 - x^2} - l_1, & \text{if } (x < \sqrt{L^2 - l_1^2}) \& (L > l_1), \\ 0 & \text{else.} \end{cases} \quad (258)$$

B.6.3 Boundary areas A-D1

In area D1, the buoy is in contact with the ROV, so $l_3 = 0$ and $l_2 = L$. Thus (18)-(19) becomes

$$x = l_1 \sin(\gamma) - L \sin(\alpha) \quad (259)$$

$$y = l_1 \cos(\gamma) - L \cos(\alpha) \quad (260)$$

At the boundary of areas A and D1, one still have $\beta = -\alpha$ and β can still be evaluated using (25) and γ_A can be evaluate using Theorem 1. Let $\gamma_A(x)$ be the value of γ inside the area A for a position $x > 0$. Thus, one has

$$\begin{aligned} \cos(\beta) &= \cos(\text{atan}(\Lambda \tan(\gamma_A(x)))) \\ &= \frac{1}{\sqrt{1 + \Lambda^2 \tan^2(\gamma_A(x))}}. \end{aligned} \quad (261)$$

Using (261) and (379), the associate depth $y_{area D1}$ can be expressed for a given x as

$$\begin{aligned} y_{area D1}(x) &= \max([l_1 \cos(\gamma_A(x)) - L \cos(\beta), 0]) \\ &= \max\left(\left[l_1 \cos(\gamma_A(x)) - \frac{L}{\sqrt{1 + \Lambda^2 \tan^2(\gamma_A(x))}}, 0\right]\right). \end{aligned} \quad (262)$$

The ROV is inside the area D1 if $y < y_{area D1}(x)$. Remark (262) can be rewritten such

$$y_{area D1}(x) = \frac{l_1 \sqrt{1 + (\Lambda^2 - 1) \sin^2(\gamma_A(x))} - L}{\sqrt{1 + \Lambda^2 \tan^2(\gamma_A(x))}}. \quad (263)$$

B.6.4 Boundary areas A-D2

In area D2, the buoy is in contact with the ballast, so $l_3 = L$ and $l_2 = 0$. Thus (18)-(19) becomes

$$x = l_1 \sin(\gamma) + L \sin(\beta) \quad (264)$$

$$y = l_1 \cos(\gamma) + L \cos(\beta). \quad (265)$$

At the boundary of areas A and D2, β can still be evaluated using (25) and γ_A can be evaluate using Theorem 1. Let $\gamma_A(x)$ be the value of γ inside the area A for a position $x > 0$. One finds (261) again. Thus, using (261) and (383), for a given x , the associate depth $y_{area D2}$ can be expressed as

$$\begin{aligned} y_{area D2}(x) &= \max([l_1 \cos(\gamma_A(x)) + L \cos(\beta), 0]) \\ &= \max\left(\left[l_1 \cos(\gamma_A(x)) + \frac{L}{\sqrt{1 + \Lambda^2 \tan^2(\gamma_A(x))}}, 0\right]\right). \end{aligned} \quad (266)$$

The ROV is inside the area D2 if $y > y_{area D2}(x)$. Remark (266) can be rewritten such

$$y_{area D2}(x) = \max\left(\left[\frac{l_1 \sqrt{1 + (\Lambda^2 - 1) \sin^2(\gamma_A(x))} + L}{\sqrt{1 + \Lambda^2 \tan^2(\gamma_A(x))}}, 0\right]\right). \quad (267)$$

B.6.5 Boundary areas E

The limit for the area E is simple because it corresponds to the maximum length of umbilical. The ROV is always outside the area E in practice because it can not physically go inside. Area E can be expressed such that

$$y_{area E}(x) = \sqrt{l^2 - x^2} \quad (268)$$

where

$$\text{if } x > l, \quad \text{take } x = l, \quad (269)$$

$$\text{if } y > y_{area E}, \quad \text{take } y = y_{area E}. \quad (270)$$

B.7 Calculation of γ , α and β without current

B.7.1 Calculation of γ , α and β in area D1

In area D1, the buoy is in contact with the ROV, so $l_3 = 0$ and $l_2 = L$. One has $x \neq 0$ because the ROV cannot be inside the area D1 if $x = 0$ (areas A or C at $x = 0$). Consider first here $y \neq 0$. Thus (18)-(19) becomes

$$x = l_1 \sin(\gamma) - L \sin(\alpha) \quad (271)$$

$$y = l_1 \cos(\gamma) - L \cos(\alpha). \quad (272)$$

From (272), one gets

$$\cos(\alpha) = \frac{-y + l_1 \cos(\gamma)}{L} \quad (273)$$

and so $\alpha = -\text{acos}\left(\frac{-y + l_1 \cos(\gamma)}{L}\right)$.

Let find now γ . From (273), one has

$$\sin(-\alpha) = \sqrt{1 - \left(\frac{-y + l_1 \cos(\gamma)}{L}\right)^2} \quad (274)$$

By putting $X = \sin(\gamma)$, (274) becomes

$$\sin(-\alpha) = \frac{1}{L} \sqrt{L^2 - \left(-y + l_1 \sqrt{1 - X^2}\right)^2}. \quad (275)$$

Introducing (275) inside (271), one gets

$$x = l_1 X + L \left(\frac{1}{L} \sqrt{L^2 - \left(-y + l_1 \sqrt{1 - X^2}\right)^2}\right) \quad (276)$$

which can be rewritten such

$$\begin{aligned} (x - l_1 X)^2 &= L^2 - \left(-y + l_1 \sqrt{1 - X^2}\right)^2 \\ x^2 - 2l_1 x X + l_1^2 X^2 &= L^2 - \left(y^2 - 2yl_1 \sqrt{1 - X^2} + l_1^2 - l_1^2 X^2\right) \\ x^2 + y^2 + l_1^2 - L^2 - 2l_1 x X &= 2yl_1 \sqrt{1 - X^2} \\ \frac{x^2 + y^2 + l_1^2 - L^2}{2yl_1} - \frac{x}{y} X &= \sqrt{1 - X^2} \end{aligned} \quad (277)$$

Put $a_D = \frac{x^2 + y^2 + l_1^2 - L^2}{2yl_1}$ and $b_D = \frac{x}{y}$. (393) becomes

$$\begin{aligned} (a_D - b_D X)^2 &= 1 - X^2 \\ a_D^2 - 2a_D b_D X + b_D^2 X^2 &= 1 - X^2 \\ a_D^2 - 1 - 2a_D b_D X + (1 + b_D^2) X^2 &= 0 \\ C_D - B_D X + A_D X^2 &= 0 \end{aligned} \quad (278)$$

with $C_D = a_D^2 - 1$, $B_D = 2a_D b_D$ and $A_D = 1 + b_D^2$. The solution of (394) is

$$X = \frac{B_D - \sqrt{B_D^2 - 4A_D C_D}}{2A_D} = \frac{a_D b_D - \sqrt{a_D^2 b_D^2 - (1 + b_D^2)(a_D^2 - 1)}}{(1 + b_D^2)}.$$

Since $X = \sin(\gamma)$, one obtains if $y \neq 0$

$$\sin(\gamma) = \frac{a_D b_D - \sqrt{a_D^2 b_D^2 - (1 + b_D^2)(a_D^2 - 1)}}{(1 + b_D^2)}. \quad (279)$$

Consider now the case $y = 0$ and $x \neq 0$. Following the same steps, one gets

$$\cos(\alpha) = \frac{l_1 \cos(\gamma)}{L} \quad (280)$$

$$\sin(\gamma) = \frac{x^2 + l_1^2 - L^2}{-2l_1 x}. \quad (281)$$

B.7.2 Calculation of γ , α and β in area D2

In area D2, the buoy is in contact with the ballast, so $l_3 = L$ and $l_2 = 0$. Thus (18)-(19) becomes

$$x = l_1 \sin(\gamma) + L \sin(\beta) \quad (282)$$

$$y = l_1 \cos(\gamma) + L \cos(\beta). \quad (283)$$

From (283), one gets

$$\cos(\beta) = \frac{y - l_1 \cos(\gamma)}{L}. \quad (284)$$

From (284), one has $\sin(\beta) = \sqrt{1 - \left(\frac{y - l_1 \cos(\gamma)}{L}\right)^2}$. By putting $X = \sin(\gamma)$, one gets

$$\sin(\beta) = \frac{1}{L} \sqrt{L^2 - \left(y - l_1 \sqrt{1 - X^2}\right)^2}. \quad (285)$$

Remark $(y - l_1 \sqrt{1 - X^2})^2 = (-y + l_1 \sqrt{1 - X^2})^2$. Thus, following the same steps developed in Section B.7.1 from (389) to (395), one gets the same evaluation of γ than for the area D1, *i.e.*

$$\sin(\gamma) = \frac{a_D b_D - \sqrt{a_D^2 b_D^2 - (1 + b_D^2)(a_D^2 - 1)}}{(1 + b_D^2)} \quad (286)$$

with $a_D = \frac{x^2 + y^2 + l_1^2 - L^2}{2yl_1}$ and $b_D = \frac{x}{y}$.

B.7.3 Calculation of γ and β in area B

In area B, the buoy is on the surface but ballast can still taut the cables l_1 and L , so $\gamma \geq 0$, $l_2 > 0$ and $l_3 > 0$. Moreover, since the buoy is on the surface, one has $y = l_3 \cos(\beta)$. Thus, (19) becomes

$$\begin{aligned} l_3 \cos(\beta) &= l_1 \cos(\gamma) - l_2 \cos(\alpha) + l_3 \cos(\beta) \\ 0 &= l_1 \cos(\gamma) - l_2 \cos(\beta) \end{aligned} \quad (287)$$

From $y = l_3 \cos(\beta)$, one has

$$\cos(\beta) = \frac{y}{l_3}. \quad (288)$$

Injecting (288) into (287), one gets

$$\begin{aligned} 0 &= l_1 \cos(\gamma) - (L - l_3) \frac{y}{l_3} \\ 0 &= l_3 l_1 \cos(\gamma) - (L - l_3) y \\ Ly &= l_3 (l_1 \cos(\gamma) + y) \\ l_3 &= \frac{Ly}{l_1 \cos(\gamma) + y}. \end{aligned} \quad (289)$$

and so $l_2 = L - \frac{Ly}{l_1 \cos(\gamma) + y}$. Remark since $\gamma \in [0, \frac{\pi}{2}]$ and $l_1 > 0$, one has $\frac{y}{l_1 \cos(\gamma) + y} \leq 1$, thus (289) guarantees that $0 \leq l_3 \leq L$.

Let find the value of γ now. From (288), one has

$$\sin(\beta) = \sqrt{1 - \left(\frac{y}{l_3}\right)^2} \quad (290)$$

and injecting (289) inside (290), one obtains

$$\sin(\beta) = \sqrt{1 - \left(\frac{l_1 \cos(\gamma) + y}{L}\right)^2}. \quad (291)$$

By putting $X = \sin(\gamma)$, one gets

$$\sin(\beta) = \frac{1}{L} \sqrt{L^2 - \left(l_1 \sqrt{1 - X^2} + y\right)^2}. \quad (292)$$

Using X , $\alpha = -\beta$ and (292) inside (18), one gets

$$\begin{aligned} x &= l_1 \sin(\gamma) + L \sin(\beta) \\ x &= l_1 X + \sqrt{L^2 - \left(y + l_1 \sqrt{1 - X^2}\right)^2} \end{aligned} \quad (293)$$

which can be rewritten such

$$\begin{aligned} (x - l_1 X)^2 &= L^2 - \left(y + l_1 \sqrt{1 - X^2}\right)^2 \\ x^2 - 2l_1 x X + l_1^2 X^2 &= L^2 - \left(y^2 + 2yl_1 \sqrt{1 - X^2} + l_1^2 - l_1^2 X^2\right) \\ x^2 + y^2 + l_1^2 - L^2 - 2l_1 x X &= -2yl_1 \sqrt{1 - X^2} \\ \frac{x^2 + y^2 + l_1^2 - L^2}{2yl_1} - \frac{x}{y} X &= -\sqrt{1 - X^2} \end{aligned} \quad (294)$$

Put $a_D = \frac{x^2 + y^2 + l_1^2 - L^2}{2yl_1}$ and $b_D = \frac{x}{y}$. (393) becomes

$$(a_D - b_D X)^2 = 1 - X^2 \quad (295)$$

Remark the same a_D and b_D used here are exactly the same that the ones used in Section B.7.1. Thus, following the same steps developed in Section B.7.1 from (389) to (395), one gets the same evaluation of γ than for the area D1 and D2, *i.e.*

$$\sin(\gamma) = \frac{a_D b_D - \sqrt{a_D^2 b_D^2 - (1 + b_D^2)(a_D^2 - 1)}}{(1 + b_D^2)} \quad (296)$$

with $a_D = \frac{x^2 + y^2 + l_1^2 - L^2}{2yl_1}$ and $b_D = \frac{x}{y}$. However, the evaluation of β is different and one has

$$\begin{aligned} \cos(\beta) &= \frac{y}{l_3} \\ &= \frac{y + l_1 \cos(\gamma)}{L}. \end{aligned} \quad (297)$$

B.7.4 Calculation of γ and β in area E

Remind the ROV can not physically go inside area E. In view of the practical case, we suppose the measurement of the depth is easier to obtain than the distance x (using a barometer for example) and more accurate. So

$$\text{if } y > l, \quad \text{put } y = l, \quad (298)$$

$$\text{if } y > y_{\text{area E}}(x), \quad \text{put } x = \sqrt{l^2 - y^2} \quad (299)$$

and $\cos(\gamma) = \frac{y}{l}$, $\beta = \gamma$, $l_2 = 0$, $l_3 = L$.

C Proof for umbilical for sea exploration with horizontal current

C.1 Proof of (70)

Since \vec{T}_1 , \vec{T}_2 and \vec{T}_3 are unknown, we project (67) and (68) on the axis perpendiculars to \vec{T}_1 and \vec{T}_3 , noted respectively $\vec{v}_{\perp T1}$ and $\vec{v}_{\perp T3}$:

$$\Sigma_M \vec{F} \cdot \vec{v}_{\perp T1} = F_{tm,x} \sin(\gamma - \psi_{P,x}) - T_2 \sin(\gamma - \alpha) \quad (300)$$

$$\Sigma_B \vec{F} \cdot \vec{v}_{\perp T3} = F_{tb,x} \sin(\beta - \psi_{B,x}) - T_2 \sin(\beta - \alpha). \quad (301)$$

Since $\Sigma_M \vec{F} \cdot \vec{v}_{\perp T1} = 0$ and $\Sigma_B \vec{F} \cdot \vec{v}_{\perp T3} = 0$, one gets

$$T_2 = F_{tm,x} \frac{\sin(\gamma - \psi_{P,x})}{\sin(\gamma - \alpha)} \quad (302)$$

$$T_2 = F_{tb,x} \frac{\sin(\beta - \psi_{B,x})}{\sin(\beta - \alpha)} \quad (303)$$

so

$$F_{tm,x} \frac{\sin(\gamma - \psi_{P,x})}{\sin(\gamma - \alpha)} = F_{tb,x} \frac{\sin(\beta - \psi_{B,x})}{\sin(\beta - \alpha)}. \quad (304)$$

In the case where the buoy does not touch the surface, one has $\alpha = 2\psi_{B,x} - \beta$ and so (304) becomes

$$F_{tm,x} \frac{\sin(\gamma - \psi_{P,x})}{\sin(\gamma - 2\psi_{B,x} + \beta)} = F_{tb,x} \frac{\sin(\beta - \psi_{B,x})}{\sin(2(\beta - \psi_{B,x}))}. \quad (305)$$

By introducing notation $\Gamma = \gamma - \psi_{P,x}$, $B = \beta - \psi_{B,x}$ and $\Delta\psi_x = \psi_{P,x} - \psi_{B,x}$, (305) becomes

$$F_{tm,x} \frac{\sin(\Gamma)}{\sin(\Gamma + B + \Delta\psi_x)} = F_{tb,x} \frac{\sin(B)}{\sin(2B)}. \quad (306)$$

From (306), one may write

$$\frac{F_{tm,x}}{F_{tb,x}} \sin(\Gamma) \sin(2B) = \sin(B) \sin(\Gamma + B + \Delta\psi_x) \quad (307)$$

$$2 \frac{F_{tm,x}}{F_{tb,x}} \sin(\Gamma) (\sin(B) \cos(B)) = \sin(B) (\sin(\Gamma) \cos(B + \Delta\psi_x) + \cos(\Gamma) \sin(B + \Delta\psi_x)) \quad (308)$$

$$2 \frac{F_{tm,x}}{F_{tb,x}} \sin(\Gamma) \cos(B) = \sin(\Gamma) \cos(B + \Delta\psi_x) + \cos(\Gamma) \sin(B + \Delta\psi_x) \quad (309)$$

Since $|\Gamma| \neq \frac{\pi}{2}$ so $\gamma \neq \frac{\pi}{2} - \psi_{P,x}$ or $\gamma \neq -\frac{\pi}{2} + \psi_{P,x}$ and $|B| \neq \frac{\pi}{2}$ so $\beta \neq \frac{\pi}{2} - \psi_{B,x}$ or $\beta \neq -\frac{\pi}{2} + \psi_{B,x}$, one has

$$2 \frac{F_{tm,x}}{F_{tb,x}} \tan(\Gamma) \cos(B) = \tan(\Gamma) [\cos(B) \cos(\Delta\psi_x) - \sin(B) \sin(\Delta\psi_x)] + [\sin(B) \cos(\Delta\psi_x) + \cos(B) \sin(\Delta\psi_x)] \quad (310)$$

$$2 \frac{F_{tm,x}}{F_{tb,x}} \tan(\Gamma) = \tan(\Gamma) [\cos(\Delta\psi_x) - \tan(B) \sin(\Delta\psi_x)] + [\tan(B) \cos(\Delta\psi_x) + \sin(\Delta\psi_x)] \quad (311)$$

$$\left(2 \frac{F_{tm,x}}{F_{tb,x}} - \cos(\Delta\psi_x)\right) \tan(\Gamma) - \sin(\Delta\psi_x) = \tan(B) (\cos(\Delta\psi_x) - \tan(\Gamma) \sin(\Delta\psi_x)) \quad (312)$$

$$\tan(B) = \frac{\left(2 \frac{F_{tm,x}}{F_{tb,x}} - \cos(\Delta\psi_x)\right) \tan(\Gamma) - \sin(\Delta\psi_x)}{\cos(\Delta\psi_x) - \tan(\Gamma) \sin(\Delta\psi_x)} \quad (313)$$

Thus (313) provides a relation between γ and β .

C.2 Calculation of the boundary between areas with current

C.2.1 Boundary areas B-C or A-C with current

The area C can correspond to two cases : 1) if $L \geq l_1$, the buoy is on the surface but ballast can not taut the cable L , 2) if $L < l_1$, the cable l_1 is not taut because the ROV is too close to the surface. Note at the boundary of areas B and C, the following system is still valid

$$x = l_1 \sin(\gamma) - l_2 \sin(\alpha) + l_3 \sin(\beta) \quad (314)$$

$$y = l_1 \cos(\gamma) - l_2 \cos(\alpha) + l_3 \cos(\beta). \quad (315)$$

Let's studied the two cases.

Case 1: $L \geq l_1$

The area C does not exist theoretically when $L > l_1$ because the umbilical can always be stretched by the current: $\alpha, \beta, \gamma, l_2, l_3$ can always be found such the umbilical is taut. Thus

$$y_{\text{area C}}(x) = 0 \quad \text{if } L \geq l_1. \quad (316)$$

Case 2: $L < l_1$

In this configuration, area B does not exist and the buoy is in contact with the ROV, so the boundary of areas D1 and C is searched. Since the buoy is in contact with the ROV in area D1, one has $l_2 = L$ and $l_3 = 0$, and the ballast can apply a tension simultaneously on the cable l_1 and L only if $\alpha \in [-\pi, 0]$ when $x > 0$ and $\alpha \in [0, \pi]$ when $x \leq 0$. For its limit angle $\alpha = 0$ and since $l_3 = 0$, one can deduce from (314) that

$$x = l_1 \sin(\gamma) \quad \sin(\gamma) = \frac{x}{l_1} \quad (317)$$

which is possible only if $|x| \leq l_1$.

Using (317), $l_2 = L$ and $l_3 = 0$ inside (315), one gets

$$y_{area C,2}(x) = \begin{cases} l_1 \cos\left(\text{asin}\left(\frac{x}{l_1}\right)\right) - L & \text{if } |x| < \sqrt{l_1^2 - L^2} \\ 0 & \text{else.} \end{cases} \quad (318)$$

which is equal to

$$y_{area C,2}(x) = \begin{cases} \sqrt{l_1^2 - x^2} - L & \text{if } |x| < \sqrt{l_1^2 - L^2} \\ 0 & \text{else.} \end{cases} \quad (319)$$

Conclusion

The result of the two previous cases can be summarized by

$$y_{area C}(x) = \begin{cases} \sqrt{l_1^2 - x^2} - L & \text{if } (|x| \leq \sqrt{l_1^2 - L^2}) \& (l_1 > L), \\ 0 & \text{else.} \end{cases} \quad (320)$$

C.2.2 Boundary areas A-F

There are two boundaries between the areas A-F, the first corresponding to $|\alpha - \beta| = 0$, the second to $|\alpha - \gamma| = 0$. To take into account the rigidity of the umbilical and a safety margin, this proof is evaluated defining $|\alpha - \beta| = \theta_{\min}$ and $|\alpha - \gamma| = \theta_{\min}$, where $\theta_{\min} \geq 0$ is the value defined in (53) in Section 5.6. Let $y_{area F1}$ and $y_{area F2}$ be the two boundaries, and consider the ROV is inside the area F if $y_{area F1} \leq y \leq y_{area F2}$.

Boundary areas A-F, side $|\alpha - \beta| = \theta_{\min}$

Let's find the limit $|\alpha - \beta| = \theta_{\min}$. Since $\beta = 2\psi_{B,x} - \alpha$, one has

$$\beta = \psi_{B,x} - \frac{\theta_{\min}}{2}s \quad (321)$$

$$\alpha = \psi_{B,x} + \frac{\theta_{\min}}{2}s \quad (322)$$

where $s = \text{sign}(\psi_{B,x})$ if $\psi_{B,x} \neq 0$, $s = -\text{sign}(x)$ else. Injecting (321)-(322) inside the system (18)-(20), one gets

$$x = l_1 \sin(\gamma) - (L - l_3) \sin\left(\psi_{B,x} + \frac{\theta_{\min}}{2}s\right) + l_3 \sin\left(\psi_{B,x} - \frac{\theta_{\min}}{2}s\right) \quad (323)$$

$$y = l_1 \cos(\gamma) - (L - l_3) \cos\left(\psi_{B,x} + \frac{\theta_{\min}}{2}s\right) + l_3 \cos\left(\psi_{B,x} - \frac{\theta_{\min}}{2}s\right) \quad (324)$$

The value of γ can be evaluated with (70) using the value of β defined in (321). Consider first (323):

$$x = l_1 \sin(\gamma) - L \sin\left(\psi_{B,x} + \frac{\theta_{\min}}{2}s\right) + l_3 \left(\sin\left(\psi_{B,x} + \frac{\theta_{\min}}{2}s\right) + \sin\left(\psi_{B,x} - \frac{\theta_{\min}}{2}s\right) \right) \quad (325)$$

$$l_3 = \frac{x - l_1 \sin(\gamma) + L \sin\left(\psi_{B,x} + \frac{\theta_{\min}}{2}s\right)}{\sin\left(\psi_{B,x} + \frac{\theta_{\min}}{2}s\right) + \sin\left(\psi_{B,x} - \frac{\theta_{\min}}{2}s\right)}$$

Consider the value of l_3 found using (325). If $l_3 > L$ or $l_3 < 0$, the buoy is in contact with the ballast (area D2) or the ROV (area D1), and the value $y_{area F1} = l$ and $y_{area F1} = 0$ are taken to close the area with the surface or the umbilical length. Else, the value of $y_{area F1}$ is evaluated using (324).

The value of $y_{area F1}$ can be expressed as

$$y_{area F1} = \begin{cases} l_1 \cos(\gamma) - (L - l_{33}) \cos\left(\psi_{B,x} + \frac{\theta_{\min}}{2}s\right) + l_{33} \cos\left(\psi_{B,x} - \frac{\theta_{\min}}{2}s\right) & \text{if } 0 \leq l_{33} \leq L \\ l & \text{if } l_{33} > L \\ 0 & \text{else,} \end{cases} \quad (326)$$

with

$$l_{33} = \frac{x - l_1 \sin(\gamma_{F1}) + L \sin\left(\psi_{B,x} + \frac{\theta_{\min}}{2}s\right)}{\sin\left(\psi_{B,x} + \frac{\theta_{\min}}{2}s\right) + \sin\left(\psi_{B,x} - \frac{\theta_{\min}}{2}s\right)} \quad (327)$$

where γ_{F1} is evaluated with (70) using $\beta = \psi_{B,x} - \frac{\theta_{\min}}{2}s$ with $s = \text{sign}(\psi_{B,x})$ if $\psi_{B,x} \neq 0$, $s = -\text{sign}(x)$ else.

Boundary areas A-F, $|\alpha - \gamma| = \theta_{\min}$

The cross between l_1 and l_2 can happened only for $\gamma = \psi_{P,x}$, i.e. when the ballast cannot pull the cable l_1 . Let's find the limit $|\alpha - \gamma| = \theta_{\min}$ when γ comes close to $\psi_{P,x} + \frac{\theta_{\min}}{2}s$, where $s = \text{sign}(\psi_{B,x})$ if $\psi_{B,x} \neq 0$, $s = -\text{sign}(x)$ else. Thus, one gets

$$\alpha = \psi_{P,x} - \frac{\theta_{\min}}{2}s \quad (328)$$

$$\beta = 2\psi_{B,x} - \alpha = 2\psi_{B,x} - \psi_{P,x} + \frac{\theta_{\min}}{2}s \quad (329)$$

Injecting (328)-(329) inside the system (18)-(20), one gets

$$x = l_1 \sin\left(\psi_{P,x} + \frac{\theta_{\min}}{2}s\right) - l_2 \sin\left(\psi_{P,x} - \frac{\theta_{\min}}{2}s\right) + (L - l_2) \sin\left(2\psi_{B,x} - \psi_{P,x} + \frac{\theta_{\min}}{2}s\right) \quad (330)$$

$$y = l_1 \cos\left(\psi_{P,x} + \frac{\theta_{\min}}{2}s\right) - l_2 \cos\left(\psi_{P,x} - \frac{\theta_{\min}}{2}s\right) + (L - l_2) \cos\left(2\psi_{B,x} - \psi_{P,x} + \frac{\theta_{\min}}{2}s\right) \quad (331)$$

Consider first (330):

$$x = l_1 \sin\left(\psi_{P,x} + \frac{\theta_{\min}}{2}s\right) - l_2 \sin\left(\psi_{P,x} - \frac{\theta_{\min}}{2}s\right) + (L - l_2) \sin\left(2\psi_{B,x} - \psi_{P,x} + \frac{\theta_{\min}}{2}s\right) \quad (332)$$

$$x = l_1 \sin\left(\psi_{P,x} + \frac{\theta_{\min}}{2}s\right) + L \sin\left(2\psi_{B,x} - \psi_{P,x} + \frac{\theta_{\min}}{2}s\right) - l_2 \left[\sin\left(2\psi_{B,x} - \psi_{P,x} + \frac{\theta_{\min}}{2}s\right) + \sin\left(\psi_{P,x} - \frac{\theta_{\min}}{2}s\right) \right]$$

$$l_2 = \frac{l_1 \sin\left(\psi_{P,x} + \frac{\theta_{\min}}{2}s\right) + L \sin\left(2\psi_{B,x} - \psi_{P,x} + \frac{\theta_{\min}}{2}s\right) - x}{\sin\left(2\psi_{B,x} - \psi_{P,x} + \frac{\theta_{\min}}{2}s\right) + \sin\left(\psi_{P,x} - \frac{\theta_{\min}}{2}s\right)}$$

Consider the value of l_2 found using (332). If $l_2 < 0$ or $l_2 > L$, the buoy is in contact with the ballast (area D2) or the

ROV (area D1), and the value $y_{area F2} = l$ and $y_{area F2} = 0$ are taken to close the area with the surface or the umbilical length. Else, the value of $y_{area F2}$ is evaluated using (331).

The value of $y_{area F2}$ can be expressed as

$$y_{area F2} = \begin{cases} l_1 \cos(\psi_{P,x} + \frac{\theta_{min}}{2}s) - l_{22} \cos(\psi_{P,x} + \frac{\theta_{min}}{2}s) \\ + (L - l_{22}) \cos(2\psi_{B,x} - \psi_{P,x} - \frac{\theta_{min}}{2}s) & \text{if } 0 \leq l_{22} \leq L \\ l & \text{if } (l_{22} < 0) \& (l_{33} \geq L) \\ 0 & \text{else,} \end{cases} \quad (333)$$

with $l_{22} = \frac{l_1 \sin(\psi_{P,x} + \frac{\theta_{min}}{2}s) + L \sin(2\psi_{B,x} - \psi_{P,x} + \frac{\theta_{min}}{2}s) - x}{\sin(2\psi_{B,x} - \psi_{P,x} + \frac{\theta_{min}}{2}s) + \sin(\psi_{P,x} - \frac{\theta_{min}}{2}s)}$, and $s = \text{sign}(\psi_{B,x})$ if $\psi_{B,x} \neq 0$, $s = -\text{sign}(x)$ else.

D Evaluation of strengths apply on the ROV with presence of current

Let's find the value of T_3 by performing the fundamental principle of static on B:

$$\begin{aligned} \Sigma_B \vec{F} \cdot \vec{x} &= 0 \\ T_3 \cos(\beta) &= T_2 \cos(\alpha) - F_{cx,b}. \end{aligned} \quad (334)$$

From (303), one has $T_2 = F_{tb,x} \frac{\sin(\beta - \psi_{B,x})}{\sin(\beta - \alpha)}$, so (334) becomes

$$T_3 \cos(\beta) = F_{tb,x} \frac{\sin(\beta - \psi_{B,x})}{\sin(\beta - \alpha)} \cos(\alpha) - F_{cx,b} \quad (335)$$

Since the ROV is not inside the area B or C, one has $\alpha = 2\psi_{B,x} - \beta$, thus

$$T_3 \cos(\beta) = F_{tb,x} \frac{\sin(\beta - \psi_{B,x})}{\sin(2(\beta - \psi_{B,x}))} \cos(2\psi_{B,x} - \beta) - F_{cx,b} \quad (336)$$

$$T_3 = F_{tb,x} \frac{\cos(2\psi_{B,x} - \beta)}{2 \cos(\beta - \psi_{B,x}) \cos(\beta)} - \frac{F_{cx,b}}{\cos(\beta)} \quad (337)$$

The strengths $F_{ROV,x}$ and $F_{ROV,y}$ can so be expressed as

$$\begin{aligned} \vec{F}_{ROV,x} \cdot \vec{x} &= - \left(F_{tb,x} \frac{\cos(2\psi_{B,x} - \beta)}{2 \cos(\beta - \psi_{B,x})} - F_{cx,b} \right) \tan(\beta) \\ &+ F_{cx,ROV} \end{aligned} \quad (338)$$

$$\vec{F}_{ROV,y} \cdot \vec{y} = F_{tb,x} \frac{\cos(2\psi_{B,x} - \beta)}{2 \cos(\beta - \psi_{B,x})} - F_{cx,b} + F_{cy,ROV}. \quad (339)$$

E Proof for sea exploration, 3D case

E.1 Calculation of l_{1x}, l_{2x}, l_{3x} and l_{1z}, l_{2z}, l_{3z}

Let define y_M and y_B the coordinate of the ballast M and the buoy B on the axis \vec{Oy} . Since y_M and y_B can be evaluated in the plans (O, x, y) and (O, z, y) , one has

$$y_M = l_{1x} \cos(\gamma) = l_{1z} \cos(\phi) \quad (340)$$

$$y_B = y - l_{3x} \cos(\beta) = y - l_{3z} \cos(\eta) \quad (341)$$

$$y_B = l_{1x} \cos(\gamma) - l_{2x} \cos(\alpha) = l_{1z} \cos(\phi) - l_{2z} \cos(\mu). \quad (342)$$

Using (340)-(342), one gets

$$l_{1x} = l_{1z} \frac{\cos(\phi)}{\cos(\gamma)} \quad (343)$$

$$l_{2x} = l_{2z} \frac{\cos(\mu)}{\cos(\alpha)} \quad (344)$$

$$l_{3x} = l_{3z} \frac{\cos(\eta)}{\cos(\beta)}. \quad (345)$$

Using (343) and (90), one gets

$$\begin{aligned} l_1^2 &= l_{1x}^2 + \sin(\phi)^2 l_{1z}^2 \\ l_1^2 &= l_{1x}^2 + \sin(\phi)^2 \left(\frac{\cos(\gamma)}{\cos(\phi)} \right)^2 l_{1x}^2 \\ l_1^2 &= \left(1 + \tan(\phi)^2 \cos(\gamma)^2 \right) l_{1x}^2 \\ l_{1x}^2 &= \frac{l_1^2}{\left(1 + \tan(\phi)^2 \cos(\gamma)^2 \right)}. \end{aligned} \quad (346)$$

In the same way, one gets

$$\begin{aligned} l_1^2 &= l_{1x}^2 + \sin(\phi)^2 l_{1z}^2 \\ l_1^2 &= l_{1z}^2 \left(\frac{\cos(\phi)}{\cos(\gamma)} \right)^2 + \sin(\phi)^2 l_{1z}^2 \\ l_{1z}^2 &= \frac{l_1^2}{\left(\sin(\phi)^2 + \left(\frac{\cos(\phi)}{\cos(\gamma)} \right)^2 \right)}. \end{aligned} \quad (347)$$

Same calculation can be made for l_{2x}^2, l_{2z}^2 and l_{3x}^2, l_{3z}^2 , using respectively (344)-(91) and (345)-(92).

F Proof for umbilical for diving exploration with presence of large obstacles

F.1 Proof of (127)

Let perform the principle of the fundamental principle of static on $B1$ and $B2$ illustrates in Figure 16:

$$\Sigma_{B2} \vec{F} = -F_{b2} \vec{y} + \vec{T}_3 + \vec{T}_4 \quad (348)$$

$$\Sigma_{B1} \vec{F} = -F_{b1} \vec{y} - \vec{T}_3 + \vec{T}_2 \quad (349)$$

where \vec{T}_4 is the tension of the cable l_4 on $B2$ and \vec{T}_2, \vec{T}_3 are the tension on the cable on $B1$ as defined in Section 5.2. Since \vec{T}_2, \vec{T}_3 and \vec{T}_4 are unknown, (348)-(349) is projected on the axis perpendicular to \vec{T}_2 and \vec{T}_4 , respectively noted $\vec{v}_{\perp T2}$ and $\vec{v}_{\perp T4}$:

$$\Sigma_{B2} \vec{F} \cdot \vec{v}_{\perp T4} = -F_{b2} \sin(\eta) + T_3 \sin(\beta - \eta) \quad (350)$$

$$\Sigma_{B1} \vec{F} \cdot \vec{v}_{\perp T2} = -F_{b1} \sin(\beta) + T_3 \sin(\beta - \alpha). \quad (351)$$

Since $\Sigma_{B2} \vec{F} \cdot \vec{v}_{\perp T4} = 0$ and $\Sigma_{B1} \vec{F} \cdot \vec{v}_{\perp T2} = 0$, one gets from (350)-(351)

$$F_{b2} \frac{\sin(\eta)}{\sin(\beta - \eta)} = F_{b1} \frac{\sin(\beta)}{\sin(\beta - \alpha)} \quad (352)$$

Since $\alpha = -\beta$, one gets

$$\begin{aligned} F_{b2} \frac{\sin(\eta)}{\sin(\beta - \eta)} &= F_{b1} \frac{\sin(\beta)}{\sin(2\beta)} \\ \frac{F_{b2}}{F_{b1}} \frac{\sin(\eta)}{\sin(\beta - \eta)} &= \frac{1}{2 \cos(\beta)} \\ 2 \frac{F_{b2}}{F_{b1}} \cos(\beta) \sin(\eta) &= \sin(\beta) \cos(\eta) - \cos(\beta) \sin(\eta) \\ 2 \frac{F_{b2}}{F_{b1}} \tan(\eta) &= \tan(\beta) - \tan(\eta) \\ \left(2 \frac{F_{b2}}{F_{b1}} + 1\right) \tan(\eta) &= \tan(\beta) \\ \tan(\beta) &= \Lambda_2 \tan(\eta) \end{aligned} \quad (353)$$

with $\Lambda_2 = 2 \frac{F_{b2}}{F_{b1}} + 1$.

F.2 Proof of Theorem 7

Using $\beta = -\alpha = \gamma$, the system (121)-(122) becomes

$$x = (l_1 + L) \sin(\beta) + l_4 \sin(\eta) \quad (354)$$

$$y = (l_1 - l_2 + l_3) \cos(\gamma) + l_4 \cos(\eta). \quad (355)$$

From (354) and (127), one can observe that the value of η can be obtained following the same step that for Theorem 1 by replacing l_1 , L and Λ by l_4 , $(l_1 + L) = 2l_1$ and Λ_2 , which is summarized in Theorem 8 and described in Appendix F.3.

From (355), one has

$$\begin{aligned} y &= (l_1 - l_2 + (L - l_2)) \cos(\gamma) + l_4 \cos(\eta) \\ \frac{y - l_4 \cos(\eta)}{\cos(\gamma)} &= (L + l_1 - 2l_2) \\ l_2 &= \frac{L + l_1}{2} - \frac{y - l_4 \cos(\eta)}{2 \cos(\gamma)}. \end{aligned} \quad (356)$$

and $l_3 = L - l_2$.

Let's find now the values of F_{b2} and x_{\max} such $\eta \leq \eta_{\max}$ inside $[x_{\min}, x_{\max}] \times [y_{\min}, y_{\max}]$. Considering first x_{\max} , one has x_{\max} when $\eta = \eta_{\max}$, so

$$x_{\max} = (l_1 + L) \sin(\beta_{\min}) + l_4 \sin(\eta_{\max}) \quad (357)$$

with β_{\min} is evaluated using (127) for $\eta = \eta_{\max}$. Thus, using (127), one may write

$$\begin{aligned} \sin(\beta_{\min}) &= \sin(\operatorname{atan}(\Lambda_2 \tan(\eta_{\max}))) \\ &= \frac{\Lambda_2 \tan(\eta_{\max})}{\sqrt{1 + (\Lambda_2 \tan(\eta_{\max}))^2}} \end{aligned} \quad (358)$$

where the value of Λ_2 is unknown here because the value of F_{b2} has not been defined yet. Continue to focus on (357):

$$x_{\max} = \frac{\Lambda_2 \tan(\eta_{\max}) (l_1 + L)}{\sqrt{1 + (\Lambda_2 \tan(\eta_{\max}))^2}} + l_4 \sin(\eta_{\max})$$

$$\begin{aligned} \Lambda_2 \tan(\eta_{\max}) (l_1 + L) &= (x_{\max} - l_4 \sin(\eta_{\max})) \\ &\quad \times \sqrt{1 + (\Lambda_2 \tan(\eta_{\max}))^2} \end{aligned}$$

$$\begin{aligned} \Lambda_2^2 \tan(\eta_{\max})^2 (l_1 + L)^2 &= (x_{\max} - l_4 \sin(\eta_{\max}))^2 \\ &\quad \times \left(1 + (\Lambda_2 \tan(\eta_{\max}))^2\right). \end{aligned} \quad (359)$$

Remind $L = l_1$ and put $\Gamma = x_{\max} - l_4 \sin(\eta_{\max})$. Then

$$\begin{aligned} \Lambda_2^2 \tan(\eta_{\max})^2 (4l_1^2) &= \Gamma^2 \left(1 + (\Lambda_2 \tan(\eta_{\max}))^2\right) \\ \Lambda_2^2 \tan(\eta_{\max})^2 (4l_1^2 - \Gamma^2) &= \Gamma^2 \\ \Lambda_2 &= \frac{|\Gamma|}{\tan(\eta_{\max}) \sqrt{4l_1^2 - \Gamma^2}} \end{aligned} \quad (360)$$

where $4l_1^2 - \Gamma^2 > 0$ if

$$\begin{aligned} 4l_1^2 &> (x_{\max} - l_4 \sin(\eta_{\max}))^2 \\ 2l_1 + l_4 \sin(\eta_{\max}) &> x_{\max}. \end{aligned} \quad (361)$$

(361) provides a condition on x_{\max} . Go back to (360):

$$\begin{aligned} \Lambda_2 &= \frac{|x_{\max} - l_4 \sin(\eta_{\max})|}{\tan(\eta_{\max}) \sqrt{4l_1^2 - (x_{\max} - l_4 \sin(\eta_{\max}))^2}} \\ 2 \frac{F_{b2}}{F_{b1}} + 1 &= \frac{|x_{\max} - l_4 \sin(\eta_{\max})|}{\tan(\eta_{\max}) \sqrt{4l_1^2 - (x_{\max} - l_4 \sin(\eta_{\max}))^2}} \\ F_{b2} &= \frac{F_{b1}}{2} \left(\frac{|x_{\max} - l_4 \sin(\eta_{\max})|}{\tan(\eta_{\max}) \sqrt{4l_1^2 - (x_{\max} - l_4 \sin(\eta_{\max}))^2}} - 1 \right). \end{aligned} \quad (362)$$

The value of F_{b2} must so be chosen equal or larger than $\frac{F_{b1}}{2} \left(\frac{|x_{\max} - l_4 \sin(\eta_{\max})|}{\tan(\eta_{\max}) \sqrt{4l_1^2 - (x_{\max} - l_4 \sin(\eta_{\max}))^2}} - 1 \right)$ to guarantee $\eta \leq \eta_{\max}$ inside $[x_{\min}, x_{\max}]$.

F.3 Proof of Theorem 8

Let first remind $\Lambda_2 \tan(\eta) = \tan(\beta)$ and let's write

$$\begin{aligned} \sin(\beta) &= \sin(\operatorname{atan}(\Lambda_2 \tan(\eta))) \\ &= \frac{\Lambda_2 \tan(\eta)}{\sqrt{1 + (\Lambda_2 \tan(\eta))^2}}. \end{aligned} \quad (363)$$

Put $X = \sin(\eta)$. One has

$$\tan(\eta) = \frac{X}{\sqrt{1 - X^2}} \quad (364)$$

and so (363) becomes

$$\begin{aligned} \sin(\beta) &= \frac{\frac{\Lambda_2 X}{\sqrt{1 - X^2}}}{\sqrt{1 + \left(\frac{\Lambda_2 X}{\sqrt{1 - X^2}}\right)^2}} \\ &= \frac{\Lambda_2 X}{\sqrt{1 + (\Lambda_2^2 - 1) X^2}}. \end{aligned} \quad (365)$$

By introducing (21),(20), (126) inside (121) and since $l_1 = L$, one gets

$$\begin{aligned} x &= l_1 \sin(\gamma) + L \sin(\beta) + l_4 \sin(\eta) \\ x &= 2L \sin(\beta) + l_4 \sin(\eta). \end{aligned} \quad (366)$$

Let's introduce X and (365) inside (366):

$$x = l_4 X + \frac{2L\Lambda_2 X}{\sqrt{1 + (\Lambda_2^2 - 1) X^2}}$$

$$(x - l_4 X) \sqrt{1 + (\Lambda_2^2 - 1) X^2} = 2L\Lambda_2 X$$

$$(x - l_4 X)^2 (1 + (\Lambda_2^2 - 1) X^2) = (2L\Lambda_2 X)^2$$

$$(x^2 - 2xl_4 X + l_4^2 X^2) (1 + (\Lambda_2^2 - 1) X^2) = 4L^2 \Lambda_2^2 X^2$$

$$\begin{aligned} x^2 + x^2 (\Lambda_2^2 - 1) X^2 - 2xl_4 X - 2xl_4 (\Lambda_2^2 - 1) X^3 \\ + l_4^2 X^2 + l_4^2 (\Lambda_2^2 - 1) X^4 - 4L^2 \Lambda_2^2 X^2 = 0 \end{aligned} \quad (367)$$

which can be reorganised such

$$aX^4 + bX^3 + cX^2 + dX + E = 0 \quad (368)$$

with

$$a = l_4^2 (\Lambda_2^2 - 1) \quad (369)$$

$$b = -2xl_4 (\Lambda_2^2 - 1) \quad (370)$$

$$c = x^2 (\Lambda_2^2 - 1) - 4L^2 \Lambda_2^2 + l_4^2 \quad (371)$$

$$d = -2xl_4 \quad (372)$$

$$e = x^2. \quad (373)$$

By putting $X = Y - \frac{b}{4a}$, (368) becomes

$$Y^4 + A_\eta Y^2 + B_\eta Y + C_\eta = 0 \quad (374)$$

with

$$A_\eta = -\frac{x^2}{2l_4^2} - \frac{(4l_1^2 \Lambda_2^2 - l_4^2)}{l_4^2 (\Lambda_2^2 - 1)} \quad (375)$$

$$B_\eta = -\frac{l_4^2 + 4l_1^2 \Lambda_2^2}{l_4^3 (\Lambda_2^2 - 1)} x \quad (376)$$

$$C_\eta = \frac{x^4}{16l_4^4} + \frac{x^2 (l_4^2 - 4l_1^2 \Lambda_2^2)}{4l_4^4 (\Lambda_2^2 - 1)} \quad (377)$$

(368) is a quartic function which can be solved using Ludovico Ferrari, similarly to the model studied in Section B.5 for the Theorem 9. From these results, the Theorem 8 can be written.

F.4 Proofs of boundaries

F.4.1 Boundary areas A-B, B-C and A-C

The minimal depth y_{\min} has been chosen such $y_{\min} = \max([l_1 + h_M, l_4])$ and one has $l_1 = L$. Thus, since the ROV stay inside the working area where $y \in [y_{\min}, y_{\max}]$, the buoy can touch the surface only for $x = 0$. Areas B and C does not exist inside the working area.

F.4.2 Boundary areas A-D1

In area D1, the buoy is in contact with the ROV, so $l_3 = 0$ and $l_2 = L$. Thus (121)-(122) becomes

$$x = l_1 \sin(\gamma) - L \sin(\alpha) + l_4 \sin(\eta) \quad (378)$$

$$y = l_1 \cos(\gamma) - L \cos(\alpha) + l_4 \cos(\eta) \quad (379)$$

At the boundary between area A and D1, one still have $\gamma = \beta = -\alpha$, and since $l_1 = L$, one has

$$x = L \sin(\gamma) + l_4 \sin(\eta) \quad (380)$$

$$y = l_4 \cos(\eta) \quad (381)$$

where $y = l_4 \cos(\eta) \leq l_4$ and since $y_{\min} = \max([l_1 + h_B, l_4])$, one has $y \leq y_{\min}$ for all y inside the area D1. Thus, the area D1 is outside the working area $[x_{\min}, x_{\max}] \times [y_{\min}, y_{\max}]$ and therefore are not require for the umbilical model.

F.4.3 Boundary areas A-D2

In area D2, the buoy is in contact with the ballast, so $l_3 = L$ and $l_2 = 0$. At the boundary between area A and D2, one still has $\gamma = \beta = -\alpha$, and since $l_1 = L$, (121)-(122) becomes

$$x = 2L \sin(\beta) + l_4 \sin(\eta) \quad (382)$$

$$y = 2L \cos(\beta) + l_4 \cos(\eta) \quad (383)$$

At the boundary of areas A and D2, β can still be evaluated using (127) and η_A can be evaluated using Theorem 8. Let $\eta_A(x)$ be the value of η inside the area A for a position $x > 0$, and so an evaluation $\beta_A(x)$ from (127) and $\eta_A(x)$. Thus, for a given x , the $y_{area D2}$ can be expressed as

$$\begin{aligned} y_{area D2}(x) \\ = \max([2L \cos(\beta_A(x)) + l_4 \cos(\eta_A(x)), 0]) \\ = \max\left(\left[\frac{2L}{\sqrt{1 + \Lambda_2^2 \tan^2(\eta_A(x))}} + l_4 \cos(\eta_A(x)), 0\right]\right) \end{aligned} \quad (384)$$

F.4.4 Calculation of γ , α , β and η in area D2

In area D2, the buoy is in contact with the ballast, so $l_3 = L$ and $l_2 = 0$. Since $l_1 = L$ and $\beta = \gamma$, (121)-(122) becomes

$$x = 2L \sin(\gamma) + l_4 \sin(\eta) \quad (385)$$

$$y = 2L \cos(\gamma) + l_4 \cos(\eta) \quad (386)$$

From (386), one gets

$$\cos(\eta) = \frac{y - 2L \cos(\gamma)}{l_4}. \quad (387)$$

From (388), one has $\sin(\eta) = \sqrt{1 - \left(\frac{y - 2L \cos(\gamma)}{l_4}\right)^2}$. By putting $X = \sin(\gamma)$, one gets

$$\sin(\eta) = \frac{1}{l_4} \sqrt{l_4^2 - \left(y - 2L \sqrt{1 - X^2}\right)^2}. \quad (388)$$

Remind $y \geq y_{\min} > 0$ so $y \neq 0$. Introducing (388) inside (385), one gets

$$x = 2LX + l_4 \left(\frac{1}{l_4} \sqrt{l_4^2 - \left(-y + 2L \sqrt{1 - X^2}\right)^2}\right) \quad (389)$$

which can be rewritten such

$$(x - 2LX)^2 = l_4^2 - \left(-y + 2L \sqrt{1 - X^2}\right)^2 \quad (390)$$

$$\begin{aligned} x^2 - 4LxX + 4L^2X^2 \\ = l_4^2 - \left(y^2 - 4yL\sqrt{1-X^2} + 4L^2 - 4L^2X^2 \right) \end{aligned} \quad (391)$$

$$x^2 + y^2 + 4L^2 - l_4^2 - 4LxX = 4yL\sqrt{1-X^2} \quad (392)$$

$$\frac{x^2 + y^2 + 4L^2 - l_4^2}{4yL} - \frac{x}{y}X = \sqrt{1-X^2} \quad (393)$$

Put $a_D = \frac{x^2 + y^2 + 4L^2 - l_4^2}{4yL}$ and $b_D = \frac{x}{y}$. (393) becomes

$$\begin{aligned} (a_D - b_DX)^2 &= 1 - X^2 \\ a_D^2 - 2a_Db_DX + b_D^2X^2 &= 1 - X^2 \\ a_D^2 - 1 - 2a_Db_DX + (1 + b_D^2)X^2 &= 0 \\ C_D - B_DX + A_DX^2 &= 0 \end{aligned} \quad (394)$$

with $C_D = a_D^2 - 1$, $B_D = 2a_Db_D$ and $A_D = 1 + b_D^2$. Since $F_{b2} > F_{b1} = P$, the solution of (394) is

$$\begin{aligned} X &= \frac{B_D + \sqrt{B_D^2 - 4A_DC_D}}{2A_D} \\ &= \frac{a_Db_D + \sqrt{a_D^2b_D^2 - 4(1 + b_D^2)(a_D^2 - 1)}}{(a_D^2 - 1)}. \end{aligned}$$

Since $X = \sin(\gamma)$, one obtains if $y \neq 0$

$$\sin(\gamma) = \frac{a_Db_D + \sqrt{a_D^2b_D^2 - 4(1 + b_D^2)(a_D^2 - 1)}}{(a_D^2 - 1)}. \quad (395)$$

F.5 Study of strengths applied on the ROV

Since \vec{T}_2 , \vec{T}_3 and \vec{T}_4 are unknown, (145)-(146) are projected respectively on the axis perpendicular to \vec{T}_2 , noted $\vec{v}_{\perp T_2}$, and \vec{y} :

$$\Sigma_{B1} \vec{F} \cdot \vec{v}_{\perp T_2} = -F_{b1} \sin(\beta) + T_3 \sin(\beta - \alpha) \quad (396)$$

$$\Sigma_{B2} \vec{F} \cdot \vec{y} = F_{b2} - T_4 \cos(\eta) + T_3 \cos(\beta) \quad (397)$$

Since $\alpha = -\beta$, one gets

$$T_3 = F_{b1} \frac{\sin(\beta)}{\sin(2\beta)} \quad (398)$$

$$T_4 = \frac{F_{b2} + T_3 \cos(\beta)}{\cos(\eta)} \quad (399)$$

One has $\frac{\sin(\beta)}{\sin(2\beta)} = \frac{1}{2\cos(\beta)}$ and $\|\vec{T}_4\| = \|\vec{F}_{cable \rightarrow ROV}\|$, one has

$$F_{cable \rightarrow ROV} = \frac{F_{b2} + \frac{1}{2}F_{b1}}{\cos(\eta)}. \quad (400)$$

Since $\eta \leq \eta_{\max}$, the strength applied on the ROV can be bounded such

$$F_{cable \rightarrow ROV} \leq \frac{F_{b2} + \frac{1}{2}F_{b1}}{\cos(\eta_{\max})}. \quad (401)$$

G Proof of Section 9.2: maximum ROV velocity

Let's apply the fundamental principle of dynamic (FPD) on the axis x and y .

FPD applied on axis \vec{y}

Let use the FPD of the buoy projected on \vec{y} :

$$\begin{aligned} (m_b \vec{a}_{b,y}) \cdot \vec{y} &= \left(\vec{F}_b + \vec{F}_{fb} + \vec{F}_{cx,b} + \vec{F}_{cy,b} \right) \cdot \vec{y} \\ m_b \dot{v}_{b,y} &= (\rho_{water} V_b - m_b) g - K_b v_{b,y} + F_{cy,b} \\ \dot{v}_{b,y} &= \left(\frac{\rho_{water} V_b}{m_b} - 1 \right) g + \frac{F_{cy,b}}{m_b} - \frac{K_b}{m_b} v_{b,y} \end{aligned} \quad (402)$$

Let solve the differential equation (402). The hypothetical solution is $v_{b,y,HS} = A \exp\left(-\frac{K_b}{m_b} t\right)$ with A a constant. Using the variation of the constant method, a particular solution can be found $v_{b,y,PS} = \frac{m_b}{K_b} \left[\left(\frac{\rho_{water} V_b}{m_b} - 1 \right) g + \frac{F_{cy,b}}{m_b} \right]$. The general solution $v_{b,y} = v_{b,y,PS} + v_{b,y,HS}$ can be expressed as

$$\begin{aligned} v_{b,y}(t) &= \frac{m_b}{K_b} \left(\left(\frac{\rho_{water} V_b}{m_b} - 1 \right) g + \frac{F_{cy,b}}{m_b} \right) \\ &+ A \exp\left(-\frac{K_b}{m_b} t\right). \end{aligned} \quad (403)$$

Since the system is at its equilibrium before the umbilical is slack, on has $v_{b,y}(0) = 0$. Using this initial solution, one gets $A = -\frac{m_b}{K_b} \left(\frac{\rho_{water} V_b}{m_b} - 1 \right) g$ so

$$\begin{aligned} v_{b,y}(t) &= \frac{m_b}{K_b} \left(\left(\frac{\rho_{water} V_b}{m_b} - 1 \right) g + \frac{F_{cy,b}}{m_b} \right) \\ &\times \left(1 - \exp\left(-\frac{K_b}{m_b} t\right) \right), \end{aligned} \quad (404)$$

$$a_{b,y}(t) = \left(\left(\frac{\rho_{water} V_b}{m_b} - 1 \right) g + \frac{F_{cy,b}}{m_b} \right) \exp\left(-\frac{K_b}{m_b} t\right). \quad (405)$$

FPD applied on axis \vec{x}

Let use the FPD of the buoy projected on \vec{x} :

$$\begin{aligned} (m_b \vec{a}_{b,x}) \cdot \vec{x} &= \left(\vec{F}_b + \vec{F}_{fb} + \vec{F}_{cx,b} \right) \cdot \vec{x} \\ m_b \dot{v}_{b,x} &= F_{cx,b} - K_b v_{b,x} \end{aligned} \quad (406)$$

We desire to find an absolute value of $v_{b,x}$. Since the current $F_{cx,b}$ is the only strength applied on the buoy on the axis x and it is supposed the buoy is immobile at the initial instant, *i.e.* $v_{b,x}(0) = 0$, (406) can be rewritten such

$$m_b \dot{v}_{b,x} = |F_{cx,b}| - K_b v_{b,x}. \quad (407)$$

Let solve the differential equation (407). The hypothetical solution is $v_{b,x,HS} = B \exp\left(-\frac{K_b}{m_b} t\right)$ with B a constant. Using the variation of the constant method, a particular solution can be found $v_{b,x,PS} = \frac{|F_{cx,b}|}{K_b}$. Thus, the general solution $v_{b,x} = v_{b,x,PS} + v_{b,x,HS}$ can be expressed as

$$v_{b,x}(t) = \frac{|F_{cx,b}|}{K_b} + B \exp\left(-\frac{K_b}{m_b} t\right). \quad (408)$$

Since the system is at its equilibrium before the umbilical is slack, on has $v_{b,x}(0) = 0$. Using this initial solution, one gets $B = -\frac{|F_{cx,b}|}{K_b} g$ so

$$v_{b,x}(t) = \frac{|F_{cx,b}|}{K_b} \left(1 - \exp\left(-\frac{K_b}{m_b} t\right) \right), \quad (409)$$

$$a_{b,x}(t) = \frac{|F_{cx,b}|}{m_b} \exp\left(-\frac{K_b}{m_b} t\right). \quad (410)$$

Conclusion

From the two previous parts, one gets

$$v_b(t) = \left(1 - \exp\left(-\frac{K_b t}{m_b}\right)\right) \times \sqrt{\left(\frac{F_{cx,b}}{K_b}\right)^2 + \left(\frac{m_b}{K_b} \left(\left(\frac{\rho_{water} V_b}{m_b} - 1\right)g + \frac{F_{cy,b}}{m_b}\right)\right)^2} \quad (411)$$

$$a_b(t) = \exp\left(-\frac{K_b t}{m_b}\right) \times \sqrt{\left(\frac{F_{cx,b}}{m_b}\right)^2 + \left(\left(\frac{\rho_{water} V_b}{m_b} - 1\right)g + \frac{F_{cy,b}}{m_b}\right)^2} \quad (412)$$

with the maximal velocity and acceleration

$$v_{b,max} = \sqrt{\left(\frac{F_{cx,b}}{K_b}\right)^2 + \left(\frac{m_b}{K_b} \left(\left(\frac{\rho_{water} V_b}{m_b} - 1\right)g + \frac{F_{cy,b}}{m_b}\right)\right)^2} \quad (413)$$

$$a_{b,max} = \sqrt{\left(\frac{F_{cx,b}}{m_b}\right)^2 + \left(\left(\frac{\rho_{water} V_b}{m_b} - 1\right)g + \frac{F_{cy,b}}{m_b}\right)^2} \quad (414)$$

H Algorithm choice of umbilical length

This section proposes an algorithm to choose the parameters l , L and l_1 in function of several environmental constraints. Note this algorithm is a suggestion made on a choice of constraints order: others parameters are possible.

Remind y_{floor} is the dept of the seafloor. Let's defined

- $[y_{\text{min}}, y_{\text{max}}]$ are the desired minimum depth and maximum depths for the ROV exploration, where $y_{\text{max}} \leq y_{\text{floor}} - h_M$.
- $[x_{\text{min}}, x_{\text{max}}]$ are the desired minimum and maximum horizontal distances for the ROV exploration, where x_{min} has been defined in Section 5.6.
- Since the boat can move on the surface, the respect of parameters $[y_{\text{min}}, y_{\text{max}}]$ is favored over $[x_{\text{min}}, x_{\text{max}}]$.
- Since reaching a distance $d = \sqrt{x^2 + y^2}$ between the ROV and the boat will lead to an important strength for the ROV (see Section 5.8), it is recommend to respect $d \leq 0.9l$. An overly secure configuration is $x \leq L$ when it is possible.
- Let $\epsilon > 0$ be a constant distance of security.

The following steps described two methods to choose l_1 and L to obtain l .

Umbilical length for y_{min} favored over y_{max}

1. To go the deepest possible without the ballast touches the seafloor, take $l_1 = y_{\text{floor}} - h_M$
2. To respect y_{min} since $x = x_{\text{min}}$, $L = l_1 + y_{\text{min}}$ is chosen, so $l = l_1 + L = 2(y_{\text{floor}} - h_M) + y_{\text{min}} - h_B$. The maximum distance \underline{x} where y_{min} can be respected is so $\underline{x} = \sqrt{l^2 - y_{\text{min}}^2}$.

3. The ROV can reach the depth y_{max} for $x \leq \bar{x}$, where $\bar{x} = \sqrt{l^2 - y_{\text{max}}^2}$.
 - (a) If $x_{\text{max}} > \bar{x}$, then the research area must be restricted to $[x_{\text{min}}, x_M] \times [y_{\text{min}}, y_{\text{max}}]$ with $x_M = \sqrt{(0.9l)^2 - y_{\text{max}}^2}$.
 - (b) Else, then $x_{\text{max}} \leq \bar{x}$ and
 - i. If $\bar{x} \geq L$, then OK.
 - ii. Else, the umbilical is too long and can potentially be reduced. Take $L = \max([x_{\text{max}}, l_1 + y_{\text{min}}])$.
4. To prevent the ballast touches the seafloor, take $l_1 = l_1 - \epsilon$.

Umbilical length for y_{max} favored over y_{min}

1. To respect y_{max} for $x \in [x_{\text{min}}, x_{\text{max}}]$, one take $l^* = \frac{1}{0.9} \sqrt{x_{\text{max}}^2 + y_{\text{max}}^2}$.
2. Take $l_1^* = \frac{l^* - y_{\text{min}}}{2}$.
3. If $l_1^* \leq y_{\text{floor}} - h_M$, the ballast does not touch the seafloor. We can take $l_1 = l_1^*$ and $l \in [l^*, 2(y_{\text{floor}} - h_B) + y_{\text{min}}]$.
4. If $l_1^* > y_{\text{floor}} - h_M$, the ballast touch the seafloor. Take so $l_1 = y_{\text{floor}} - h_M$ and
$$y_{\text{min}}^* = \frac{1}{0.9} \sqrt{x_{\text{max}}^2 + y_{\text{max}}^2} - 2(y_{\text{floor}} - h_M). \quad (415)$$

Then

- (a) If $y_{\text{min}}^* \in [0, y_{\text{max}}]$, then OK. Take $l = 2(y_{\text{floor}} - h_M) + y_{\text{min}}^*$ and the research area must be restricted to $[x_{\text{min}}, x_{\text{max}}] \times [y_{\text{min}}^*, y_{\text{max}}]$ with $y_{\text{min}}^* = \max(y_{\text{min}}, y_{\text{min}}^*)$.
 - (b) If $y_{\text{min}}^* < 0$, take $y_{\text{min}}^* = 0$ and define the maximum horizontal distance
$$x_M = \sqrt{3.24(y_{\text{floor}} - h_M)^2 - y_{\text{max}}^2} \quad \text{using (415).}$$
The research area must be restricted to $[x_{\text{min}}, x_M] \times [y_{\text{min}}, y_{\text{max}}]$.
 - (c) Else, $y_{\text{min}}^* \geq y_{\text{max}}$, put $y_{\text{min}}^* = 0.9y_{\text{max}}$ and
$$x_M = \sqrt{0.81(y_{\text{min}}^* + 2(y_{\text{floor}} - h_M))^2 - y_{\text{max}}^2}$$
using (415). The research area must be restricted to $[x_{\text{min}}, x_M] \times [y_{\text{min}}^*, y_{\text{max}}]$.
5. To prevent the ballast touch the seafloor, take $l_1 = l_1 - \epsilon$.

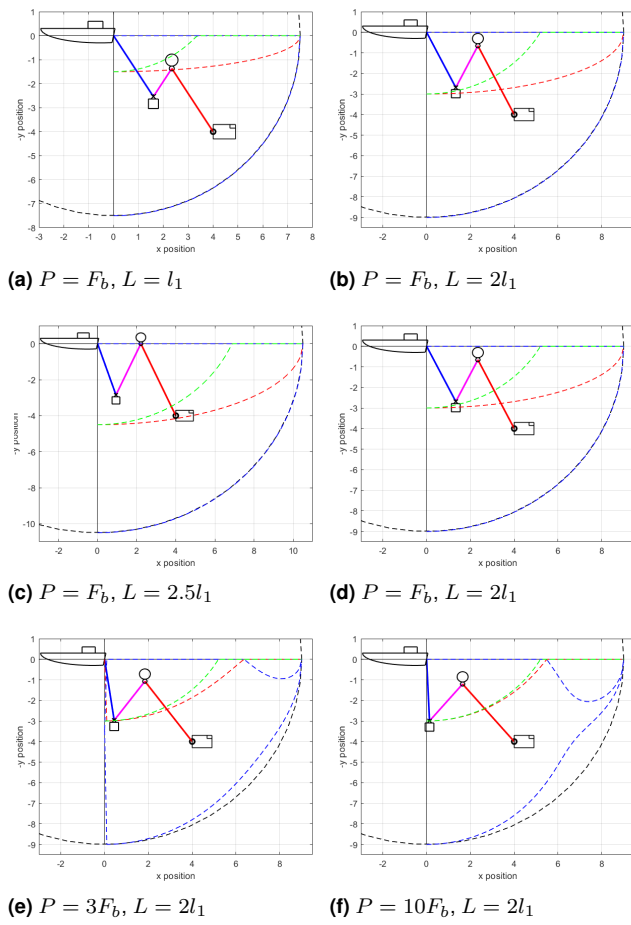


Figure 23. Influence of parameters on the areas when $l_1 < L$.

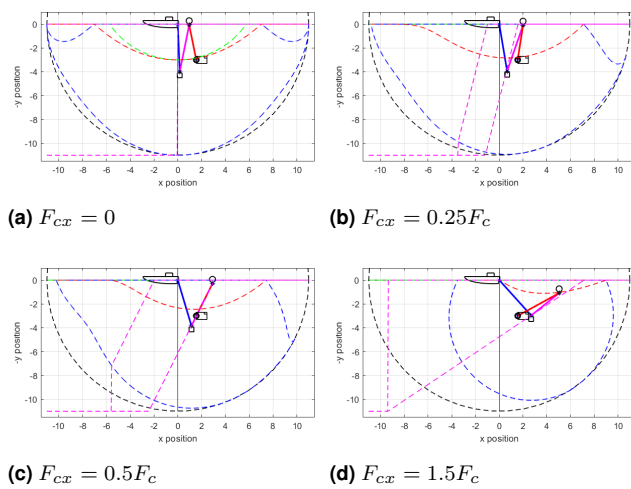


Figure 24. Influence of parameters $F_{cx} = F_{cx,m} = F_{cx,b}$, with $P = 3F_b$ and $(x, y) = (1.5, 3)$ in any case. One observes that the areas D2 and F take more space when the horizontal current rises, since other areas become smaller.